



Faculty of Life Sciences

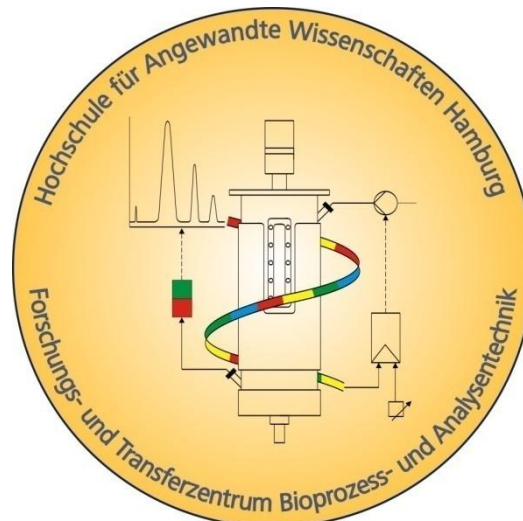
Hochschule für Angewandte Wissenschaften Hamburg

*Hamburg University of Applied Sciences*

## Master Thesis

Study course Pharmaceutical Biotechnology

# Development of a GUI to evaluate strain specific reaction parameters using Matlab App Designer



Judith Ahr



18.06.2021

1. Reviewer
2. Reviewer

Prof. Dr. Anna Rodenhausen (HAW Hamburg)

Prof. Dr. Gesine Cornelissen (HAW Hamburg)

**Title of master thesis**

Development of a GUI to evaluate strain specific reaction parameters using Matlab App Designer

**Abstract**

For the development and planning of fermentation strategies, knowledge of strain behavior is very important. For a fed batch strategy, the knowledge of strain specific global reaction parameters is needed for the development of the open-loop feed control and therefore the accurate control of the growth rate during the fed batch, which in turn is vital to achieve high production rates.

Calculation of the global reaction parameters requires lengthy calculations and large data files. The automation through an application makes this process easier and faster.

In this master thesis, an application was developed to calculate the global reaction parameters  $q_{S/X_m}$ ,  $y_{X/S_{gr}}$ ,  $q_{O/X_m}$  and  $y_{O/S_{gr}}$  for organisms grown on one substrate. The application was developed using Matlab App Designer®. For the development and verification of the application, fermentations were performed to create data that could be used in the application.

The verification of the performance of the application showed, that high quality data is vital for good results. High deviations in the data, especially the offline data, leads to unreliable results that cannot be used for process development. A data fit was performed on the fermentation data, to acquire a data set which showed optimized behavior. This data was then used to calculate the global reaction parameters, confirming the function of the application.

# Contents

<b>I</b>	<b>Table of Contents</b>	<b>II</b>
<b>I</b>	<b>List of Figures</b>	<b>V</b>
<b>II</b>	<b>List of Tables</b>	<b>VII</b>
<b>III</b>	<b>List of Acronyms</b>	<b>VIII</b>
<b>IV</b>	<b>List of variables</b>	<b>IX</b>
<b>V</b>	<b>List of indices</b>	<b>X</b>
<b>1</b>	<b>Introduction</b>	<b>1</b>
<b>2</b>	<b>Aim and purpose</b>	<b>2</b>
<b>3</b>	<b>Theoretical Background</b>	<b>3</b>
3.1	Organism . . . . .	3
3.1.1	Methanol Metabolism . . . . .	4
3.2	High Cell Density Culture . . . . .	6
3.2.1	pO <sub>2</sub> - control . . . . .	7
3.2.2	Open loop feed control . . . . .	7
3.3	Three phase model . . . . .	9
3.3.1	Liquid phase balance . . . . .	10
3.3.1.1	The bio wet phase V <sub>Z</sub> . . . . .	11
3.3.1.2	The media phase V <sub>M</sub> . . . . .	12
3.3.2	Mass transfer from gas to liquid phase . . . . .	13
3.3.3	Gas Phase Balance . . . . .	16
3.3.3.1	O <sub>2</sub> and CO <sub>2</sub> offgas balance . . . . .	17
3.3.4	Quasi steady state O <sub>2</sub> oxygen supply chain . . . . .	18
3.4	Kinetic reaction parameters . . . . .	19
3.4.1	Specific reaction rates . . . . .	19
3.4.2	Global reaction parameters . . . . .	21
3.5	Matlab 2020a® . . . . .	24
3.5.1	Curve Fitting Toolbox . . . . .	25
3.5.2	Matlab App Designer® . . . . .	27
3.5.3	Matlab Report Generator® . . . . .	28
<b>4</b>	<b>Material</b>	<b>29</b>
4.1	Organism . . . . .	29
4.2	Chemicals . . . . .	30
4.3	Media composition . . . . .	31
4.4	Reactor and measuring system . . . . .	33
4.4.1	pH electrode . . . . .	35
4.4.2	pO <sub>2</sub> electrode . . . . .	36
4.4.3	Anti foam sensor . . . . .	37
4.4.4	Offgas measurement . . . . .	38

---

4.5	Eve . . . . .	38
<b>5</b>	<b>Methods</b>	<b>39</b>
5.1	Preliminary Experiments . . . . .	39
5.1.1	Shaker flask cultivation . . . . .	39
5.1.2	Flow rates of the pumps . . . . .	39
5.2	Preculture . . . . .	40
5.3	Preparation of the reactor . . . . .	40
5.4	Inoculation . . . . .	41
5.5	Sample . . . . .	41
5.6	Offline measurement techniques . . . . .	42
5.6.1	OD <sub>600</sub> measurement . . . . .	43
5.6.2	Cell Dry Weight . . . . .	43
5.6.3	Glycerol measurement . . . . .	44
<b>6</b>	<b>Development of the Application</b>	<b>46</b>
6.1	Layout of the Application . . . . .	46
6.2	Global variables . . . . .	49
6.3	Startup Function . . . . .	51
6.4	Data Upload . . . . .	51
6.4.1	Infors Data Upload . . . . .	52
6.4.2	MFCs Data Upload . . . . .	55
6.4.3	Function for the calculation of the offgas data . . . . .	57
6.4.4	Offline Data . . . . .	57
6.4.5	Comma2pointoverwrite . . . . .	59
6.5	Plot . . . . .	59
6.6	Calculation of specific reaction rates . . . . .	59
6.6.1	Function for the calculation of the specific reaction rates . . . . .	60
6.7	Calculation of global reaction rates . . . . .	61
6.7.1	Function for the calculation of the global reaction rates . . . . .	61
6.8	Creation of a .mat-file . . . . .	62
6.9	Creation of a PDF report . . . . .	63
<b>7</b>	<b>Results</b>	<b>64</b>
7.1	Shaker flask cultivation . . . . .	64
7.2	Flow rate of the pump . . . . .	65
7.3	K <sub>XOD</sub> determination from CDW and OD measurement . . . . .	66
7.4	Glycerol measurement . . . . .	67
7.5	Fermentation 1 . . . . .	69
7.5.1	Discussion of the first fermentation . . . . .	73
7.6	Fermentation 2 . . . . .	77
7.6.1	Disussion of the second fermentation . . . . .	81
<b>8</b>	<b>Exemplary calculated data</b>	<b>84</b>
8.1	Data fit . . . . .	84
8.2	Fermentation overview using the calculated data . . . . .	87
8.2.1	Discussion of the results using the calculated data . . . . .	88
8.3	Comparison of the results . . . . .	90

---

<b>9 Summary and Conclusion</b>	<b>91</b>
9.1 Outlook . . . . .	92
<b>References</b>	<b>XI</b>

## I List of Figures

Fig. 1	Microscopic image of <i>Pichia pastoris</i> . . . . .	4
Fig. 2	Methanol metabolism of <i>Pichia pastoris</i> . . . . .	5
Fig. 3	Schematic plot of a Fed-Batch cultivation . . . . .	6
Fig. 4	Macroscopic volume element . . . . .	9
Fig. 5	Gas-liquid interface . . . . .	13
Fig. 6	Characteristics of the yield coefficients . . . . .	21
Fig. 7	Macroscopic representation of the global reaction parameters . . . . .	21
Fig. 8	Structure of an external function . . . . .	25
Fig. 9	Genome section of <i>Pichia pastoris</i> LM1 . . . . .	29
Fig. 10	Setup of the Infors reactor . . . . .	33
Fig. 11	The Infors reactor . . . . .	34
Fig. 12	Schematic presentation of a pH-electrode . . . . .	35
Fig. 13	Schematic presentation of the function of the $p_{O_2}$ -electrode . . . . .	36
Fig. 14	Sample mechanism . . . . .	41
Fig. 15	Sample division for the offline measurements . . . . .	42
Fig. 16	Tab 1 of the app . . . . .	47
Fig. 17	Tab 2 of the app . . . . .	47
Fig. 18	Tab 3 of the app . . . . .	48
Fig. 19	Basic structure of the app . . . . .	50
Fig. 20	Structure of the Button Pushed Callback function for the Infors Data . . . . .	52
Fig. 21	Section of the raw Infors data . . . . .	53
Fig. 22	Structure of the Button Pushed Callback function for the MFCS data from multiple text-files . . . . .	55
Fig. 23	Overview of the function for the upload of the offline data . . . . .	58
Fig. 24	Structure of the for loop for the extraction of the online data matching the time points in the online data . . . . .	60
Fig. 25	PDF-file of the app . . . . .	63
Fig. 26	Growth plot of the pre culture . . . . .	64
Fig. 27	Analysis of the flow rates . . . . .	65
Fig. 28	Plot for the determination of $k_{XOD}$ . . . . .	66
Fig. 29	Chromatograms of the calibration curve . . . . .	67
Fig. 30	Calibration curve of the glycerol measurement . . . . .	68
Fig. 31	Chromatograms of samples $t_0$ , $t_9$ and $t_{11}$ during the first fermentation . . . . .	68
Fig. 32	Overview of Fermentation 1 . . . . .	70
Fig. 33	Substrate uptake during fermentation 1 . . . . .	71
Fig. 34	Oxygen uptake during fermentation 2 . . . . .	72
Fig. 35	Reaction rates during the first fermentation . . . . .	73
Fig. 36	Reaction rates during the first fermentation . . . . .	74
Fig. 37	Overview of Fermentation 2 . . . . .	78
Fig. 38	Substrate uptake during fermentation 2 . . . . .	79
Fig. 39	Oxygen uptake during fermentation 2 . . . . .	80
Fig. 40	Reaction rates during the second fermentation . . . . .	81
Fig. 41	Reaction rates during the second fermentation . . . . .	82

---

Fig. 42	Fermentation 2 with smoothed data . . . . .	84
Fig. 43	Fitted data using Matlab curve fitting tool . . . . .	86
Fig. 44	Substrate uptake during fermentation 2 . . . . .	87
Fig. 45	Oxygen uptake during fermentation 2 . . . . .	88
Fig. 46	Reaction rates calculated using the smoothed and calculated data . . . . .	89

## II List of Tables

Tab. 1	Components and callbacks of the app designer . . . . .	28
Tab. 2	List of chemicals used during this thesis . . . . .	30
Tab. 3	FM22 media composition for shaking flask pre cultures . . . . .	31
Tab. 4	FM22 media composition for batch medium . . . . .	31
Tab. 5	Media composition for the feeding solution . . . . .	31
Tab. 6	composition of PTM4 stock solution . . . . .	32
Tab. 7	composition of Biotin stock solution . . . . .	32
Tab. 8	Measurement system of the reactor . . . . .	34
Tab. 9	HPLC LaChrom system (Merck, Darmstadt, Germany) used for the glycerol measurement . . . . .	44
Tab. 10	Dilution range for the calibration of the glycerol measurement . . . . .	45
Tab. 11	Components of the app and their callback functions . . . . .	49
Tab. 12	Global variables used in the application . . . . .	51
Tab. 13	Table containing the results of the offgas function saved in the mat-file . . . . .	62
Tab. 14	Table containing the specific reaction rates saved in the mat-file . . . . .	62
Tab. 15	Table containing the ranges saved in the mat-file . . . . .	62
Tab. 16	Table containing the global reaction parameters saved in the mat-file . . . . .	62
Tab. 17	Set points for fermentation 1 . . . . .	69
Tab. 18	Ranges for the calculations of the reaction parameters . . . . .	75
Tab. 19	Reaction rates calculated from the OD <sub>600</sub> - and Cell Dry Weight (CDW)-data from the first fermentation . . . . .	75
Tab. 20	Global reaction parameters calculated using data from the first fermentation . . . . .	75
Tab. 21	Set points for fermentation 2 . . . . .	77
Tab. 22	Ranges for the calculations of the reaction parameters . . . . .	82
Tab. 23	Reaction rates calculated from the CDW-data from the second fermentation . . . . .	83
Tab. 24	Global reaction parameters calculated using data from the second fermentation of <i>P. pastoris</i> . . . . .	83
Tab. 25	Evaluation of fit . . . . .	85
Tab. 26	Ranges for the calculations of the reaction parameters using the calculated data . . . . .	89
Tab. 27	Reaction rates calculated using the fitted data . . . . .	89
Tab. 28	Global reaction parameters calculated using the fitted data . . . . .	89
Tab. 29	Comparison of the results from the actual and fitted data from the second fermentation . . . . .	90
Tab. 30	Comparison of the global reaction parameters using the actual and fitted data from the second fermentation . . . . .	90



### III List of Acronyms

**CDW** Cell Dry Weight

**DOM** Document Object Model

**GUI** Graphic User Interface

**HCDC** High Cell Density Culture

**HPLC** High Performance Liquid Chromatography

**MFCS** Multi Fermentor Control System

**NaN** Not a Number

**OD** Optical Density

**RMSE** root mean squared error

**SSE** sum of squared due to error

**WCB** Working Cell Bank

## IV List of variables

$A_G$	:=	bubble surface area	$m^2$
$c_{IK}$	:=	concentration of component I in subsystem K	$g/l$
$c_{IK}^*$	:=	steady state concentration of component I in subsystem K	$g/(l\ h)$
$F_K$	:=	flow rate from subsystem K	$l/h$
$H_I$	:=	Henry coefficient of component I	$N\ m/kg$
$K_{IL}$	:=	transport coefficient of component I from the gas to the liquid phase	$l/m^2h$
$k_{IK}$	:=	conductance value of component I into subsystem K	$l/m^2h$
$k_{La}$	:=	volumetric $O_2$ transfer coefficient	$1/h$
$M_I$	:=	mole mass of component I	$g/mol$
$m_{IK}$	:=	mass of the component I in subsystem K	$g$
$n_{IK}$	:=	amount of component I in subsystem K	$mol$
$N_{St}$	:=	agitation rate	$1/min$
OTR	:=	Oxygen Transfer Rate	$g/(l\ h)$
OUR	:=	Oxygen Uptake Rate	$g/(L\ h)$
$p_{IK}$	:=	partial pressure of component I in subsystem K	$bar$
$p_I$	:=	pressure of component I	$bar$
$Q_{O_2}$	:=	volumetric oxygen supply	$g/(l\ h)$
$q_{I/X}$	:=	cellspecific reaction rate of component I	$1/h$
$R$	:=	gas constant	$N\ m\ K/kmol$
RQ	:=	Respiratory Quotient	
$T_G$	:=	temperature of the gas phase	$K$
$V_K$	:=	volume of subsystem K	$l$
$x_{IG}$	:=	mole fraction of component I in the gas phase	
$y_{X/I}$	:=	yield coefficient of component I	
$\alpha_{Z/X}$	:=	ratio of the bio dry to wet phase	
$\mu$	:=	growth rate of the cells	$1/h$
$\rho_Z$	:=	density of the bio wet phase	$g/l$

## V List of indices

AF	:=	Antifoam
AIR	:=	Air
cal	:=	calibration
C,CO <sub>2</sub>	:=	Carbon dioxide
G	:=	gas phase
gr	:=	growth phase
in	:=	ingoing
L	:=	liquid phase
m	:=	maintenance part
M	:=	media phase
max	:=	maximal
n	:=	norm conditions
O,O <sub>2</sub>	:=	Oxygen
out	:=	outgoing
S	:=	sample
S1	:=	substrate 1 (glycerol)
T1	:=	Titration agent 1 (Acid)
T2	:=	Titration agent 2 (Base)
R	:=	reservoir
w	:=	set point
X	:=	bio dry mass
Z	:=	bio wet mass

# 1 Introduction

In 1982 the first recombinant protein - Insulin - was produced and used for the treatment of diabetes. The bacteria *Escherichia coli* was used in this process. Since then, the industry has expanded rapidly, with pro- and eukaryotic organism being used for the production of proteins. The organisms needed for the production of the proteins are grown with many different strategies.

In the pharmaceutical industry, fed batch cultivations are often employed to grow organisms to a high cell concentration. In contrast to a batch cultivation, where all substrate is made available at the beginning of the fermentation, a fed batch cultivation employs a feeding strategy after all available substrate has been consumed.

In a fed batch cultivation, the cell concentration can reach very high densities, due to the constant feeding of substrate. A batch cultivation can not reach those concentrations, as the amount of substrate that would need to be provided at the beginning of the fermentation would have an inhibitory effect on the growth of the cells.

Knowledge of strain characteristics is very important in the development of fed batch fermentation processes for the control of the growth rate. The feed rate can be used to control the growth rate ( $\mu$  or  $q_{X/X}$ ) of the organism. A well controlled growth rate leads to higher product yields, as the highest product formation is not be expected at the maximal growth rate but at growth rates of  $\mu_w < \mu_{max}$ .

Global reaction parameters that are specific to each strain are needed to calculate the feed rate for growth rate control. They describe the maintenance reaction parameters of the metabolism and growth yield rates of oxygen and substrate.

## 2 Aim and purpose

The aim of this master thesis was the development of a Graphic User Interface (GUI) that can reliably calculate the global reaction parameters of *Pichia pastoris* with data from the Infors Minifors reactor using Matlab App Designer.

The reaction parameters are calculated using data from previously performed fermentations. The calculation process is tedious, as the data sets are large and many equations are involved. The automation through an application eases and accelerates the calculation.

A prototype of the app was developed, and fermentations were performed for testing and further development of the app. Finally, the fermentation data was analyzed using the app and the reaction parameters were calculated.

## 3 Theoretical Background

### 3.1 Organism

*Pichia pastoris* is an expression system that is widely used in the industry for the production of recombinant proteins. It was reclassified as *Komagataella* and split into the sub-species *pastoris* and *phaffii* because of the discovery of a tRNA-divergence (Kurtzman 2009). It is still referred to as *P. pastoris* for simplicity. A microscopic image of *P. pastoris* can be seen in figure 9.

It was first discovered in the 1960s as an expression system because of its ability to grow on methanol as its only carbon source, which during the time was very inexpensive, as it was synthesized from natural gas source (Li et al. 2007).

The usual fermentation strategy for *P. pastoris* is a three stage strategy, that utilises a batch and fed batch phase with glucose or glycerol as substrate. In the batch phase, the substrate is abundant, therefore the growth rate is at its maximum, while during the fed batch phase, the feed is limited for a limited growth rate. The last stage is the induction of production using methanol (Li et al. 2007). The advantage to bacteria is that yeasts are eukaryotes with a nucleus, possessing many of the post-translational capabilities of other eukaryotes, leading to correct folding and better stability of the product. In contrast to bacteria, they have the ability for glycosilation, disulphide bond formation and proteolytic processing, all of which are not possible in bacteria.

It also offers the advantages of prokaryotic expression systems, such as easy cultivation and high expression. It is also very similar to the very well characterized *Saccharomyces cerevisiae* and is able to use methanol as its only carbon source (Ogata, Nishikawa, and Ohsugi 1969)

Furthermore, unlike *Escherichia coli*, *P. pastoris* is nonpathogenic, and does therefore not cause disease in other organisms. There is also no risk of an endotoxin contamination (Li et al. 2007).

*P. pastoris* also has an advantage against other yeasts, especially the well studied *S. cerevisiae*, as it prefers respiratory growth over the fermentation of sugars, meaning no energy is wasted on the conversion of sugar, but all energy is spent on cell growth. Thus it can be grown to higher cell densities with less toxic byproducts, and the given substrate is converted into biomass, which will lead to higher product yields (Higgins and James M. Cregg 2000, Lopes, Belo, and Mota 2012). The maximal growth rates of *P. pastoris* lie between 0.28/h to 0.16/h. A lower growth rate generally leads to a higher productivity, while the substrate uptake re-

mains unchanged. Therefore, at lower growth rates more resources are used for the production than for growth (Heyland et al. 2011).

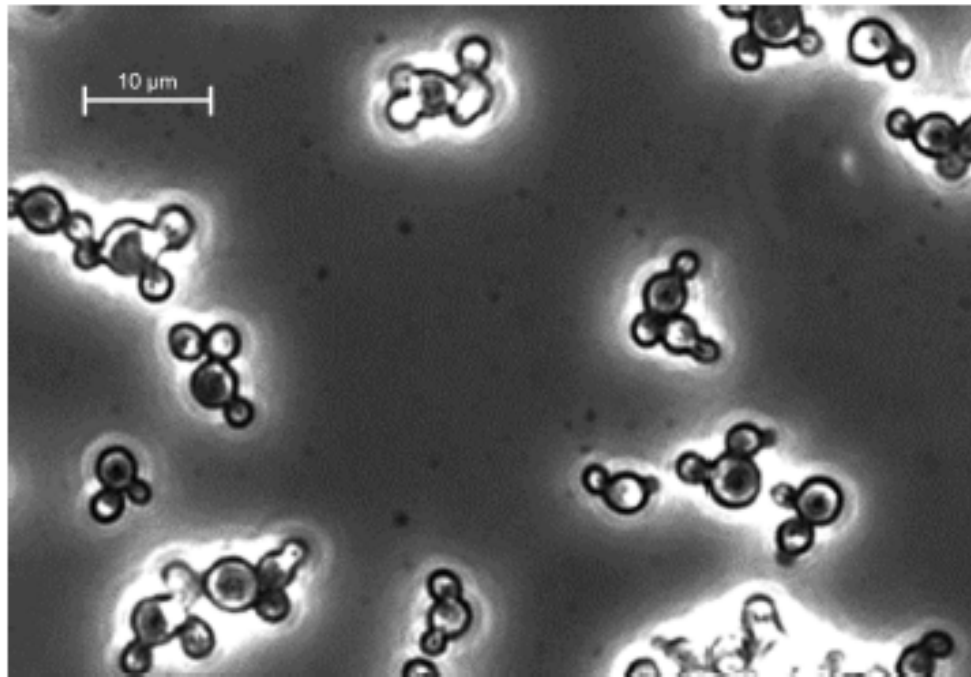


**Fig. 1:** *Pichia pastoris* under a fluorescence microscope in phase contrast. Source: Scheunemann 2020

### 3.1.1 Methanol Metabolism

*P. pastoris* ability to grow on methanol depends on the two genes AOX1 and AOX2, which transcribe alcohol oxidase and are induced by the presence of methanol. This gives *P. pastoris* the ability to use methanol as its only carbon source. If glucose or glycerol are in sufficiently high concentrations in the medium, the transcription of the oxidase is repressed.

This repression of the transcription by the presence of other carbon sources makes the promoters easily regulated. When the glycerol is used up and methanol is added to the culture, the AOX-genes are induced and transcription of alcohol oxidase begins, making it possible for *P. pastoris* to metabolize the methanol (Krainer et al. 2012).

The metabolization of methanol is done by oxidation of methanol to formaldehyde and hydrogen peroxide, which are further broken down into formate and carbon dioxide, producing energy and water and oxygen respectively. The first step takes places in a special organelle, the peroxisome, to avoid the toxicity of the hydrogen peroxide (Higgins and James M. Cregg 2000). The methanol metabolism is

shown in figure 2.

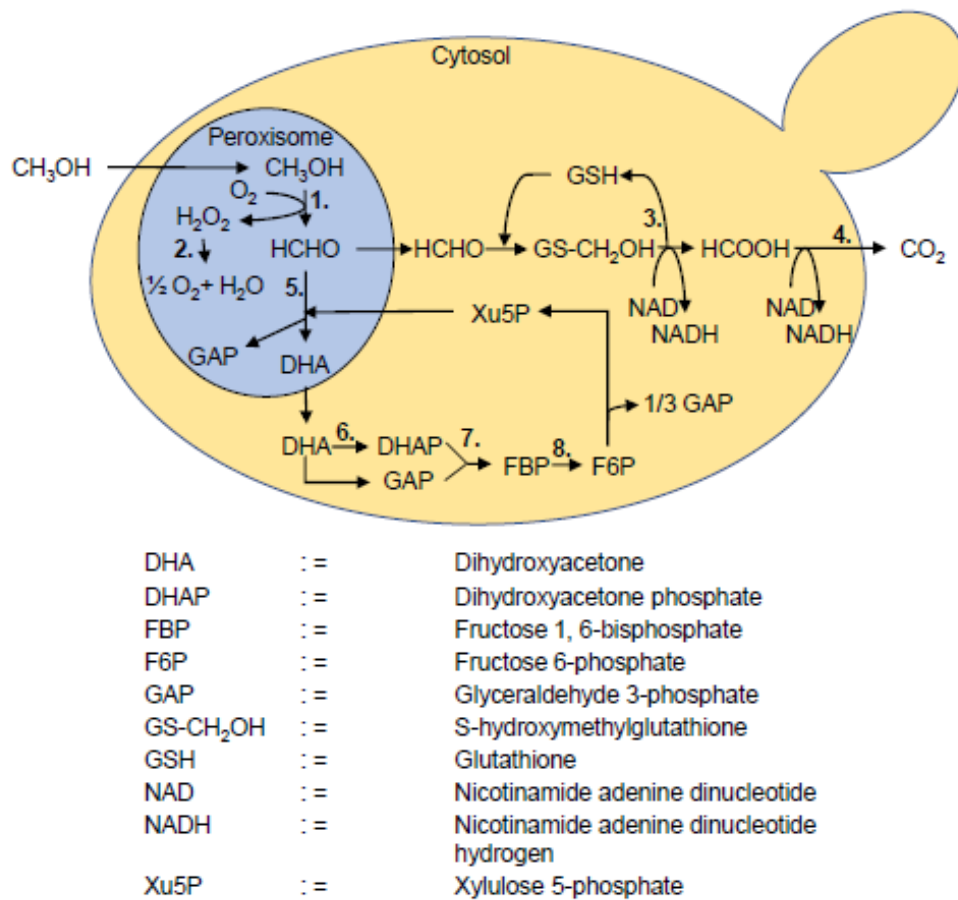


**Fig. 2:** Methanol metabolism of *P. pastoris*: 1. alcohol oxidase; 2. catalase; 3. formaldehyde dehydrogenase; 4. formate dehydrogenase; 5. dihydroxyacetone synthase; 6. dihydroxyacetone kinase; 7. fructose 1, 6-bisphosphate aldolase; 8. fructose 1,6-bisphosphatase Source: Scheunemann 2020

After activating the AOX1 promoter, alcohol oxidase makes up about 30% of the total proteins produced by the yeast. By adding the gene sequence of the wanted protein upstream of the promoter, an equivalent amount of product can be expected (Trinh, Phue, and Shiloach 2003). The AOX2 promoter is less productive, accounting for about 15% of the AOX activity (J M Cregg et al. 1989).

Three different phenotypes of *P. pastoris* exist, in which one or both AOX promoters are knocked out. The wildtype Mut<sup>+</sup> contains both promoters, while the Mut<sup>s</sup> has the AOX1 promoter knocked out. The Mut<sup>s</sup>-strain commonly has lower growth rates, leading to an employment of a mixed feed strategy with glycerol and methanol to increase growth rates. The Mut<sup>+</sup>-strain is characterized by higher growth rates and productivity. However, the high methanol consumption of Mut<sup>+</sup> also leads to problems, requiring a higher oxygen supply, as well as a sensitivity



to the high methanol concentrations needed.

The Mut<sup>-</sup>-strain contains none of the promoters and is unable to grow on methanol as its only carbon source (Krainer et al. 2012).

### 3.2 High Cell Density Culture

A High Cell Density Culture (HCDC) is, as the name suggests, a culture in which the cell density or concentration is grown to a very high value. The culture broth can have a paste-like consistency, owing to the high concentration of cells in the medium.

In a HCDC, a batch and fed batch phase are employed, to grow the cells to very high cell densities.

In the batch phase, the growth rate of the cells is unlimited, as an abundance of substrate is available. To ensure no oxygen limitation occurs, the oxygen supply has to be controlled by a  $pO_2$  control. In the first phase, the  $pO_2$  is uncontrolled until it reaches a set point  $pO_{2w}$ . The agitation control is started, increasing  $N_{St}$  to keep the  $pO_2$  stable. If all available substrate is used up, the batch phase ends, and the fed batch phase begins. This can be seen by a strong increase in the  $pO_2$ .

A schematic plot of a HCDC can be seen in figure 3

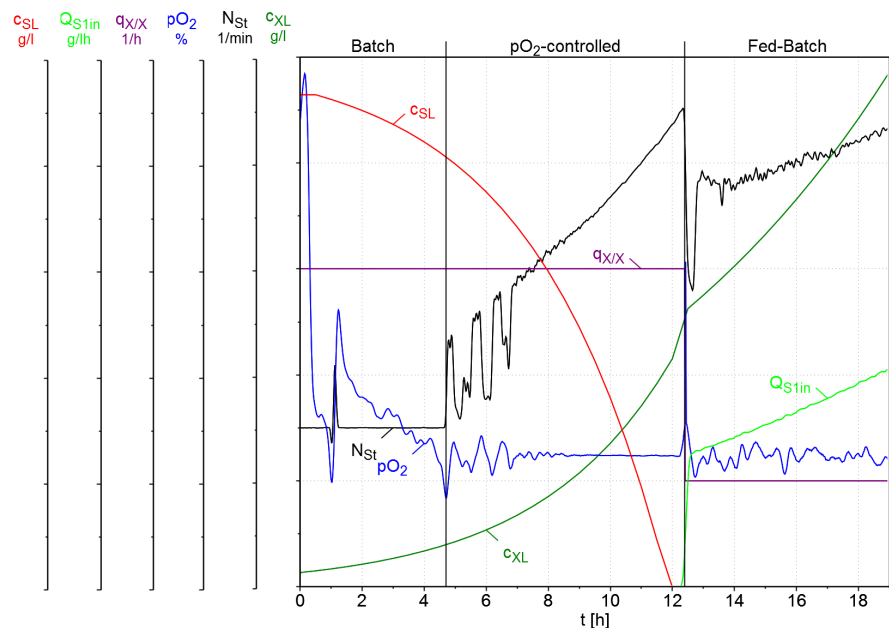


**Fig. 3:** Schematic plot of a Fed-Batch cultivation process, with the batch phase divided into the uncontrolled and the  $pO_2$ -controlled phase, and the fed batch

During the fed batch, the growth rate  $\mu$  is controlled with quantity of substrate  $Q_{S1in}$ . The cells are growing in substrate limitation and the growth rate  $\mu$  or  $q_{X/X}$  is kept constant at its set point  $\mu_w$ .

### 3.2.1 pO<sub>2</sub>- control

After the pO<sub>2</sub> reaches its setpoint, a pO<sub>2</sub> control has to be started, to guarantee the oxygen needs of the organism are met. For this, a pO<sub>2</sub>-agitation control is employed.

The  $k_L a$  describes the mass transfer of a substance in the reactor (in this case oxygen). The  $k_L a$  is dependent on the stirrer speed  $N_{St}$ , the aeration rate  $F_{nG}$  and the liquid volume of the reactor  $V_L$ .

The control of the pO<sub>2</sub> is made possible by the following equations.

The oxygen supply rate into the reactor  $Q_{O_2}$  is calculated by

$$Q_{O_2}(t) = \frac{[F_{nGin}(t) * x_{OGin}(t) - F_{OLnGout}(t)] * M_{O_2}}{V_{nM} * V_L(t)} \quad (1)$$

with  $F_{nGin} = F_{nAir}$  and  $x_{OGin} = 0.21$ .

The bottle neck is the OTR.

$$OTR(t) = k_L a(N_{St}, \dots t) * \left[ \frac{p_G(t) * x_{OG}(t) - p_{OL}(t)}{H_{O_2}(t)} \right] \quad (2)$$

which contains the partial oxygen pressure pO<sub>2</sub>:

$$pO_2(t) = \frac{p_{OL}(t) * 100\%}{p_{OLcal}(t)} \quad (3)$$

Therefore, the pO<sub>2</sub> is controllable by a change in agitation speed  $N_{St}$ , as it is part of the equation for OTR(t) (Cornelissen 2004, Schügerl and Bellgardt 2011).

### 3.2.2 Open loop feed control

The open loop feed control for the control of  $\mu_w$  is set up by the following equation

$$F_{Rw} = F_{Rwj} * e^{\mu_w(t-t_j)} \quad (4)$$

with the starting value

$$F_{Rwj} = \frac{(\mu_{wj} + q_{S1/Xm} * y_{X/S1gr}) * V_L * c_{XLj}}{y_{X/S1gr} * c_{S1R}} \quad (5)$$

The parameters  $c_{XL}$  and  $V_L$  can be measured during fermentation or predicted using data from earlier fermentations, while  $c_{S1R}$  is known. The feeding will start after all the available substrate in the medium is used up by the cells. This will be noticeable by a spike in the  $p_{O_2}$ , as the oxygen demand decreases. In turn the controlled agitation rate will decrease. Through those two parameters a batch end detection can be set up, after which the feeding will start.

### 3.3 Three phase model

To characterize and plan a HCDC, a model is needed that describes the the reactions during the fermentation.

The model is built by (1) the concentration balances during the process, (2) the kinetic reactions of the organism and (3) the process parameters.

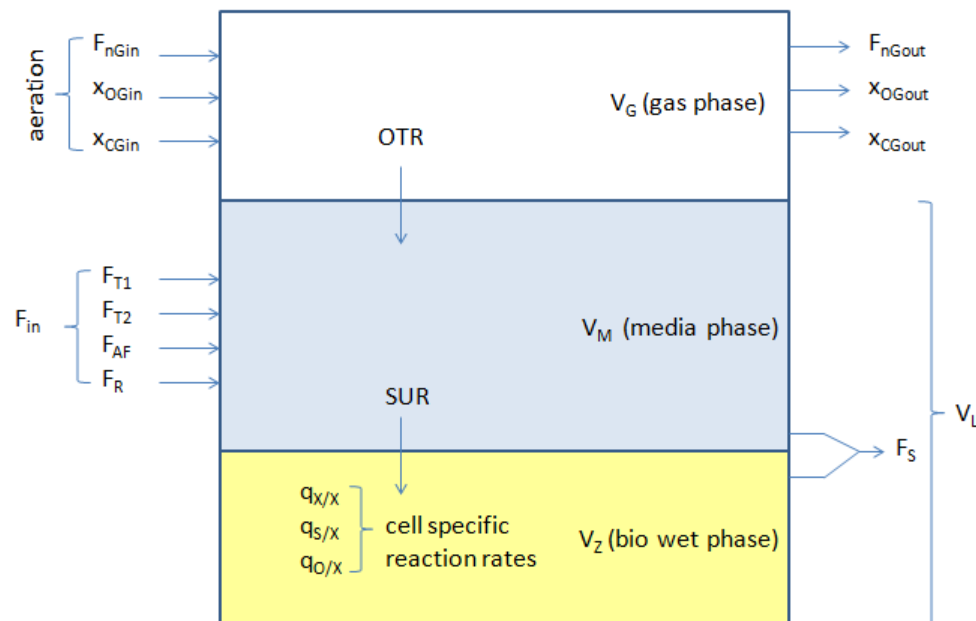


**Fig. 4:** Macroscopic volume element of all incoming and outgoing flows as well as the transfer between the phases. After: Schügerl and Bellgardt 2011, Cornelissen 2004

In a HCDC the cell mass can take up an extensive percentage of the liquid volume. Therefore the liquid volume of the reactor has to be divided into the two subspaces  $V_M$ , which is the volume of the cellfree media, and  $V_Z$ , the bio wet phase containing the cells, to acquire accurate mass balances. The third phase is the gas phase,  $V_G$ . For the calculations of all parameters of the fermentation, the concentration balances have to be considered, as liquid volume is added to the reactor through the flow rates of feed, titration and antifoam ( $F_R$ ,  $F_{T1}$ ,  $F_{T2}$  and  $F_{AF}$ ) and volume is removed by sampling ( $F_S$ ). In an ideally stirred bioreactor, the concentrations can be considered as equal everywhere, with no pockets of deviations.

The ingoing flows change the concentrations in the reactor, while sampling ( $F_S$ ) removes volume but does not change concentration. In figure 4 all incoming and outgoing flows, as well as the transfer between the gas and liquid phase are depicted.

The substrate reaches the bio wet phase  $V_Z$  through the SUR. In the bio wet phase, the cell specific reaction rates  $q_{X/X}$ ,  $q_{S1/X}$  and  $q_{O/X}$  change the concentrations of cells, substrate and oxygen.

The oxygen is transported into the liquid phase through the OTR. The oxygen concentration in the gas phase is influenced by the aeration rate and the offgas.

### 3.3.1 Liquid phase balance

The liquid reactor volume  $V_L$  is made up of the bio wet phase  $V_Z$  and the media phase  $V_M$ .

$$V_L = V_M + V_Z \quad (6)$$

with

- $V_L$  = volume of the liquid phase l
- $V_M$  = volume of the media phase l
- $V_Z$  = volume of the bio wet phase phase l

The volume of the liquid phase is influenced by the ingoing and outgoing flows with

$$F_{in}(t) = F_R(t) + F_{T1}(t) + F_{T2}(t) + F_{AF}(t) \quad (7)$$

with

- $F_{in}$  = sum of all ingoing flows l/h
- $F_R$  = flow rate from the reservoir with the feed solution l/h
- $F_{T1}$  = flow rate of the acid l/h
- $F_{T2}$  = flow rate of the base l/h
- $F_{AF}$  = flow rate of the anti foam l/h

and  $F_{out}$

$$F_{out} = F_S \quad (8)$$

- $F_{out}$  = sum of all outgoing flows l/h
- $F_S$  = sample flow rate l/h

Therefore the change in the liquid volume is described by

$$\dot{V}_L = F_{in} - F_{out} \quad (9)$$

The mass balance of the cell mass is described by

$$\dot{m}_{XL} = \left[ \frac{F_S(t)}{V_L(t)} + q_{X/X}(t) \right] * m_{XL}(t) \quad (10)$$

- $m_{XL}$  = mass of the cells in the liquid phase g
- $q_{X/X}$  = cell specific growth rate 1/h

With the volume and mass balance, the concentration balance can be set up

$$\dot{c}_{XL} = \left[ \frac{F_{in}(t)}{V_L(t)} + q_{X/X}(t) \right] * c_{XL}(t) \quad (11)$$

- $c_{XL}$  = concentration of the cells in the liquid phase g/l

### 3.3.1.1 The bio wet phase $V_Z$

The volume of the bio wet phase can be calculated by

$$V_Z(t) = \frac{\alpha_{Z/X} * m_{XL}(t)}{\rho_Z} = \frac{\alpha_{Z/X} * V_L(t) * c_{XL}(t)}{\rho_Z} \quad (12)$$

with

- $\alpha_{Z/X}$  = ratio of the bio dry to wet phase
  - $\rho_Z$  = density of the bio wet phase g/l
- with the change in the volume described by

$$\dot{V}_Z = F_Z - F_S * \frac{V_Z(t)}{V_L(t)} \stackrel{!}{=} \frac{\alpha_{Z/X} * \dot{m}_{XL}(t)}{\rho_Z} \quad (13)$$

with

- $F_Z$  = Volume loss rate of the medium l/h

calculated by

$$F_Z(t) = \frac{\alpha_{Z/X} * q_{X/X}(t) * m_{XL}(t)}{\rho_Z} = q_{X/X}(t) * V_Z(t) \quad (14)$$

which is only influenced by the growth rate  $q_{X/X}$  and the volume of the bio wet phase  $V_Z$ .

### 3.3.1.2 The media phase $V_M$

For the balance of the substrate in the media phase, first the mass balance is set up, with the inflowing, outgoing and reaction terms

$$\begin{aligned} \dot{m}_{S1M}(t) &= \dot{m}_{S1Min}(t) - \dot{m}_{S1Mout}(t) + \dot{m}_{S1Mreac}(t) \\ &= \sum F_R * c_{S1R} - \frac{F_{S1}}{V_L} * m_{S1M}(t) + q_{S1/X}(t) * m_{XL}(t) \end{aligned} \quad (15)$$

with

- $m_{S1M}$  = mass of the substrate in the media phase g
- $m_{S1Min}$  = ingoing mass of the substrate in the media phase g
- $m_{S1Mout}$  = outgoing mass of the substrate in the media phase g
- $m_{S1Mreac}$  = reaction term of the mass of the substrate in the media phase g
- $c_{S1R}$  = concentration of the substrate in the reservoir g/l
- $q_{S1/X}$  = cell specific substrate uptake rate 1/h

For the concentration balance we need the following equations

$$m_{S1M}(t) = V_M(t) * c_{S1M}(t) \quad (16)$$

- $c_{S1M}$  = concentration of the substrate in the media phase g/l

and

$$\dot{m}_{S1M}(t) = \dot{V}_M(t) * c_{S1M}(t) + V_M(t) * \dot{c}_{S1M}(t) \quad (17)$$

to calculate the mass and the change in mass over time of the substrate in the media phase.

The volume balance of the media phase is described by

$$\dot{V}_M(t) = F_{in} - F_S(t) * \frac{V_M(t)}{V_L(t)} - F_Z \quad (18)$$

The concentration balance can now be set up with

$$\begin{aligned} \dot{c}_{S1M}(t) = & \frac{\sum F_R(t) * c_{S1R}}{V_M(t)} - \frac{\rho_Z * F_{in}(t) - \alpha_{Z/X} * q_{X/X}(t) * V_L(t) * c_{XL}(t)}{\rho_Z * V_M(t)} * c_{S1M}(t) \\ & + \frac{q_{S1/X} * V_L(t) * c_{XL}(t)}{V_M(t)} \end{aligned} \quad (19)$$

for the concentration balance of the substrate in the media phase.

### 3.3.2 Mass transfer from gas to liquid phase

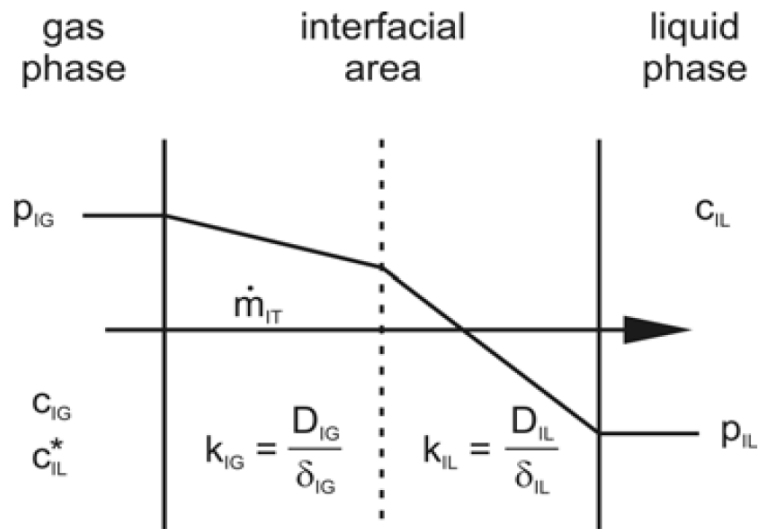


**Fig. 5:** Interface of the gas to the liquid face. Source: Cornelissen 2004

The mass transfer of oxygen between the liquid and the gas phase is explained with the double film theory shown in figure 5.

With Henry's Law we can set up the dissolved concentration in the liquid phase

$$c_{OL}(t) = \frac{p_{OG}(t)}{H_{O2}(t)} = \frac{p_G(t) * X_{OG}(t)}{H_{O2}(t)} \quad (20)$$

with



- $c_{OL}$  = concentration of oxygen in the liquid phase g/l
- $p_{OG}$  = partial pressure of oxygen in the gas phase bar
- $H_{O_2}$  = Henry coefficient of oxygen N m/kg
- $p_G$  = pressure of the gas phase bar
- $x_{OG}$  = oxygen mole fraction

and in the gas phase

$$c_{OL}^*(t) = \frac{p_{OL}(t)}{H_{O_2}(t)} \quad (21)$$

with

- $p_{OL}$  = partial pressure of oxygen in the liquid phase bar
- $c_{OL}^*$  = steady state concentration of oxygen g/(l h)

can be derived.

The mass transfer flow between the gas and liquid phase

$$\dot{m}_{OT} = K_{OL}(t) * A_G(t) * [c_{OL}^*(t) - c_{OL}(t)] \quad (22)$$

with

- $m_{OT}$  = mass transfer of oxygen g
- $K_{OL}$  = transport coefficient of oxygen from the gas to the liquid phase L/m<sup>2</sup>h
- $A_G$  = bubble surface area m<sup>2</sup>

is proportional to

- the concentration difference
- the contact area between gas and liquid phase
- the product of the mass transfer coefficient  $K_{iL}$

The reciprocal value of the transfer coefficient  $K_{OL}$  is calculated by

$$\frac{1}{K_{OL}(t)} = \frac{1}{k_{OL}(t)} + \frac{R * T_G(t)}{M_{O_2} * H_{O_2}(t) * k_{OG}(t)} \quad (23)$$

with

- $k_{OL}$  = conductance value of oxygen into the liquid phase  $l/m^2h$
- $R$  = gas constant  $N\ m\ K/kmol$
- $T_G$  = temperature of the gas phase  $K$
- $M_{O_2}$  = mole mass of oxygen  $g/mol$
- $k_{OG}$  = conductance value of oxygen into the gas phase  $l/m^2h$

The diffusion barrier is mainly in the liquid phase, therefore  $K_{OL}$  and  $k_{OL}$  are almost identical.

Using the volumetric oxygen transfer coefficient  $k_L a$

$$k_L a(t) = \frac{k_{OL}(t) * A_G(t)}{V_L(t)} \quad (24)$$

with

- $k_L a$  =volumetric  $O_2$  transfer coefficient  $1/h$

and the maximum saturation concentration

$$c_{OLmax}(t) = \frac{p_G(t)}{H_{O_2}(t)} \quad (25)$$

the oxygen transfer rate can be calculated

$$OTR(t) = OTR_{max}(t) * [x_{OG}(t) - \frac{c_{OL}(t)}{c_{OLmax}(t)}] \quad (26)$$

with

- $OTR$  =Oxygen Transfer Rate  $g/(lh)$

Since the concentration of oxygen  $c_{OL}$  is not measurable, it has to be replaced by the partial oxygen pressure in the liquid phase  $p_{OL}$

$$p_{OL}(T) = H_{O_2}(t) * c_{OL}(t) \quad (27)$$

The relative partial oxygen pressure can accessed by the  $pO_2$ -probe and the  $O_2$ -calibration partial pressure  $p_{OLcal}$ .

$$pO_2(t) = \frac{p_{OL}(t)}{p_{OLcal}} * 100\% \approx \frac{p_{OL}(t)}{p_{Gcal} * x_{OGcal}} * 100\% = \frac{H_{O_2}(t) * 100\%}{p_{Gcal} * x_{OGcal}} * c_{OL}(t) \quad (28)$$

with

- $p_{O_2}$  =relative partial pressure of oxygen in the gas phase %

This leads to this equation

$$OTR(t) = OTR_{max}(t) * [x_{OG}(t) - \frac{p_{Gcal} * x_{OGcal}}{p_G(t)} * \frac{p_{O_2}(t)}{N_{100\%}}] \quad (29)$$

for the calculation of the Oxygen Transfer Rate.

### 3.3.3 Gas Phase Balance

The balancing of oxygen in the gas phase is started with the general mass balance.

$$\dot{m}_{OG}(t) = \dot{m}_{OGin}(t) - \dot{m}_{OGout}(t) - \dot{m}_{OT}(t) \quad (30)$$

with

- $m_{OG}$  =mass of oxygen in the gas phase g

The ingoing mass flow is calculated by

$$\dot{m}_{OGin}(t) = \frac{F_{nGin}(t) * M_{O_2} * x_{OGin}(t)}{V_{nM}} = \dot{M}_{O_2} * \dot{n}_{OGin}(t) \quad (31)$$

with

- $F_{nG}$  =gas flow l/h
- $V_{nM}$  =mole volume under norm conditions l/mol
- $n_{OG}$  =amount of gas in the gas phase mol

and the outgoing mass flow by

$$\dot{m}_{OGout}(t) = \frac{F_{nGout}(t) * M_{O_2} * x_{OGout}(t)}{V_{nM}} = \dot{M}_{O_2} * \dot{n}_{OGout}(t) \quad (32)$$

with the transfer mass flow already shown in equation 22. The flow  $F_{nGin}$  is only

comprised of air as no gas mixing was employed.

$$F_{nGin} = F_{nAIR} \quad (33)$$

### 3.3.3.1 O<sub>2</sub> and CO<sub>2</sub> offgas balance

In the balancing, the O<sub>2</sub> supply, the CO<sub>2</sub> production and the ratio of the two are considered.

$$\begin{aligned} Q_{O_2}(t) &= \frac{\dot{m}_{OGin} - \dot{m}_{OGout}}{V_L(t)} \\ &= Q_{O_2max} * \frac{x_{OGin}(t) - [1 - x_{O_2}(t)] - x_{O_2}(t) - [1 - x_{CGin}(t)]}{1 - x_{O_2} - x_{CO_2}} \end{aligned} \quad (34)$$

with

- Q<sub>O<sub>2</sub></sub> = volumetric oxygen supply g/(l h)
- x<sub>CG</sub> = carbon dioxide mole fraction

and the maximal oxygen supply rate Q<sub>O<sub>2</sub>max</sub>

$$Q_{O_2max}(t) = \frac{F_{nG}(t) * M_{O_2}}{V_{nM} * V_L(t)} \quad (35)$$

The CO<sub>2</sub> discharge rate can be calculated in the same way.

$$\begin{aligned} Q_{CO_2}(t) &= \frac{\dot{m}_{CGout} - \dot{m}_{OGout}}{V_L(t)} \\ &= Q_{CO_2max} * \frac{x_{CO_2}(t) - [1 - x_{OGin}(t)] - x_{OGin}(t) - [1 - x_{O_2}(t)]}{1 - x_{O_2} - x_{CO_2}} \end{aligned} \quad (36)$$

with the maximal CO<sub>2</sub> supply rate Q<sub>CO<sub>2</sub>max</sub>

$$Q_{CO_2max}(t) = \frac{F_{nG}(t) * M_{CO_2}}{V_{nM} * V_L(t)} \quad (37)$$

with

- M<sub>CO<sub>2</sub></sub> = mole mass of CO<sub>2</sub> g/mol

From this the respiration quotient can be calculated

$$RQ(t) = \frac{Q_{CO_2}(t) * M_{O_2}}{M_{O_2} * Q_{O_2}(t)} \quad (38)$$

which describes the molar ratio of produced CO<sub>2</sub> to consumed O<sub>2</sub>.

### 3.3.4 Quasi steady state O<sub>2</sub> oxygen supply chain

In studying the relationship between the components in equation 30, it is discernable that the oxygen accumulation in the gas phase is negligible in comparison to the oxygen transfer rate.

In the liquid phase, the oxygen transfer rate is described by

$$\dot{m}_{OT}(t) > \dot{m}_{OLin}(t) - \dot{m}_{OLout}(t) - \dot{m}_{OL}(t) \quad (39)$$

where both the oxygen flow as well as the accumulation term are negligible in relation to the the transfer.

Therefore the following relationship can be found.

$$\dot{m}_{OGin}(t) - \dot{m}_{OGout}(t) = \dot{m}_{OT} = V_L(t) * OUR(t) \quad (40)$$

This confirms the quasi steady state transfer equilibrium of oxygen.

$$Q_{O_2}(t) = OTR(t) = OUR(t) \quad (41)$$

with

- OUR = Oxygen Uptake Rate g/(L h)

with the oxygen supply chain

$$\begin{aligned} Q_{O_2}(t) &= Q_{O_2max} * \frac{x_{OGin}(t) - x_{OGout}(t)}{1 - [1 - RQ(t)] * x_{OGin}(t)} = \\ OTR(t) &= OTR_{max} * [x_{OG}(t) * \frac{p_{Gcal} * x_{OGcal}}{p_G(t)} * \frac{p_{O_2}(t)}{100\%}] = \\ OUR(t) &= q_{O/X}(t) * c_{XL}(t) \end{aligned} \quad (42)$$

which is in accordance with the three phase model.

### 3.4 Kinetic reaction parameters

#### 3.4.1 Specific reaction rates

The specific reaction parameters are used to describe the metabolization of oxygen and substrate as well as the growth of the cells. The yield coefficients are the ratio of the formed biomass to the used substrate/ oxygen.

They are calculated by first setting up the equations for the change in the concentration of either substrate or the cell concentration over time with

$$\frac{dc_{XL}}{dt} = \frac{c_{XL}(t_{i+1}) - c_{XL}(t_{i-1})}{t_{i+1} - t_{i-1}} \quad (43)$$

for the change in the cell concentration and

$$\frac{dc_{SL}}{dt} = \frac{c_{SL}(t_{i+1}) - c_{SL}(t_{i-1})}{t_{i+1} - t_{i-1}} \quad (44)$$

for the change in the substrate concentration.

After this, the reaction rates at the time points can be calculated by setting up the concentration balances and rearranging them to the cell specific reaction rates.

The cell specific growth rate  $q_{X/X}$  is calculated by

$$q_{X/X}(t) = \frac{F_{in}(t_j)}{V_L(t_j)} + \frac{\dot{c}_{XL}(t_j)}{c_{XL}(t_j)} \quad (45)$$

The outgoing flows do not change the concentrations in the liquid and can therefore be ignored. They only have to be considered in the liquid volume of the reactor.

For the concentration balance of the substrate, the concentration and flow rate of the feed have to be considered, as well as the volume of the cell mass in the liquid. It is again rearranged to the cell specific substrate uptake rate  $q_{S/X}$ .

$$q_{S1/X}(t_i) = \frac{F_{R1}(t_i) * c_{S1R}}{V_L(t_i) * c_{XL}(t_i)} * \left[ \frac{F_{in}(t_i)}{V_L(t_i)} - \frac{\alpha_{Z/X} * q_{X/X}(t_i) * c_{XL}(t_i)}{\rho_Z} \right] * \frac{c_{S1L}(t_i)}{c_{XL}(t_i)} - \frac{\rho_Z - \alpha_{Z/X} * c_{XL}(t_i)}{\rho_Z} * \left[ \frac{\dot{c}_{S1L}(t_i)}{c_{XL}(t_i)} \right] \quad (46)$$

Finally, the cell specific oxygen uptake rate is calculated by using the offgas bal-

ance, dividing the  $Q_{O_2}$  calculated with equation 34 by the cell concentration.

$$q_{O/X}(t_j) = \frac{Q_{O_2}(t_j)}{c_{XL}(t_j)} \quad (47)$$

To calculate the medians for the two growth phases max and w, the constant phases have to be identified in the course of the cell specific reaction rates. The equations are then rearranged to an overdetermined system and the medians are calculated for the chosen ranges.

$$c_{XL}(t_i) * \bar{q}_{S1/X}(t_i) = \frac{F_{R1}(t_i) * c_{S1R}}{V_L(t_i)} * \left[ \frac{F_{in}(t_i)}{V_L(t_i)} - \frac{\alpha_{Z/X} * q_{X/X}(t_i) * c_{XL}(t_i)}{\rho_Z} \right] * c_{S1M}(t_i) - \frac{\rho_Z - \alpha_{Z/X} * c_{XL}(t_i)}{\rho_Z} * \frac{c_{S1M}(t_{i+1}) - c_{S1M}(t_{i-1})}{t_{i+1} - t_{i-1}} \quad (48)$$

$$a * \bar{q}_{I/Xk} = b \quad (49)$$

For the calculation of the median ranges, the backslash operator of Matlab® is used.

$$\bar{q}_{I/Xk} = b \setminus a \quad (50)$$

The yield coefficients are calculated by dividing the reaction rates, as

$$q_{X/X}(t) = q_{S1/X}(t) * y_{X/S1}(t) = q_{O/X}(t) * y_{X/O}(t) \quad (51)$$

can be rearranged to

$$y_{X/Ik}(t) = \frac{q_{X/Xk}(t)}{q_{I/Xk}(t)} \quad (52)$$

In figure 6 the characteristics of theyield coefficients can be observed. In the maximal growth phase, the yield coefficients are at their maximal value  $y_{X/I\max}$  and in the controlled growth phase the values are lower with  $y_{X/Iw}$ , depending on  $q_{X/Xw}$ .

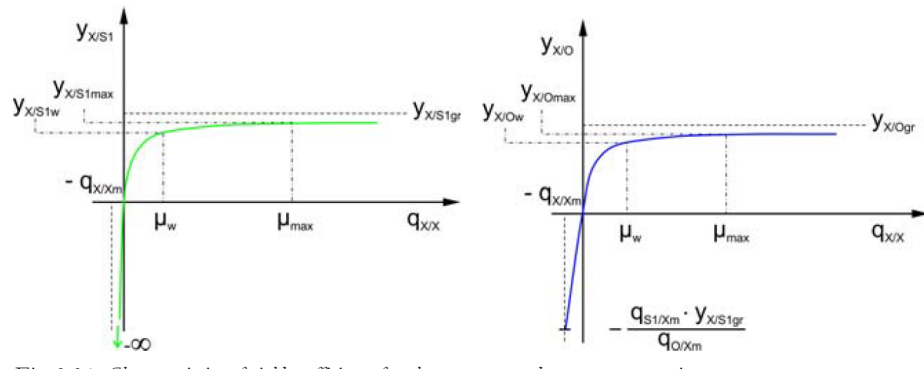


**Fig. 6:** Characteristics of the yield coefficients of glycerol and oxygen against the growth rate  $q_{X/X}$

### 3.4.2 Global reaction parameters

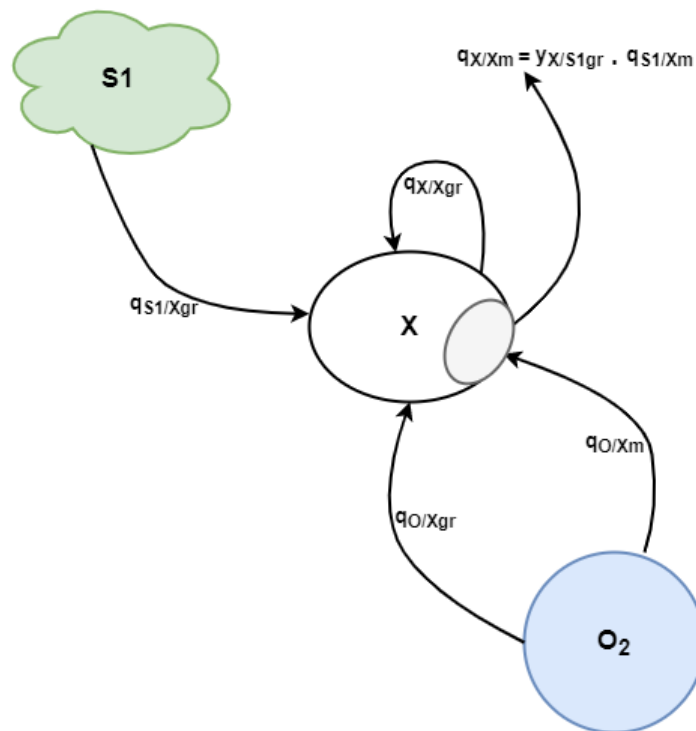


**Fig. 7:** Macroscopic representation of the global reaction parameters in relation to the cell. After: Cornelissen 2004

As shown in equation 6, the cells are in steady state equilibrium dependent on substrate and oxygen with the time variant yield coefficients.

The growth rate of the cell  $q_{X/X}$  is made up of the growth rate  $q_{X/Xgr}$  and the artificial maintenance part  $q_{X/Xm}$ , which can also be considered as the mortality rate of the



cells.

$$q_{X/Xm} = q_{X/Xgr} - q_{X/Xm} \quad (53)$$

This can be derived from the steady state equilibrium of  $q_{X/Xgr}$

$$q_{X/Xgr} = y_{X/S1gr} * q_{S1/X}(t) = y_{X/Ogr} * q_{O/X}(t) \quad (54)$$

with the time invariant yield coefficients  $y_{X/S1gr}$  and  $y_{X/Ogr}$ . Therefore the time invariant maintenance metabolism of the cells is made up of

$$q_{X/Xm} = y_{X/S1gr} * q_{S1/Xm} \quad (55)$$

To avoid a zeroth order reaction, where the reaction rate is independent of the concentration of the substrate, the substrate uptake  $q_{X/S1}$  is equal to the growth part of the substrate reaction rate

$$q_{S1/X}(t) = q_{S1/Xgr}(t) \quad (56)$$

while the cell specific oxygen uptake rate is made up of the maintenance and the growth part.

$$q_{O/X}(t) = q_{O/Xgr}(t) + q_{O/Xm} \quad (57)$$

The growth dependent yield coefficient  $y_{X/S1}$  and  $y_{X/O}$  are calculated by

$$y_{X/S1}(t) = \frac{q_{X/X}(t)}{q_{X/X}(t) + y_{X/S1gr} * q_{S1/Xm}} * y_{X/S1gr} \quad (58)$$

and

$$y_{X/O}(t) = \frac{q_{X/X}(t)}{q_{X/X}(t) + y_{X/S1gr} * q_{S1/Xm} + y_{O/S1gr} * q_{O/Xm}} * y_{X/Ogr} \quad (59)$$

The yield coefficients  $y_{X/S1gr}$  and  $y_{X/Ogr}$  are time independent global metabolism parameters, that describe the substrate and oxygen metabolism together with the maintenance reaction parameters  $q_{S1/Xm}$  and  $q_{O/Xm}$ . After calculation of the reaction parameters of the maximal growth phase and the controlled growth phase, they can be calculated by the following formulas and used for an exact control of the growth rate.

$$q_{S1/Xm} = \frac{(y_{X/S1max} - y_{X/S1w}) * q_{X/Xmax} * q_{X/Xw}}{(q_{X/Xmax} - q_{X/Xw}) * y_{X/S1max} * y_{X/S1w}} \quad (60)$$

$$y_{X/S1gr} = \frac{y_{X/S1w} * q_{X/Xw}}{q_{X/Xw} - y_{X/S1w} * q_{S1/Xm}} \quad (61)$$

$$q_{O/Xm} = \frac{(y_{X/Omax} - y_{X/Ow}) * q_{X/Xmax} * q_{X/Xw} + (y_{X/Omax} * q_{X/Xw} - y_{X/Ow} * q_{X/Xmax}) * y_{X/S1gr} * q_{S1/Xm}}{(y_{X/Omax} * y_{X/Ow}) * (q_{X/Xmax} - q_{X/Xw})} \quad (62)$$

$$y_{X/Ogr} = \frac{(q_{X/Xw} + y_{X/S1gr} * q_{S1/Xm}) * y_{X/Ow}}{q_{X/Xw} - y_{X/Ow} * q_{O/Xm}} \quad (63)$$

### 3.5 Matlab 2020a®

Matlab® is a programming language and computing environment by MathWorks®, used for matrix manipulation and calculations. The name is derived from the abbreviation of MATrix LABoratories, as the software's main uses are the analysis of measurements or simulation of processes, which are stored in matrices, as they produce a large amount of data.

Matlab® can be used for a wide range of applications, from simple calculations to complex models. The programming language is part of the fourth-generation programming languages, aiming to be more programmer-friendly and easily accessible and mainly employed in the STEM-field.

Matlab® is an array programming language, which easily loads data into data types in less line of code than traditional languages. For creating matrices and variables, data can either be loaded from external files through different functions saving into different data types, or created in the code.

#### Data types

There are many different data types that can be used in Matlab® for data storage. Numeric data is saved as a double precision floating point by default. Numeric data can be saved in arrays and vectors, which can be addressed by row- and column number, or by position.

Character data is stored in character arrays or strings, which are used to save text.

Data can also be organized in a table, where each column gets a name by which it can be addressed. Each column can contain a different data type.

The last important organizational structure is the cell array, which contains different fields, that can contain different data types.

Data types can be transformed into each other with Matlab® functions. Numeric data can be transformed into strings, a numeric array can be transformed into a table array by using the function *array2table*, adding headers to the data and vice versa by using *table2array*, removing the headers.

#### Internal functions

Matlab® possesses many different functions for the data upload, data transformation, calculations and pre processing. The data transformation functions are an example of an internal function. Matlab® contains many functions for calculations and many possibilities for visualizing the results in plots, which can be saved in different formats.

Some functions, which are used in this thesis are explained below. One of the functions used is the backslash operator  $\backslash$ , which solves the linear equation system.

$$A * x = B \quad (64)$$

for  $x$ . It returns the least squares solution to the system of equations.

The `smoothdata` function is another internal function of Matlab®, which smoothes a vector along a fixed window using a moving average.

### External functions

Matlab® has the option to program function files, which can be called and used in many different programs.

A function has to start with the word *'function'*, otherwise it will be saved as a normal Matlab® script. The output vector, or vectors, follow. After that, the function name is declared, with the input variables in parenthesis.

Now the body of the function can be programmed, using the input variables. The function is finished by *'end'*.

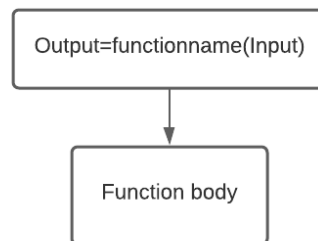


**Fig. 8:** Structure of an external function

### 3.5.1 Curve Fitting Toolbox

The curve fitting toolbox is a Matlab® app that can be used to fit a function to data. The data can be loaded into the Matlab® workspace in any way, and used in the toolbox.

In the toolbox, the  $x$ - and  $y$ -data has to be specified, as well as the equation type. A custom equation can also be used for a fit.

After the data and the equation have been specified, Matlab® will fit a function to the data and give the resulting parameters, as well as a summary of the goodness of fit.

### Evaluation of the Goodness of Fit

After fitting a curve, the fit has to be evaluated. The summary of fit gives sum of squared due to error (SSE),  $R^2$ ,  $R^2$  adjusted to the degrees of freedom and the root mean squared error (RMSE).

The SSE measures the sum of the deviation of the fit values to the data and is calculated by

$$SSE = \sum_{i=1}^n w_i (y_i - \hat{y}_i)^2 \quad (65)$$

The lower the SSE, the better the fit of the data, as the random error component of the fit is lower.

The  $R^2$  measures the goodness of the fit concerning the variation of the data. It is calculated by

$$R^2 = \frac{SSR}{SST} \quad (66)$$

with

$$SSR = \sum_{i=1}^n w_i (\hat{y}_i - \bar{y})^2 \quad (67)$$

and

$$SST = \sum_{i=1}^n w_i (y_i - \bar{y})^2 \quad (68)$$

The closer the  $R^2$  is to 1, the higher proportion of variance is explained by the model. A higher number of data points leads to a higher  $R^2$ , but not necessarily to a better fit. Therefore the degrees of freedom adjusted  $R^2$  is employed. The degrees of freedom are defined by

$$v = n - m \quad (69)$$

with  $n$  being the number of response values and  $m$  being the number of fitted coefficients. The adjusted  $R^2$  is calculated by

$$adjustedR^2 = 1 - \frac{SSE(n-1)}{SST(v)} \quad (70)$$

Just as with the  $R^2$ , the closer the value to 1, the better.

The last evaluation tool is RMSE, which estimates the standard deviation of the random error of the data

$$RMSE = s = \sqrt{MSE} \quad (71)$$

with

$$MSE = \frac{SSE}{v} \quad (72)$$

A value closer to 0 indicates a better fit.

### 3.5.2 Matlab App Designer®

Matlab App Designer® is a development environment for creation of standalone apps using Matlab® code. Through the use of different components and callback functions, a GUI for different uses can be created.

The aim of the GUI is the creation of an interactive platform for the user with the program, reducing the need of a deeper understanding of the programming language. The user can use the functions of the programming language without having to understand them.

The App Designer contains two main views, the *Design View* in which different components, such as buttons and tables, can be added to the app and the *Code View* where the callback functions are edited. When an object is added to the app layout, the code for the layout is automatically added in the *Code View*.

The interaction with the different objects has to be done through callback functions, that are triggered when the user interacts with one of the objects. The callback function contains the code for the interaction. Different components of the App Designer have different callback functions. For example, *Button* objects have a *ButtonPushed* Callback that is triggered everytime the button is pushed, while the *TableCellEdit* Callback triggers when a cell in a table is edited. Some objects have no callback functions, for example the *Axes* object.

**Table 1:** Components and callbacks of the app designer

<b>Component</b>	<b>Callback</b>
Table	TableCellEdit Callback
Axes	-
Button	ButtonPushedCallback
DropDownMenu	DropDownValueChanged Callback
Edit Field	-
Label	-

After creating the *ButtonPushed* Callback for the button, code can be added to the callback in the code view. For example, pressing a button could save a variable or start a calculation.

### 3.5.3 Matlab Report Generator®

The Matlab Report Generator® can be used to automatically create reports containing Matlab® data and figures. A report includes Document Object Model (DOM) objects, such as paragraphs, tables and images, which make up the report. The DOM objects can be organized in the report in any order, creating a customizable report that is automatically created when the reporter is compiled. The Report Generator can be used with template files using Microsoft Word and Microsoft PowerPoint, where the template is created first, and empty spaces can be filled with the report generator. Furthermore pdf and html files can be created.

## 4 Material

### 4.1 Organism

The specific strain used in this thesis is *Pichia pastoris* LM1, which is genetically modified BSYBG11 to produce and secrete a fusion protein when induced by methanol. As a Mut<sup>s</sup> strain, the AOX1 gene was removed, therefore growth on methanol is slow (Krainer et al. 2012). The AOX1 promoter was used for the induction of the production of the fusion protein 8His\_eGFP\_TEV(G)\_NK2\_ALG, which is secreted extracellularly (see Appendix).

The cells were stored in a Working Cell Bank (WCB) in glycerol at  $-80^{\circ}\text{C}$  in cryo micro vials with screw caps.

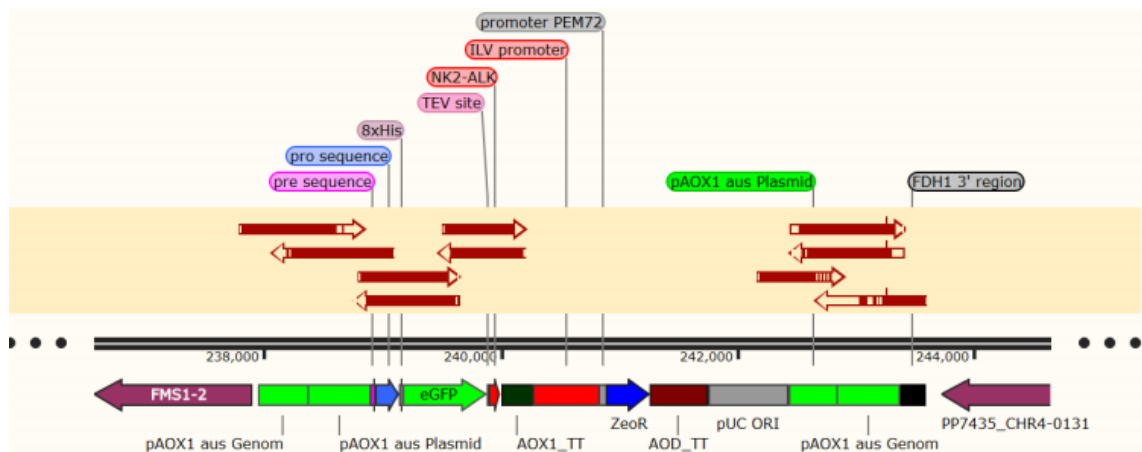


**Fig. 9:** Genome section of *Pichia pastoris* LM1 from the protocol of the organism (see Appendix)



## 4.2 Chemicals

**Table 2:** List of chemicals used during this thesis

product	manufacturer	article no.	chemical formula
Glycerol 99.5 %	Carl Roth GmbH + Co. KG	3785.3	$C_3H_8O_3$
Ortho-phosphoric acid 85 %	Carl Roth GmbH + Co. KG	6366.1	$H_3PO_4$
Ammonia 25 %	Carl Roth GmbH + Co. KG	5460.2	$NH_3 + H_2O$
Potassium hydrogenphosphate	Carl Roth GmbH + Co. KG	3904.3	$KH_2PO_4$
Ammonium sulfate	Carl Roth GmbH + Co. KG	3746.	$H_4N_2O_4S_4$
Potassium sulfate	Carl Roth GmbH + Co. KG	P022.3	$K_2SO_4$
Calcium sulfate- dihydrate	Carl Roth GmbH + Co. KG	P741.2/ 0256.1	$CaSO_4 + 2 H_2O$
Magnesium sulfate- heptahydrate	Carl Roth GmbH + Co. KG	T888.3	$MgSO_4 + 7 H_2O$
Sodium hydrogen phosphate- dihydrate	Carl Roth GmbH + Co. KG	T879.3	$Na_2HPO_4 + 2 H_2O$
Copper sulfate	Carl Roth GmbH + Co. KG	CP86.2	$CuSO_4$
Sodium iodide	Carl Roth GmbH + Co. KG	8783.1	NaI
Manganese (III) sulfate monohydrate	Carl Roth GmbH + Co. KG	X890.1	$MnSO_4 + H_2O$
Sodium molybdate- dihydrate	Carl Roth GmbH + Co. KG	0845.1	$Na_2MoO_4 + 2 H_2O$
Boric acid	Carl Roth GmbH + Co. KG	6943.2	$H_3BO_3$
Cobalt(III) chloride- hexahydrate	Carl Roth GmbH + Co. KG	7095.1	$CoCl_2 + 6 H_2O$
Zinc sulfate- heptahydrate	Carl Roth GmbH + Co. KG	T884.1	$ZnSO_4 + 7 H_2O$
Iron(II) sulfate- heptahydrate	Carl Roth GmbH + Co. KG	P015.1	$FeSO_4 + 7 H_2O$

### 4.3 Media composition

**Table 3:** FM22 media composition for shaking flask pre cultures

<b>Chemical</b>	<b>Concentration</b>
Glycerol	10 g/L
KH <sub>3</sub> PO <sub>4</sub>	6.43 g/L
H <sub>8</sub> N <sub>2</sub> O <sub>4</sub> S <sub>4</sub>	1.25 g/L
K <sub>2</sub> SO <sub>4</sub>	2.15 g/L
CaSO <sub>4</sub> + 2 H <sub>2</sub> O	0.35 g/L
CaSO <sub>4</sub> + 2 H <sub>2</sub> O	4.1 g/L
NaH <sub>2</sub> PO <sub>4</sub> + 2 H <sub>2</sub> O	1.47 g/L
Biotin Stock	8 mL/L
PTM4 Stock	4 mL/L

**Table 4:** FM22 media composition for batch medium

<b>Chemical</b>	<b>Concentration</b>
Glycerol	25 g/L
KH <sub>3</sub> PO <sub>4</sub>	6.43 g/L
H <sub>8</sub> N <sub>2</sub> O <sub>4</sub> S <sub>4</sub>	1.25 g/L
K <sub>2</sub> SO <sub>4</sub>	2.15 g/L
CaSO <sub>4</sub> + 2 H <sub>2</sub> O	0.35 g/L
CaSO <sub>4</sub> + 2 H <sub>2</sub> O	4.1 g/L
NaH <sub>2</sub> PO <sub>4</sub> + 2 H <sub>2</sub> O	1.47 g/L
Biotin Stock	8 mL/L
PTM4 Stock	4 mL/L

**Table 5:** Media composition for the feeding solution

<b>Chemical</b>	<b>Concentration</b>
Glycerol	200 g/L
Biotin Stock	8 mL/L
PTM4 Stock	4 mL/L

**Table 6:** composition of PTM4 stock solution

<b>Chemical</b>	<b>Concentration</b>
$\text{CuSO}_4 + 5 \text{H}_2\text{O}$	2 g/L
NaI	0.8 g/L
$\text{MnSO}_4 + \text{H}_2\text{O}_4$	3 g/L
$\text{Na}_2\text{MoO}_4 + 2 \text{H}_2\text{O}$	0.2 g/L
$\text{H}_3\text{BO}_3$	0.2 g/L
$\text{CaSO}_4 + 2 \text{H}_2\text{O}$	0.5 g/L
$\text{CoCl}_2 + 6 \text{H}_2\text{O}$	0.5 g/L
$\text{ZnSO}_4 + 7 \text{H}_2\text{O}$	7 g/L
$\text{FeSO}_4 + 7 \text{H}_2\text{O}$	22 g/L
$\text{H}_2\text{SO}_4$	1 mL/L

**Table 7:** composition of Biotin stock solution

<b>Chemical</b>	<b>Concentration</b>
$\text{C}_{10}\text{H}_{16}\text{N}_2\text{O}_3\text{S}$ (Biotin)	0.2 g/L

## 4.4 Reactor and measuring system

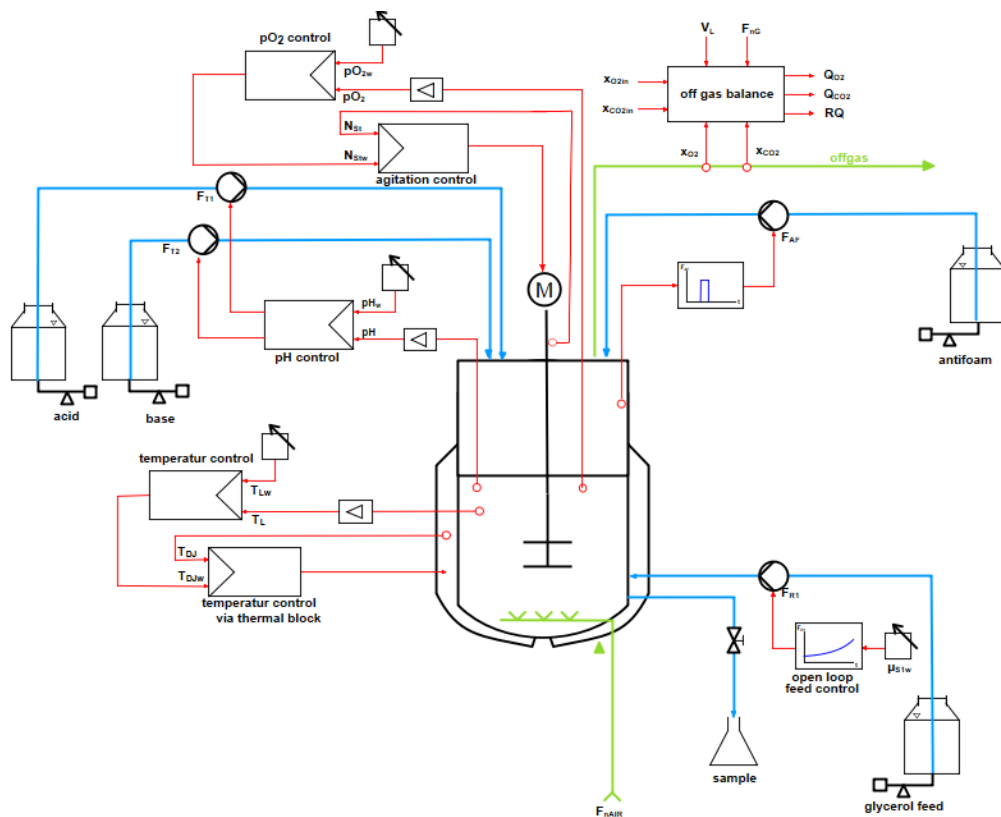


**Fig. 10:** Setup of the Infors reactor and its control structures

The Minifors (Infors, Bottmingen, Switzerland) reactor with a 3 L total volume set up is shown in figure 10. It was used with a pH-controller, which controlled the feed rates of acid and base and an open loop feed control, controlling the glycerol feed rate. The foam production was suppressed by anti foam using an anti foam sensor. A  $pO_2$  sensor was used for a  $pO_2$ -agitation control, controlling the stirrer speed. A thermal block was used for the temperature control.

The aeration was done with air and the offgas data was measured with the Blue-Vary (BlueSens, Herten, Germany) offgas sensors. A mechanism for samples was also added to the reactor. In figure 11 the setup can be seen.

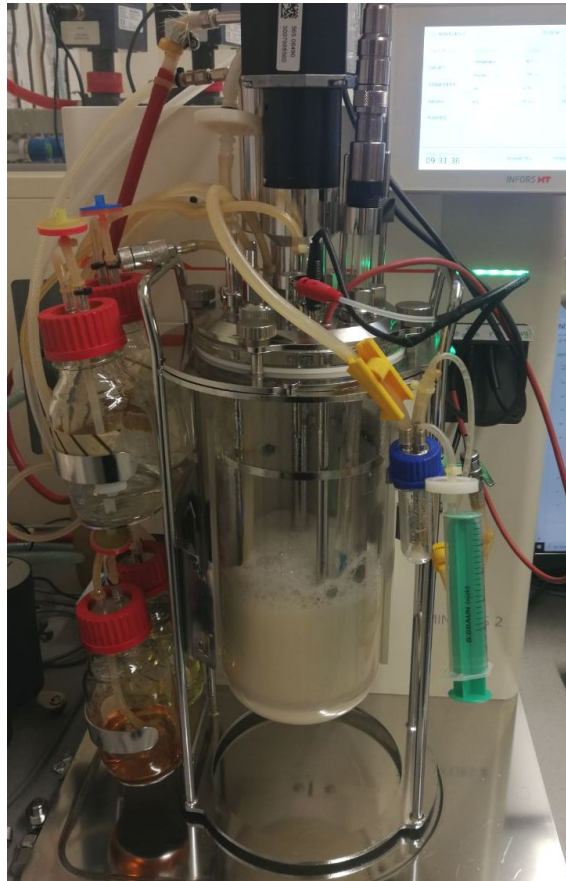


**Fig. 11:** The Infors reactor during fermentation

**Table 8:** Overview of the measurement system used for the Minifors 2 bioreactor

parameter	probe name	measurement range	manufacturer
Temperature - $\vartheta_L$			Infors, Bottmingen, Switzerland
pH - pH	EasyFerm Plus Arc 325	0-14	HAMILTON Company, Reno, USA
partial oxygen pressure - $p_{O_2}$	VisiFerm DO Arc 325	4 ppm to 2 ppm	HAMILTON Company, Reno, USA
oxygen mole fraction - $x_{O_2}$	BCP-O2	1-50 %	BlueSens gas sensor GmbH, Herten, Deutschland
carbon dioxide mole fraction - $x_{CO_2}$	BCP-O2	0-25 %	BlueSens gas sensor GmbH, Herten, Deutschland

### 4.4.1 pH electrode

The pH-electrode is a HAMILTON EasyFerm Plus Arc 325 combination electrode, which combines measurement and reference electrode in one single rod. The measurement electrode contains a conductive glass membrane, which forms a gel layer from the solution inside and outside. This gel layer is permeable for hydrogen ions. The solution inside the electrode has a pH of 7.

The hydrogen concentration difference in the measured medium to the solution in the electrode leads to a potential difference over the glass membrane, leading to a voltage, which can be used to calculate the concentration of the hydrogen ion concentration by using the NERNST-equation.

$$E = \frac{R \cdot T}{n \cdot F} * \log \frac{C_1}{C_2} \quad (73)$$

with

- E = potential difference [mV]
- R = gas constant (8.314 39 J K/mol)
- F = Faraday constant 96 495.7 C/mol
- T = Temperature [K]
- n = charge number of the measured ion
- C<sub>1</sub> = active hydrogen ion concentration in solution 1
- C<sub>2</sub> = active hydrogen ion concentration in solution 2

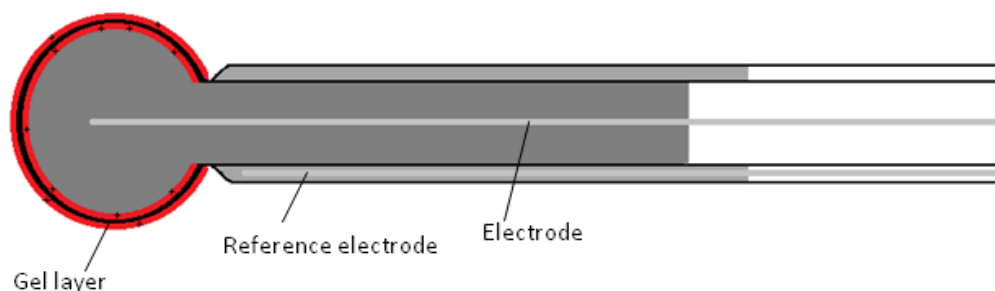


**Fig. 12:** Schematic presentation of a pH-electrode

### Calibration

On paper the voltage for each pH is always the same, with a 58.13 mV difference between each pH value and a voltage of 0 mV at pH 7. But since aging of the

electrode leads to a change in these values, a calibration has to be performed at 2 points of the pH-range to find the correct slope and x-intercept.

Therefore 2 measurements are performed at pH 4 and 7, which are used to find the new slope and x-intercept. Those values are used for all subsequent measurements.

#### 4.4.2 pO<sub>2</sub> electrode

The pO<sub>2</sub> electrode utilises an optical measurement. It excites a luminophore in the electrode membrane with a blue light. When returning to its ground state the luminophore gives off a red light. Oxygen will absorb some of this red light, if present. The electrode can then compare the intensity of the excited and emitted light and determine the amount of dissolved oxygen by the difference in intensity. The function of the measurement can be seen in figure 13

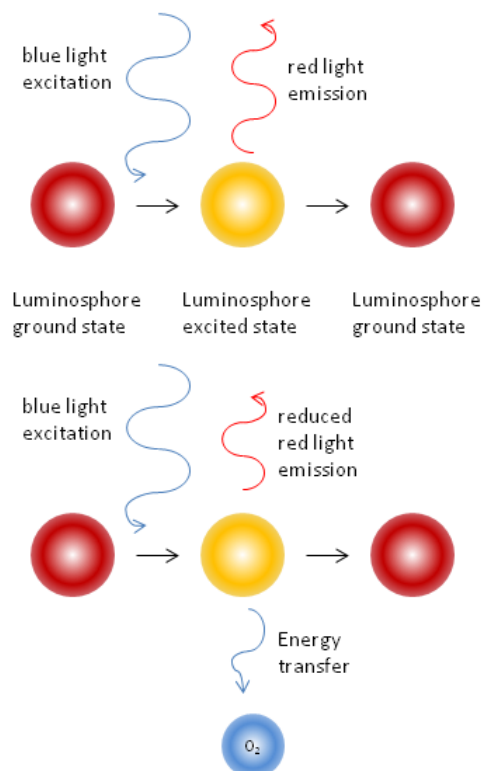


**Fig. 13:** Schematic presentation of the function of the pO<sub>2</sub>-electrode. After: Hamilton Company

**Calibration**

The pO<sub>2</sub>-electrode is calibrated before each use. After heating the reactor to the fermentation temperature, the aeration is switched to nitrogen, dissipating all oxygen in the liquid, establishing the zero value. Afterwards the aeration is set to air, and the slope is calibrated with the 100 % measurement.

**4.4.3 Anti foam sensor**

Foam can hinder the exchange of gas between the liquid and gas phase and therefore needs to be regulated through the addition of anti foam to the medium. For the detection of foam, the lid of the reactor is fitted with an anti foam sensor that activates the anti foam-pump when the foam reaches it and anti foam is dispensed through its integrated dispensing nozzle.



#### 4.4.4 Offgas measurement

The combination sensor BlueVary (BlueSens, Herten, Germany) was used for the offgas measurement, with a O<sub>2</sub> and CO<sub>2</sub>-cartridge.

##### Oxygen measurement

For the offgas measurements an off gas sensor based on the galvanic element using a zirconium dioxide (ZrO<sub>2</sub>) element is used. The element does not need a reference gas for the measurement.

When a voltage is supplied to the cell, oxygen ions wander from the cathode to the anode. When a gas diffusion barrier is formed at the cathode, a saturation current is formed. This current is the measurement for the oxygen concentration in the atmosphere surrounding the probe.

##### Carbon dioxide measurement

The carbon dioxide measurement is based on the reflection of infrared light. The infrared light is reflected inside the measuring cell. The surrounding carbon dioxide weakens the intensity of the light. The difference in intensity can be measured.

##### Calibration

A one-point calibration with air has to be performed before the sensor can be used. The sensor is flushed with air for at least 30 min and the calibration is performed in both cartridges. The calibration is needed to increase the accuracy of the measurements during fermentation.

## 4.5 Eve

Eve® by Infors is the software used to plan and automate the fermentation. The fermentation strategy as well as fermentation parameters are added to the software.

The strategy can be planned and saved in so called *recipes*, which can be reused. The fermentation is divided into different phases, where conditions have to be met for the beginning of the next phase.

The control parameters for all control tasks are also saved within eve®. For the open loop feed control, a custom function was used. The parameters can be changed within the function and eve® then controls the feed rate.

Eve® is also used for the online data display during fermentation and the data download after fermentation.

## 5 Methods

### 5.1 Preliminary Experiments

#### 5.1.1 Shaker flask cultivation

Prior to the main cultivations, a preculture in a shaker flask was done to gain information about the time frame for the inoculation of the bioreactor.

99 mL of FM22 medium (table 3) is prepared and autoclaved in a 1 L shaker flask with chicanes and complemented with sterile filtrated stock solutions PTM4 and Biotin after sterilisation (see table 3). It is inoculated with 300  $\mu$ L of the WCB and an initial sample  $t_0$  is taken. The optical density of the sample is measured with the Optical Density (OD)<sub>600</sub> method.

The shaking flask is placed into the shaker at 30 °C at 150 rpm.

After 18 hours, samples are taken hourly. This is done by placing the flask under the sterile laminar flow cabinet and pipetting 2x 1 mL into 1 mL micro vial plastic tubes, for the OD<sub>600</sub> measurement.

#### 5.1.2 Flow rates of the pumps

For the calibration of the feed rates  $F_{Rmax}$  has to be experimentally determined. The feed rate is set to 100 % and the pumped volume is weighed after 5 min. This is done three times and the mean was determined. The calculated flow rate in mL/min is used as  $F_{Rmax}$  in the system.

Since the feed rates are used for the concentration balances and are therefore crucial for the calculations, the deviation between the flow rate calculated by the system versus the actual flow rate is checked.

The pump rate is set to different rates and the pumped liquid is weighed. The volume calculated by the reactor is also noted to calculate the deviation between the actual and measured volume of the pump. Each setpoint is checked in triplicates. The setpoints are 1 %, 1 %, 2 %, 5 %, 10 %, 25 %, 50 % and 100 %.

## 5.2 Preculture

For the preculture 99 mL are mixed with 1 mL of sterile filtrated stock solutions in a 1 L shaking flask with chicanes and inoculated with 500  $\mu$ L of the WCB. The media composition is shown in table 3. Two precultures are prepared for every fermentation and incubated for 24 h at 30 °C at 150 rpm, which achieved an OD<sub>600</sub> of around 8, corresponding to a cell concentration of 4.8 g/L.

## 5.3 Preparation of the reactor

After filling the reactor with 800 mL of FM22 medium without stock solution, all the instrumentation is added to the lid and the lid is placed on the reactor.

The pH-electrode is calibrated with buffers with pH 4 and 7 before it is added to the reactor lid. The reservoir bottles are prepared with antifoam, 20 % phosphoric acid and feed solution (table 5) without stock solution. The ammonia bottle is left empty at this stage, as it is volatile and will evaporate during sterilization, which would lead to harmful vapors.

The reactor is placed in the autoclave for sterilisation. All tubes have to be clamped, to prevent the reservoir bottles from emptying into the reactor. The filters and the stirrer motor have to be covered with aluminium foil. The connectors for the pH and pO<sub>2</sub> electrode are not covered in aluminium foil, as the connectors would get damaged. Instead, a glass vial is placed over the connector and the gap is covered in aluminium foil to keep the connectors dry. The reactor is then autoclaved on the fluids program at 121 °C for 20 min.

After sterilizing, the feed bottle is completed with sterile filtrated stock solution to a concentration of 8 mL/L for the biotin stock solution and 4 mL/L for the PTM4-solution (table 5) under the clean bench. The ammonia bottle is also added in the sterile environment.

All cables are connected to the lid of the reactor and the cultivation is started with the software. Stock solution is added to the reactor medium with a sterile inoculation bottle through the connectors. The pO<sub>2</sub>-electrode can be calibrated, after the reactor has reached the cultivation temperature. A two-point calibration is performed. The aeration is switched to 100 % nitrogen to set the 0 % value. Aeration is switched to 21 % oxygen and the process is repeated for the 100 % pO<sub>2</sub> value. After the calibration is finished, the reactor is ready for fermentation.

## 5.4 Inoculation

A medium sample is taken before inoculation of the reactor for a starting measurement of the glycerol concentration in the medium.

When the preculture has reached an OD of around 8 after 24 h the reactor is inoculated with the cells. The 200 mL of cell culture from the two flasks, which corresponds to 20% of the fermentation volume are transferred into a sterile inoculation bottle under the clean bench after clamping the tube of the bottle. The inoculation bottle is connected to the reactor through a connector in the lid.

The aeration is stopped, so there is no counter pressure hindering the medium from flowing into the reactor. The clamp is removed from the inoculation bottle, allowing the cell broth to flow into the reactor. After the bottle is emptied and the connectors are disconnected, the aeration is restarted. A sample is taken immediately after inoculation.

## 5.5 Sample

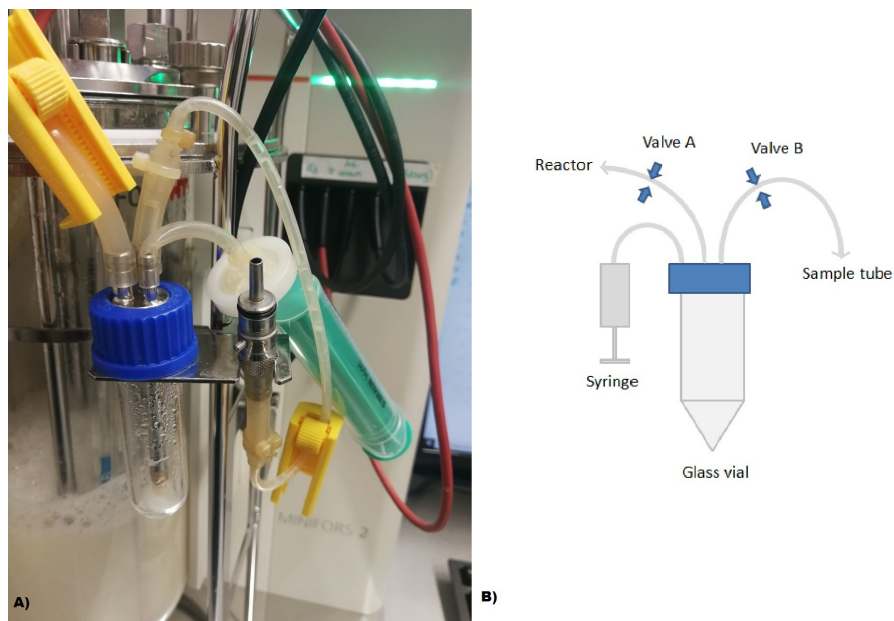


**Fig. 14:** A) Sample mechanism of the Infors reactor with the glass vial, the syringe, the filter and the clamps on the tubes, B) Schematic presentation of the sample mechanism

During cultivation, samples are taking hourly. The sampling mechanism can be seen in figure 14, containing two valves, a glass tube and a filter. It is connected to the culture broth through an immersion tube in the reactor. It is vital to be very

careful during the sampling procedure, to prevent any contamination of the reactor content.

At the beginning of the sampling procedure valve B is closed and valve A is opened, closing the tube to the outside and opening the connection from the reactor to the glass vial. A vacuum is created inside the glass vial with a syringe attached to the filter, aspirating culture broth through the immersion tube into it. Valve A is then closed, which closes the connection to the reactor and valve B is opened to open the way into the sample tube. The syringe is used to push the medium into the sample tube through the now open tube.

The tubes have to be flushed once and the sample has to be discarded, as culture broth left in the tube from the last sample will influence the sample composition. After flushing the tubes, the process is repeated as described above and the sample is saved. The sample volume was noted for the volume balance of the reactor, as well as the volume of the discarded 'flushed' sample.

The OD is measured via photometer and two 1 mL samples are centrifuged for the CDW measurement described in chapter 5.6.

## 5.6 Offline measurement techniques

Two different methods were used to measure the growth of the cells. The concentration of the substrate in the medium was also determined. The division of the sample is shown in figure 15.

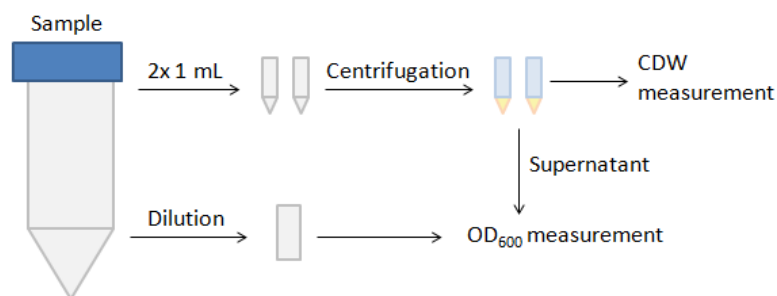


**Fig. 15:** Sample division for the offline measurements

### 5.6.1 OD<sub>600</sub> measurement

The OD measurement is based on the turbidity of the sample, measuring mainly the light scattering of particles in the sample, causing less light to reach the detector. The difference in light intensity between source and detector is measured. The measurement was done at 600 nm wavelength in a single use plastic cuvette. The result of the measurement has to be between 0 and 0.5 AU to ensure a linear correlation of cell concentration and measurement. Therefore, the sample is diluted with deionized water if the result is outside of these boundaries.

The samples are centrifuged at 1300 rpm for 10 min. The supernatant is transferred into a plastic cuvette and the OD<sub>600</sub> is determined. This ensures that no particles in the medium effect the result. The resulting measurement is subtracted from the OD<sub>600</sub> of the sample.

The OD<sub>600</sub> has to be converted into the cell concentration. For this the factor  $K_{XOD}$  is calculated, by using the CDW measurements taken at the same time points during the fermentation. The determination of the  $K_{XOD}$  is described in chapter 7.3.

$$OD_{600} = OD_{600Sample} - OD_{600Supernatant} \quad (74)$$

### 5.6.2 Cell Dry Weight

For the CDW measurement, micro vial tubes are prepared by drying and weighing before the samples were taken. They are dried at 80 °C for at least 24 h and weighed with an analytical scale.

The prepared vials are filled with 1 mL of cell broth and centrifuged at 1300 rpm for 10 min. The supernatant is pipetted into another vial for use in the substrate measurement or used for an OD<sub>600</sub> measurement.

After drying the pellet at 80 °C for at least 24 h, the vial is again weighed. The CDW was calculated by

$$c_{XLCDW} = \frac{m_{filledvial} - m_{emptyvial}}{V_{sample}} \quad (75)$$

### 5.6.3 Glycerol measurement

For the measurement of the glycerol concentration in the supernatant, a cation exchange chromatography is performed. Depending on the charge of the molecule, the retention time in the column is longer due to their interaction with the resin. For the separation of the glycerol from the rest of the sample, a Alltech IOA-1000 (Hichrom, Theale, UK) column is used. The separation is done at 60 °C with a volume flow of 0.1 mL/min with the High Performance Liquid Chromatography (HPLC) LaChrom system (Merck, Darmstadt, Germany).

**Table 9:** HPLC LaChrom system (Merck, Darmstadt, Germany) used for the glycerol measurement

Name	Number
Autosampler	L-7250
Diode Array Detector	L-7455
Interface	D-7000
RI-Detector	L-7490
Column Oven	L-7360
Pump	L-7100

To remove particulates from the flow, a carbo-H pre column (Phenomenex, Torrance, United States) is used in order to prevent pressure from building up during the measurement.

The eluent used for this measurement is 5 mM sulfuric acid, which is filtrated with a 45 µm pore filter and degassed with a vacuum pump. The column is pre-heated to 60 °C and equilibrated with 5 mM sulfuric acid before the measurement is started.

A standard dilution range, shown in table 10, is prepared for the calibration of the measurement. The standards are prepared in the same way as the samples.

The samples for the measurement have to be prepared to make sure that they are particle free and in the right buffer, as supernatants from the fermentation are used. These could contain impurities, which could block the column.

The samples are first taken out of the freezer and defrosted. Then 10 µL of 5 M H<sub>2</sub>SO<sub>4</sub> are added to 1 mL of sample to reach a concentration of 5 mM in the sample, which matched the concentration of the eluent. The sample is then centrifuged at 1200 rpm for 10 min to remove precipitated particles and the supernatant is filtrated through a 0.2 µm pore filter with a syringe.

The samples are transferred to HPLC-glass vials with a volume of 300 µL and the

vials are closed with a septum.

After the measurement, the column is stored in the elution buffer.

**Table 10:** Dilution range for the calibration of the glycerol measurement

	<b>S1</b>	<b>S2</b>	<b>S3</b>	<b>S4</b>	<b>S5</b>	<b>S6</b>	<b>S7</b>	<b>S8</b>	<b>S9</b>	<b>S10</b>
$c_{\text{Gly}}$ [g/L]	0.25	3	5.75	8.5	11.25	14	16.75	19.5	22.25	25



## 6 Development of the Application

In this chapter, the process of developing the application for the calculation of the global reaction parameters using data from fermentations is explained. In order to calculate the parameters, data from the fermentation has to be uploaded into the app. This data is then used to calculate the reaction rates.

### 6.1 Layout of the Application

The basic structure of the app consists of three tabs.

The first tab, called the *data tab*, contains all structures necessary for uploading all relevant data for the calculation into the app. It can be seen in figure 16. The two buttons at the top are used for uploading the online data from the fermentation. As the data structure is different between the two systems used in the lab, two different buttons had to be created. The data upload is executed through the *ButtonPushed* Callbacks, which read the data from files.

The data is displayed in a *Table* object, called the *TableOnlineData*. For the offline data, there is a table called *TableOfflineData* and another button for the data upload. Through this button an especially created text-file can be uploaded into the app with another *ButtonPushed* Callback function.

The last table is the *TableFeedData*, which is used for all further parameters needed for the calculation, which are parameters concerning the cell line and the reservoirs. The data from this table is saved through the *CellEdit* Callback.

The last component on tab 1 is the *CalculateButton*. After pushing this button, the calculation of the time specific reaction parameters is done, through another *ButtonPushed* Callback function.

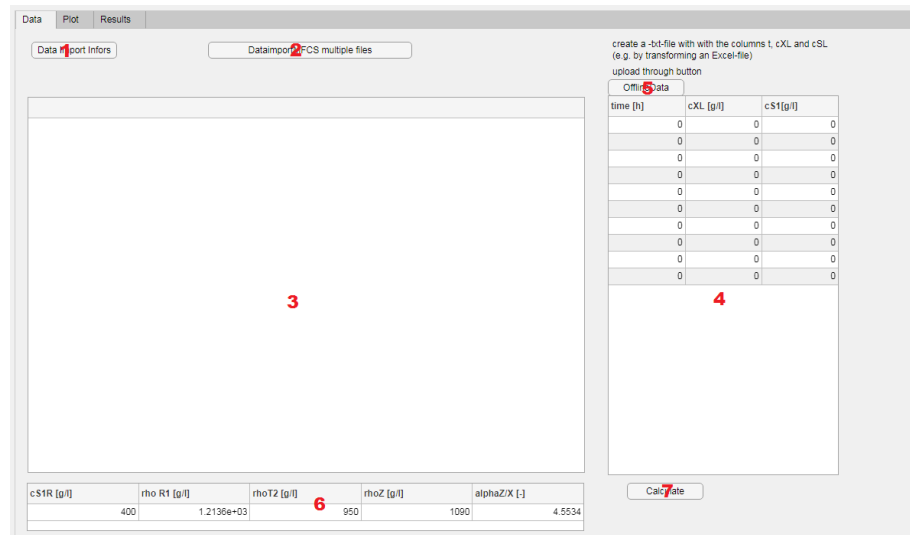


**Fig. 16:** Screenshot of tab 1 of the app, with the data upload buttons and tables displaying the data

The second tab contains a *Axes* object, the *FermentationPlot* and a *DropDownMenu*. It is shown in figure 25. One of the variables from the online data, chosen through the *DropDownMenu* can be plotted here. This tab is called the *plot tab*.

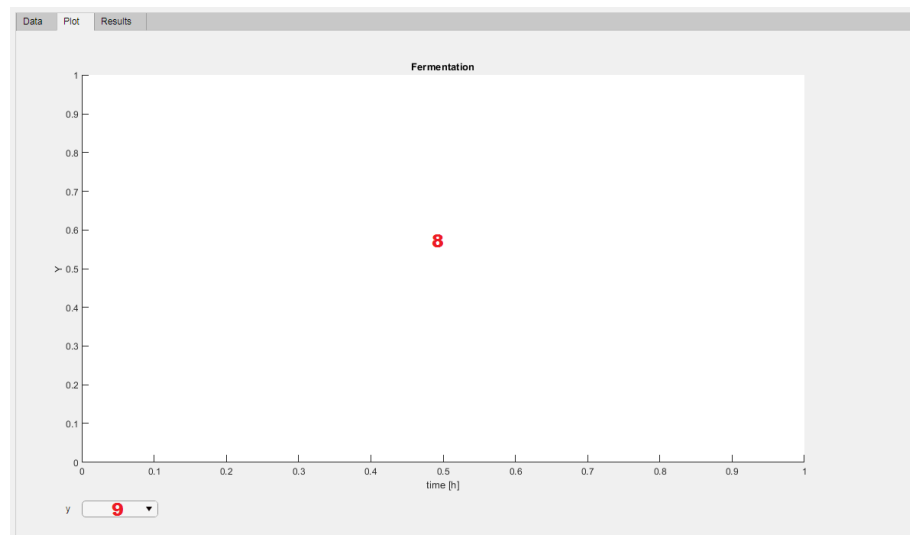


**Fig. 17:** Screenshot of tab 2 of the app, the dropdown menu and the plot to display the online data

The third tab is the *results tab*, shown in figure 18. Here three plots are displayed, containing the results of the first calculation. There is one plot for each variable, the *plotqxx*, *plotqyx* and the *plotqox*, which are plotted after the *ButtonPushed* Callback function of the *CalculateButton* in tab 1 is executed.

Again, there are multiple buttons and 4 display fields. Two of the buttons are for saving the constant ranges of the batch and fed batch through *ButtonPushed* Callbacks, which are displayed in the *display fields*. The third button is for the calculation of the global reaction parameters, which are displayed in the table *TableResults*. The last two buttons are for either creating a summary PDF-file or a -mat-file containing all the results.

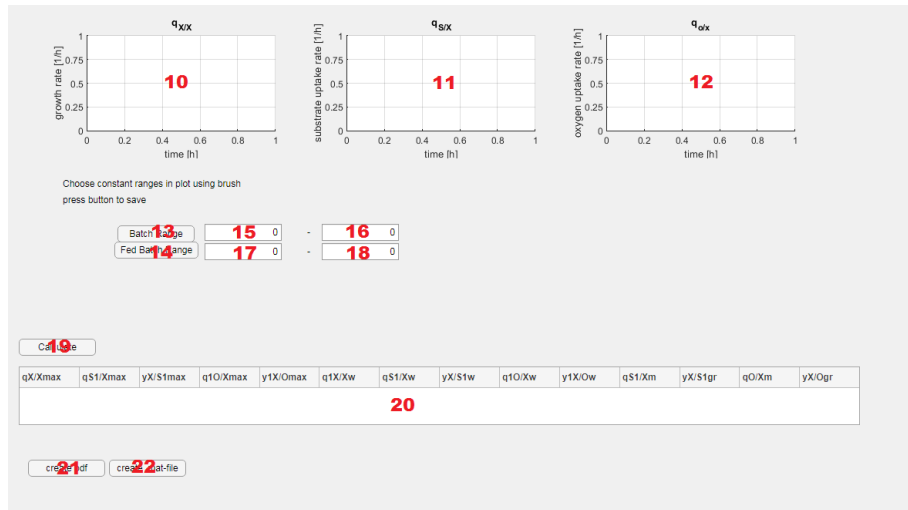


**Fig. 18:** Screenshot of tab 3 of the app, with the plots for the time specific reaction rates, the buttons and number fields for the ranges, the result table and the buttons for saving the data to a .PDF and .mat-file

The division in three tabs was chosen so the data upload and the calculations are separated from each other. The plot has its own tab so it could be a sensible size. The basic sequence of the callbacks can be seen in figure 19

**Table 11:** Components of the app and their callback functions

No.	Name	Callback Action
1	DataImportInforsButton	ButtonPushed
2	DataImportMFCSmultiplefilesButton	ButtonPushed
3	TableOnlineData	-
4	TableOfflineData	-
5	OfflineDataButton	ButtonPushed
6	TableFeedData	TableDataCellEdit
7	CalculateButton	ButtonPushed
8	plotFermentation	-
9	yDropDown	ValueChanged
10	plotqxx	-
11	plotqsx	-
12	plotqox	-
13	BatchRangeButton	ButtonPushed
14	FedBatchRangeButton	ButtonPushed
15	Batcht0EditField	-
16	BatchtendEditField	-
17	FedBatcht0EditField	-
18	FedBatchtendEditField	-
19	CalculateButton_2	ButtonPushed
20	TableResults	-
21	createpdfButton	ButtonPushed
22	creatematfileButton	ButtonPushed

## 6.2 Global variables

Global variables are variables that can be used in every function of the code without having to be defined every time. They have to be declared at the start of the code and called with '*app.Variable Name*' to be used in the callback functions. Variables that are not declared as a global variable and not saved with '*app.Variable Name*' can only be used in their own function.

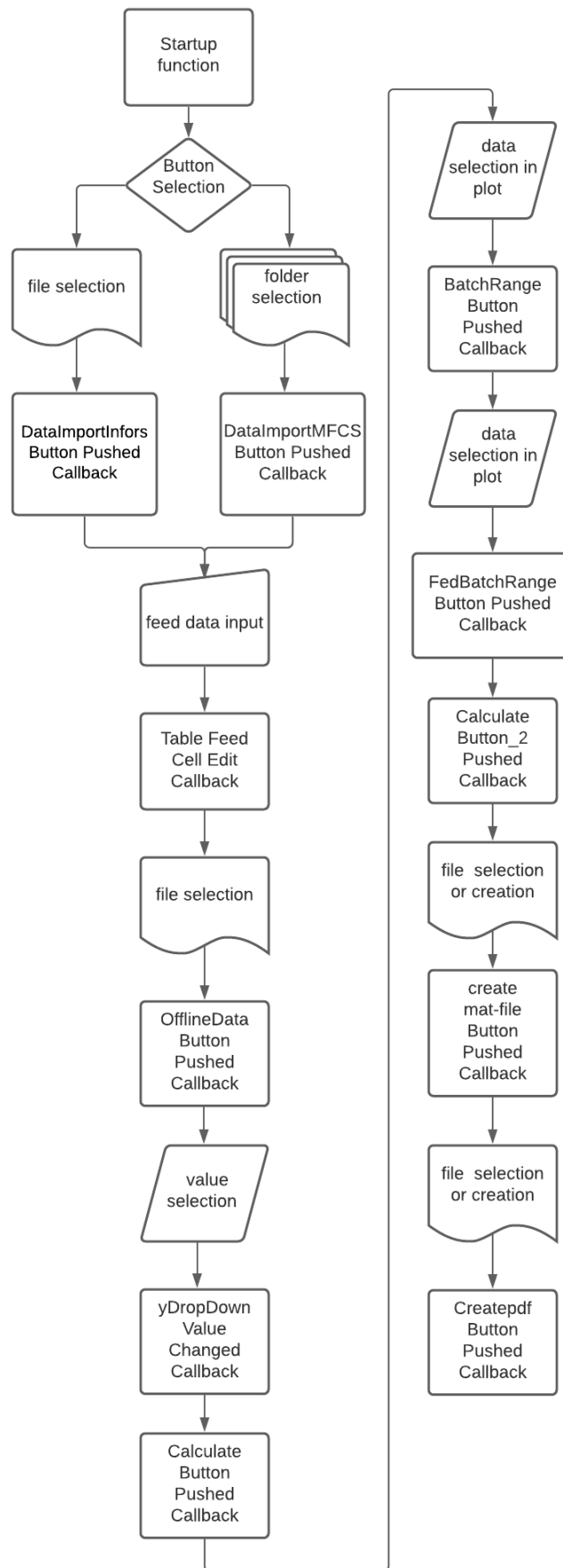


Fig. 19: Basic structure of the application

**Table 12:** Global variables used in the application

Variable name	Description
MatrixData	Online data uploaded from the file in matrix form without headers
TableData	Online data uploaded from the file in table form with headers
CalcData	Data necessary for the calculations at the extracted time points matching the offline data in matrix form
OfflineData	Offline data from the fermentation uploaded from a text file
t	time vector
qnx	matrix with the time, $q_{X/X}$ , $q_{S1/X}$ , $q_{O/X}$ , $dc_{XL}$ and $F_{in}$
tb1	index of data chosen for batch $t_0$
tb2	index of data chosen for batch $t_{end}$
tfb1	index of data chosen for fed batch $t_0$
tfb2	index of data chosen for fed batch $t_{end}$
file	filename of file chosen for online data
path	path to file chosen for online data
Res	result vector of the calculation for the global reaction parameters
p	vector containing $c_{S1R}$ , $\rho_{S1R}$ , $\rho_{T2}$ , $\rho_Z$ and $\alpha_{Z/X}$

### 6.3 Startup Function

The startup function is, as the name indicates, executed as soon as the app is started. The app and all its components are created. the global variable *app.p* is created and filled with zeroes. The table *TableFeedData* is filled with *app.p*.

### 6.4 Data Upload

Since fermentations are regularly done with two different bioreactors running with two different softwares -Multi Fermentor Control System (MFCS) win and eve- two different upload functions have to be created to account for the difference in the data structure given by these systems. Therefore, there are two buttons in the first tab of the program labelled '*Data Import Infors*' and '*Data Import MFCS*'

to upload data from the Infors reactor or the MFCS reactors respectively, which activate different *ButtonPushed* Callback functions.

### 6.4.1 Infors Data Upload

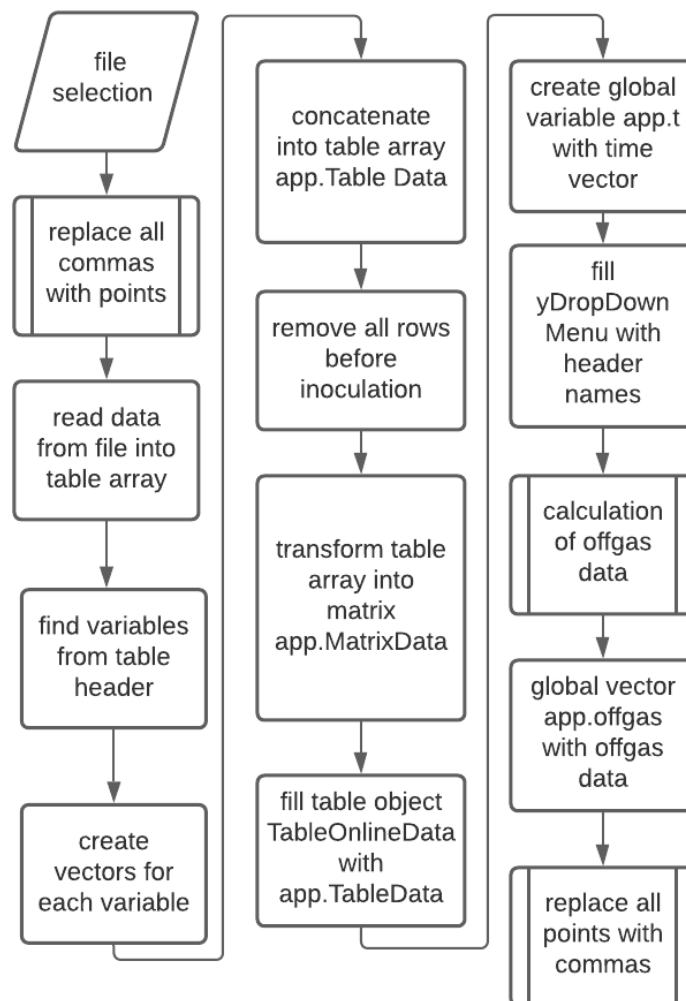


**Fig. 20:** Structure of the Button Pushed Callback function for the Infors Data

The Infors reactor works with the eve system. The output of that system after fermentation is one big .csv-file, with each column containing one variable. The headers of the table contain the name and unit of the variable. The raw data can be seen in figure 21.

After pressing the *Infors* button, you are directed to choose a .csv file from the directory. After selecting a file, the path to the file and the filename are saved in the global variables `app.path` and `app.file`. The data from the file is processed through





the column '*Batch time since Inoculation*', the time will be Not a Number (NaN) before inoculation. All rows in which batch time since inoculation is NaN are searched for and removed in the whole table. The data is displayed in the table on tab 1, using the headers from the .csv-file. Since calculations cannot be done with data in table form, the data is transformed into a matrix, removing the headers, with the function *table2array*. The new matrix is saved in the global variable *app.MatrixData*.

$$app.MatrixData = \left[ t \quad x_{O_2} \quad x_{CO_2} \quad V_L \quad \vartheta \quad V_{T1} \quad V_{T2} \quad V_{AF} \quad V_{S1} \quad pH \quad F_{nG} \right]$$

The volumetric flow of all reservoirs is saved in mL by the eve-software. It has to be transformed into liters, which is done by dividing the correct columns by 1000. The time vector is set as the global variable *app.t* to make it accessible across all functions in the app. All the variables are put into the *DropDownMenu* here and will be used for the plot later.

The offgas data is calculated through an external function and saved in the global variable *app.offgas*.

$$app.offgas = \left[ t \quad Q_{O_2max} \quad Q_{O_2} \quad Q_{CO_2max} \quad Q_{CO_2} \quad RQ \right]$$

At the end of the callback, the points are transformed back into commas, since the Infors data is often opened with Microsoft Excel, and a point as the decimal separator leads to Excel recognizing many values as dates, which is irreversible and destroys the raw data. If the data upload is not successful, a try-case loop replaces the points with commas anyway, to conserve the data.

### 6.4.2 MFCS Data Upload

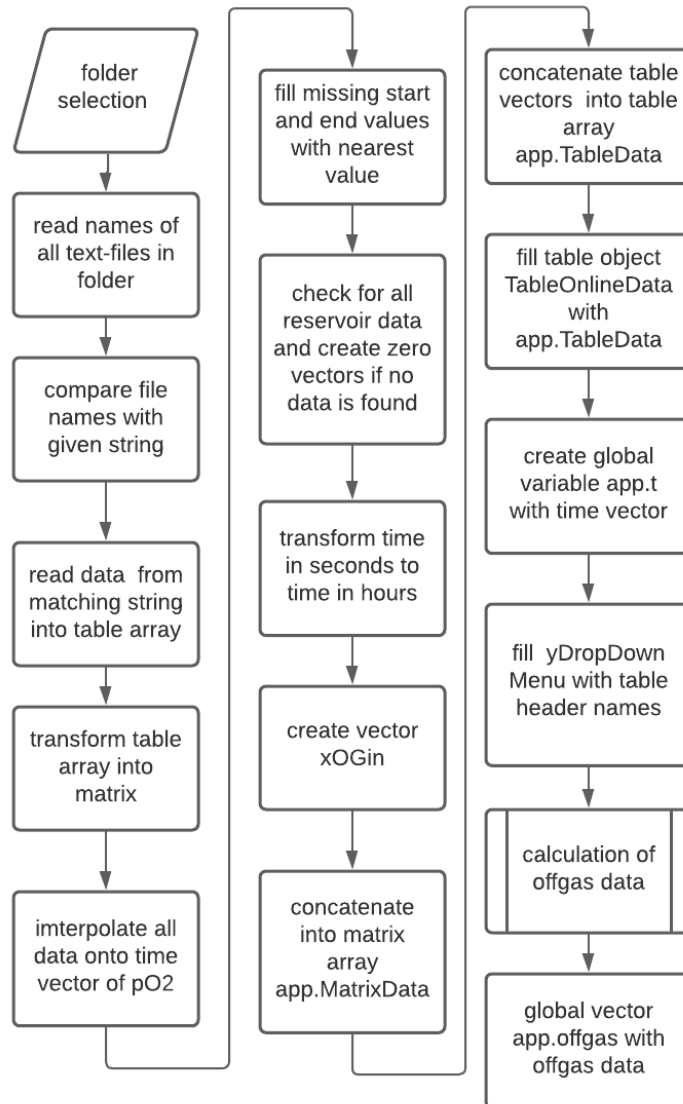


**Fig. 22:** Structure of the Button Pushed Callback function for the MFCS data from multiple text-files

In contrast to Infors, MFCS gives one text-file for every single variable, with its own time vector so the data has to be loaded into the program differently. The structure of the function can be seen in figure 22.

Instead of choosing each file separately, after pressing the MFCS-Import Button a folder is chosen from the directory. In a for-loop every file name is read and saved into the array baseFileName. The path and filename are put together into

the entire path in the variable `fullFileName`, which is changed in every iteration of the for-loop. The filename is compared to a prewritten example through a case-switch loop. If the filename matches one of the examples, the table is read into a table vector, which is given a header, and transformed into a matrix vector to make calculation possible. The data is already saved with points as the decimal separator, so in this case, the decimal separator does not need to be changed

The time vectors in each variable contain non-unique time points, meaning some time points appear multiple times, which makes interpolation impossible. To remove those, the difference between the time points in the matrices first row is calculated, and if it is zero, the row is removed from the vector. The matrix is transformed back into a table array, and the old table array is overwritten.

Now, the vectors can all be interpolated onto the same time vector, which is needed for the calculations. The time vector of `po2` is set as the general time vector and all other variables are interpolated onto that vector. This variable was chosen because it had the most time points. The `interp1`-function of Matlab® is used for the interpolation.

Some data is not written into the file starting from 0 seconds, so there are some time points missing from the data after interpolation, as Matlab® had no data to interpolate from. The missing time points are filled with the nearest data from the end or the beginning, as this is expected to be closest to the actual value at that time.

Furthermore, the feed rates are taken by the weight reduction on scales and are therefore negative. The absolute of every point in the feed rates is calculated to transform it into a positive number. Now the feed rates are divided by their densities from the vector `app.p` (if they are given) to transform the mass flow into the volume flow.

Some data is not recorded during the fermentation, but the vectors are needed for calculation.

For the reservoir bottles which were not weighed to get their mass, vectors with zeroes are created. Sometimes, two reservoir bottles are put on the same scale, so the weight of this reservoir is already accounted for. For reservoir bottles the person performing the fermentation did not think recording the data for that reservoir bottle was necessary for the accurate analysis of the fermentation. Accurate data cannot be recreated for those bottles, therefore using zeroes is the only sensible option.

In the sample data, there was also no file for `xO2` so a vector with 0.2094 is created, as the oxygen mole fraction of air, which is most often used for aeration, is 0.2094.

The data is horizontally concatenated to create a table array with headers and a matrix without headers for the calculation. The order of the variables is the same as in the other Data Upload function, which makes it possible to refer to the variables by row number later.

$$app.TableData = \begin{bmatrix} t & x_{O_2} & x_{CO_2} & V_L & \vartheta & V_{T1} & V_{T2} & V_{AF} & V_{S1} & pH & F_{nG} \end{bmatrix}$$

The data is displayed in the OnlineData Table. The batch time is set as a global variable `app.t`, and the `DropDownMenu` is filled with the property names for the plot. The external offgas function is used to calculate the offgas data, which is saved in the global variable `app.offgas`.

### 6.4.3 Function for the calculation of the offgas data

The online data from the fermentation, extracted with either of the `UploadButtonPushed` Callback functions is given to the function for the calculation of the offgas data. The necessary variables are extracted from the online data matrix by number and named after their respective variable for easier understanding of the equations.

The vector for  $x_{CGin}$  is created by subtracting  $x_{OGin}$  from 21, since  $O_2$  and  $CO_2$  make up about 21 % of the composition of the atmosphere.

The constant variables  $M_{O_2}$ ,  $V_{nM}$  and  $M_{CO_2}$  are created.

$F_{nG}$  is given in L/min and is multiplied by 60 to create L/h. The mole fraction of the inlet and outlet are all given in percent and have to be divided by 100 for the calculation.

Now equations 35, 34, 37, 36 and 38 are used to calculate  $Q_{O_2max}$ ,  $Q_{O_2}$ ,  $Q_{CO_2max}$ ,  $Q_{CO_2}$  and  $RQ$ .

The result vector given back to the app contains these variables as well as the time vector.

### 6.4.4 Offline Data

There are two tables for the offline data: one table contains the offline data from the fermentation, with  $c_{XL}$  and  $c_{S1L}$ , together with the matching times at which

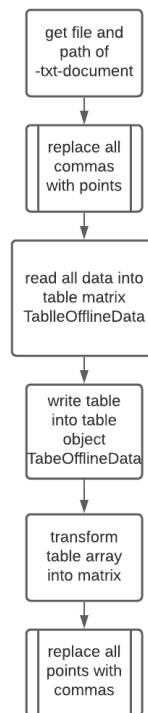


**Fig. 23:** Overview of the function for the offline data from a .txt-file

the samples were taken. This table is called *TableOfflineData*. The other table contains data from the reservoirs and some strain specific values and is called *TableFeedData*.

For the offline data a .txt-file has to be created, that contains a column for  $t$ ,  $c_{XL}$  and  $c_{S1L}$  in that order. The text-file can be chosen through the *OfflineDataButton* and the *ButtonPushed* Callback activates the upload. The file and path are saved in variables, and the *comma2point* overwrite function replaces all commas with points. The data is saved into a table array.

The app table is filled with the data and the global variable *app.OfflineData* is created by transforming the table into a matrix. The last step is replacing all points with commas again in the text-file.

$$app.OfflineData = \begin{bmatrix} t & c_{XL} & c_{S1L} \end{bmatrix}$$

The *TableFeedData* can be edited directly in the app, and the data is saved in the global vector *app.p*.

$$app.p = \begin{bmatrix} c_{S1R} & \rho_{S1R} & \rho_{T2} & \rho_Z & \alpha_{Z/X} \end{bmatrix}$$

### 6.4.5 Comma2pointoverwrite

An external function to change the decimal separator from a comma to a point had to be employed, so Matlab® saves the data as numeric data and not strings. The function receives the path and filename of the chosen file and creates a memmapfile, which maps the file to the Matlab® address space. This accelerates the data transformation. All instances of commas in the file are changed to points. There is also the opposite function *point2commaoverwrite*, which changes all points to commas. It functions in the same way.

## 6.5 Plot

For a visual check of the data, as an *Axes* object was added to tab 2 of the app. It contains the plot and a *DropDownMenu* in which the displayed variable can be chosen. The chosen variable is displayed against the time in hours on the x-axis. The headers of the table vectors, which also contain the unit, appear in the *DropDownMenu* and also as the y-axis label. This is all done in a callback function for the *DropDownMenu*.

## 6.6 Calculation of specific reaction rates

After all the data is added into the app via the upload function and the tables, the calculate button in tab 1 can be clicked. This activates the *ButtonPushed* Callback. The offline data from tables 2 and 3 is written into 2 global matrices, called *app.p* for the variables for the reservoirs and *app.ManualData* for the offline data taken from the samples. The data in the matrices is updated in *CellEdit* Callback functions, to ensure the calculations are always done with the most recent data. Since the online data is recorded much more frequently than the offline data, there are more timepoints for each variable. The data matching the time of the offline data has to be extracted from the online data. Both time vectors are put into their own vector for easier access and understanding. A for loop calculates the difference between each point in both vectors and returns the indices of the rows in the online data. The correct rows from the *MatrixData* and the data from the offgas calculation are put into their own matrices and horizontally concatenated to create one big matrix with all data needed for the calculation.

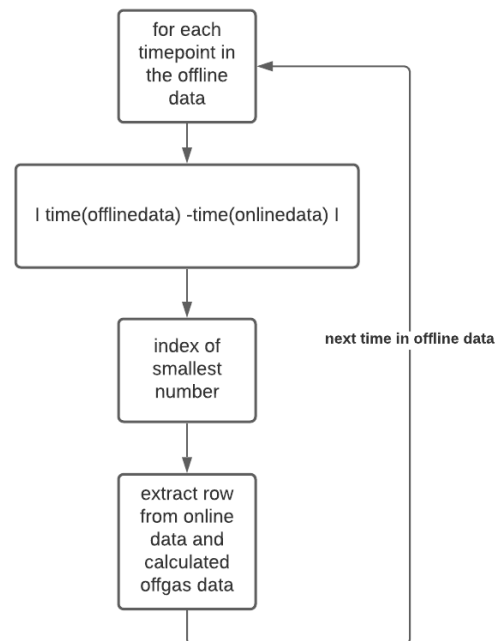


**Fig. 24:** Structure of the for loop for the extraction of the online data matching the time points in the online data

The calculations of the specific reaction rates are done with an external function. The results of the calculation are put into a vector and plotted on three diagrams in tab 3, since the constant ranges have to be visually chosen. For easier visibility, 3 different diagrams instead of one diagram for all three rates were created. The limits of the axes are set as the minimal and maximal result and the y-axis is divided into fifths by ticks.

### 6.6.1 Function for the calculation of the specific reaction rates

The matrix with all the necessary data for the calculation, which was created in the *CalculateButtonPressed* Callback function is given to the function, as well as the data from vector  $p$ , containing the concentrations and densities of the reservoirs, as well as the density of the bio wet phase density  $\rho_Z$  and  $\alpha_{Z/X}$ .

All data is written into vectors named after their respective variable for easier understanding of the calculations.

The size of the matrix is written into the variable 'index'. Since the Matlab®command

'size' returns the number of rows and columns, the first object in 'index' is used to create a for loop. The for-loop starts at an index of 2 and ends at one less than the number of rows of the matrix.

The loop calculates  $dc_{XL}/dt$  and  $dc_{S1L}/dt$  for each time point using equation 43 and 44 and does the same to the feed rates. The 4 feed rates  $F_R$ ,  $F_B$ ,  $F_A$  and  $F_{AF}$  are added together to get  $F_{in}$ . The specific reaction rates are calculated using equation 45, 46 and 47 and put into the result vector. The time vector,  $dc_{XL}$  and  $F_{in}$  are also written in the result vector for use in later calculations.

$$app.qnx = \left[ t \quad q_{X/X} \quad y_{S1/X} \quad q_{O/Xm} \quad \dot{c}_{XL} \quad F_{in} \right]$$

## 6.7 Calculation of global reaction rates

The next step is the calculation of the global reaction parameters. The constant ranges of the specific reaction rates have to be identified to set up the overdetermined system to calculate the yield coefficients  $y_{X/S1max/w}$  and  $y_{X/Omax/w}$ .

For this, two buttons were added to the app, the *BatchRange* Button and the *Fed-BatchRange* Button. In the *ButtonPressed* Callback function, brushed data from the plot is written into vectors that contain the constant ranges from the plots.

The calculation is again done by an external function, after pressing the second calculate button. The *CalculateButtonPressed* Callback function gives all necessary data to the external function for calculation and returns the results. The results are then written into *TableResults* on tab 3.

### 6.7.1 Function for the calculation of the global reaction rates

After the *ButtonPressed* Callback is activated, the external function receives the CalcData matrix, the p vector, the result vector with the specific reaction ranges qnx and the ranges from the brushed data and calculates  $q_{X/Xmax/w}$ ,  $q_{Xmax/w}$  and  $q_{O/Xmax/w}$  with the equations 45, 46 and 47 rearranged to an overdetermined system, using the backslash operator.

The results are used to calculate  $q_{S1/Xm}$ ,  $y_{X/S1gr}$ ,  $q_7O/Xm$  and  $y_{X/S1gr}$ . The result vector is given back to the main function and saved in the global variable Res.



$$app.Res = \begin{bmatrix} q_{X/Xmax} & q_{S1/Xmax} & y_{X/S1max} & q_{O/Xmax} & y_{X/Omax} \dots & \\ & q_{X/Xw} & q_{S1/Xw} & y_{X/S1w} & q_{O/Xw} & y_{X/Ow} \dots \\ & q_{S1/Xm} & y_{X/S1gr} & q_{O/Xm} & y_{X/Ogr} & \end{bmatrix}$$

## 6.8 Creation of a .mat-file

The calculated data from the functions for the specific and global reaction parameters can both be saved in a .mat-file, for further use.

After pressing the create mat-file button, the user can choose to overwrite an existing file or create a new file. The matrices app.Res containing the global reaction parameters and app.qnx with the time specific reaction parameters are transformed into table arrays with headers with the variable names. The filename of the file used for the calculation is also saved as a string. These table arrays are named after the data they contain and saved in the file previously chosen.

**Table 13:** Table containing the results of the offgas function saved in the mat-file

$Q_{O2max}$	$Q_{O2}$	$Q_{CO2max}$	$Q_{CO2}$	$RQ$
-------------	----------	--------------	-----------	------

**Table 14:** Table containing the specific reaction rates saved in the mat-file

time	$q_{X/X}$	$q_{S1/X}$	$q_{O/X}$
------	-----------	------------	-----------

**Table 15:** Table containing the ranges saved in the mat-file

Batch start	Batch end	Fed-Batch start	Fed-Batch end
-------------	-----------	-----------------	---------------

**Table 16:** Table containing the global reaction parameters saved in the mat-file

$q_{X/Xmax}$	$q_{S1/Xmax}$	$y_{X/S1max}$	$q_{O/Xmax}$	$x_{O/Xmax}$
$q_{X/Xw}$	$q_{S1/Xw}$	$y_{X/S1w}$	$q_{O/Xw}$	$x_{O/Xw}$
$q_{S1/Xm}$	$y_{S1/Xgr}$	$q_{O/Xm}$	$y_{X/Ogr}$	

## 6.9 Creation of a PDF report

A summary of the app results is given in a PDF-report, created with the Matlab® Report Generator. The report contains the name of the file used for the online data, the plot of the time specific reaction rates, the ranges of batch and fed batch and tables with the global reaction parameters.

For display in a table, all numbers are transformed into strings using `mat2str` and named after their respective variable.

The document starts with 'Summary of' and the string saved in `app.file`, so the PDF-files can later be matched with their data.

The figures for the reaction rates are taken from the app and temporarily saved in files, so they can be added to the report. All three plots are added with subtitles.

Next, the ranges for the batch and fed-batch are added, taken from the brushed data from the *Batch-* and *FedBatchButtonPushed* Callbacks.

Lastly, three tables with the global reaction parameters are added. They are taken from the matrix `app.Res` and have previously been transformed into strings. The first table contains the reaction rate of the maximal growth rate, the second one from the controlled growth phase and the last one the global reaction parameters. All tables are also given titles.

After the document is saved and opened, the graphics are deleted again. The document can now be downloaded and saved.

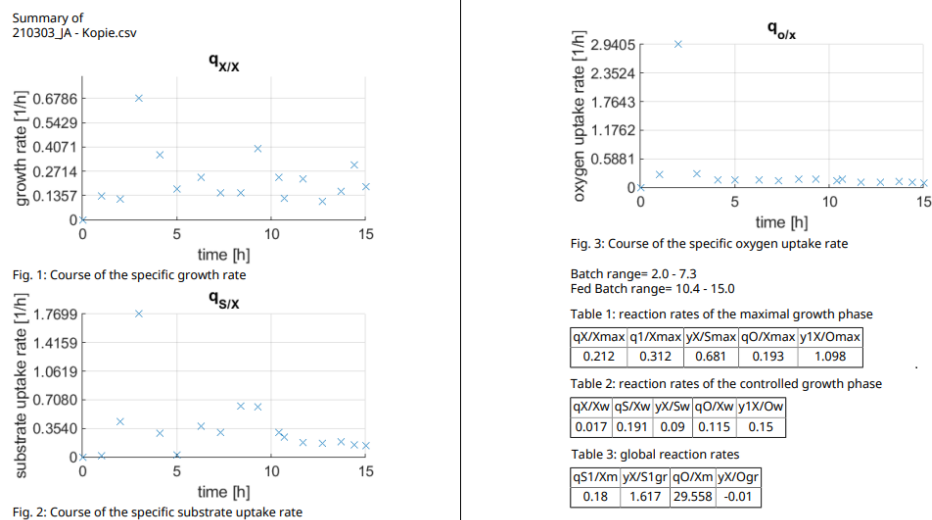


**Fig. 25:** Summary PDF file that is created after pushing the `createpdf` button containing the plots of the time specific reaction rates, the ranges of batch and fed batch, the reaction parameters of the fermentation and the calculated global reaction parameters

## 7 Results

### 7.1 Shaker flask cultivation

Two precultures were done prior to cultivation for the inoculation of the reactor. Before the fermentations were started, a growth curve of the cell line was recorded, to analyze the optimal time point for inoculation of the reactor, as it should be happening while the cells are in the exponential growth phase.

A sample was taken after inoculation. The cell concentration immediately after inoculation was 0.08 g/L.

After 18 hours, the cell concentration had reached 0.82 g/L. During the next hours, exponential growth can be observed, with the cell concentration reaching 3.1 g/L after 23 h, showing that inoculation of the reactor is possible within 18 h to 23 h of the inoculation of the pre culture.

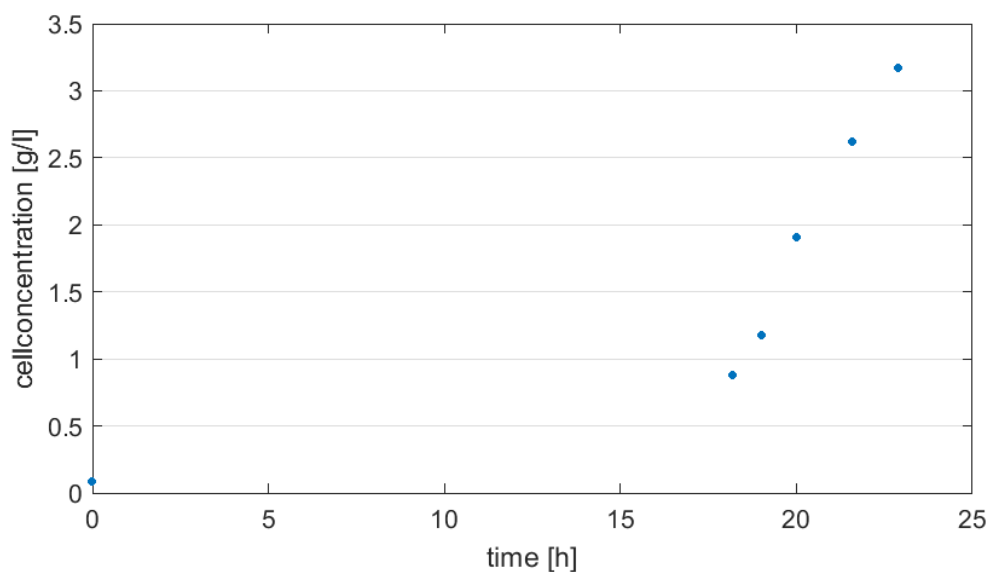


**Fig. 26:** Growth plot of the preculture inoculated with 300  $\mu$ L of the Working Cell Bank in 100 mL of medium cultivated at 30 °C at 150 rpm

## 7.2 Flow rate of the pump

The flow rates of the pumps are important in the calculation of the global reaction parameters, as they change the volume of and concentrations in the cell broth. Therefore, their accuracy was analyzed, to examine their influence on the results. The maximal feed rate  $F_{Rmax}$  was determined to be 3.37 mL/min. This value was used as the set point in the equations of the eve-system.

The data of the other flow rates shows a linear behavior of the pump over its whole range, as can be seen in figure 27 A).

In figure 27 B), the deviations in percent of the measured feed rate to the given feed rates by the system are shown in percent. The median is shown and the error bar depicts the highest and lowest deviation. High deviations can be seen at the low feed rates of 1 and 2 %, therefore those rates were avoided for more accurate results.

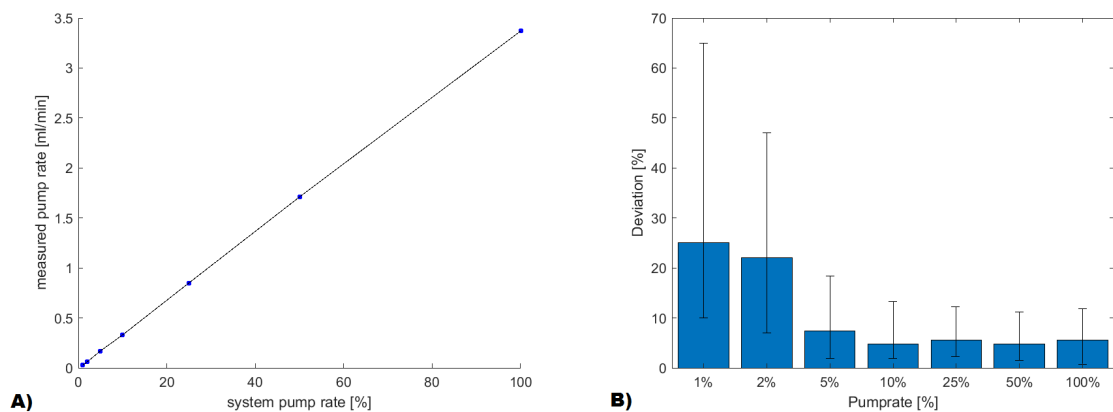


**Fig. 27:** A) Measured versus system flow rates of the eve system, B) Deviations of the measured flow rates to the flow rates given by the eve system in %, with the error bar showing the highest and lowest deviation

### 7.3 $K_{XOD}$ determination from CDW and OD measurement

To transform the  $OD_{600}$  results into cell concentration, a regression function had to be calculated to give the factor  $K_{XOD}$ .

The results of the CDW is plotted against the corresponding OD measurements, and a linear regression function with the y-intercept at 0 is calculated. The resulting function contains the factor  $K_{XOD}$ .

The  $R^2$  is 0.96, which shows a good fit of the data to the function. The constant can therefore be used to calculate the cell concentration in g/L from the  $OD_{600}$ -results. The  $K_{XOD}$  was determined to be 0.5506.

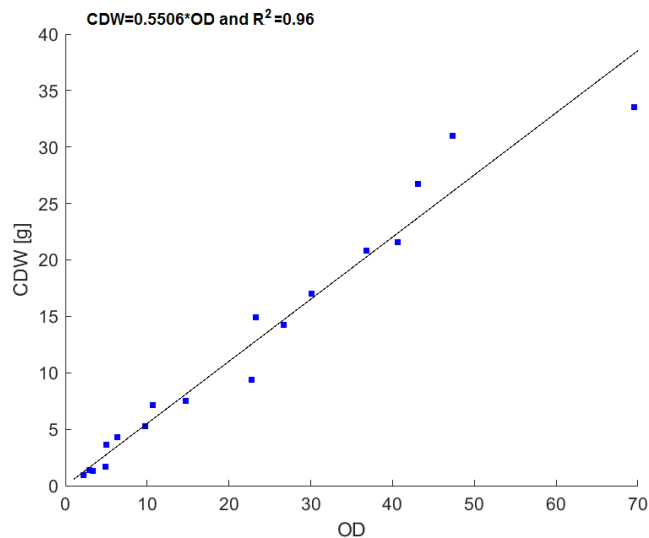


**Fig. 28:** Plot of OD against the CDW for the determination of  $k_{XOD}$

$$c_{XL} = K_{XOD} * D * OD_{600} \quad (76)$$

with

- $K_{XOD}$  = factor
- $D$  = Dilution rate of the sample
- $OD_{600}$  = result of the OD measurement

## 7.4 Glycerol measurement

For the calculation of the glycerol concentrations in the culture broth, a calibration curve was recorded for each fermentation. The calibration curve used for the analysis of the first cultivation is shown in figure 30.

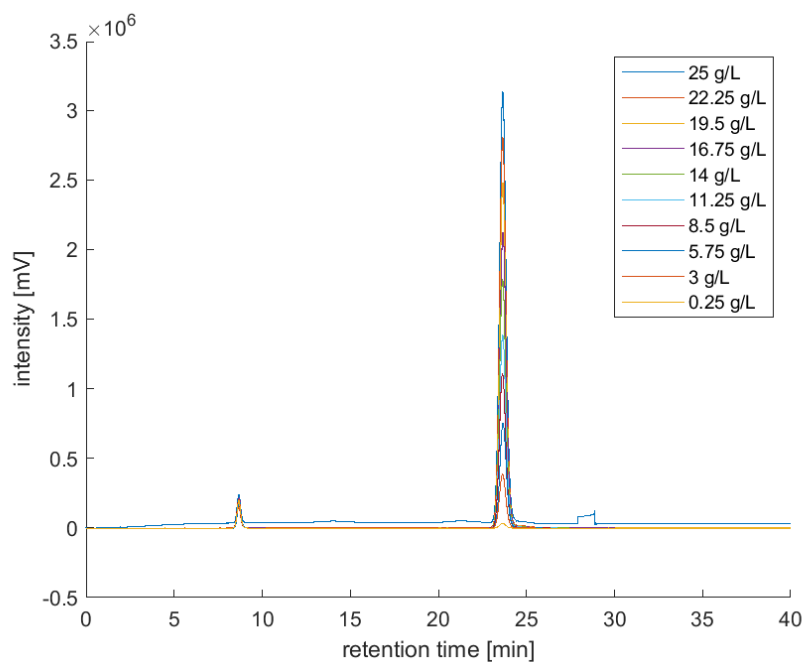


**Fig. 29:** Chromatograms of the standards used for the calibration curve for the analysis of the samples of the first cultivation

The area of the peaks at a retention time of 24 min were calculated using a Matlab script and plotted against the concentration to obtain the calibration function. Figure 29 shows the the chromatograms of the calibration standards. The chromatograms show no contaminations and the regression function shows a good fit to the data, meaning a good calibration curve was achieved.

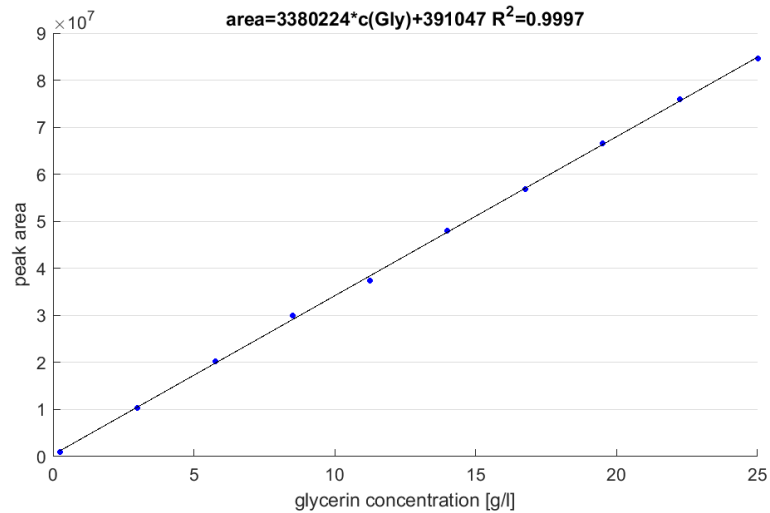


**Fig. 30:** Calibration curve of the glycerol measurement showing the peak area of the chromatograms over the glycerol concentration from 10 standards for the analysis of the samples of the first cultivation

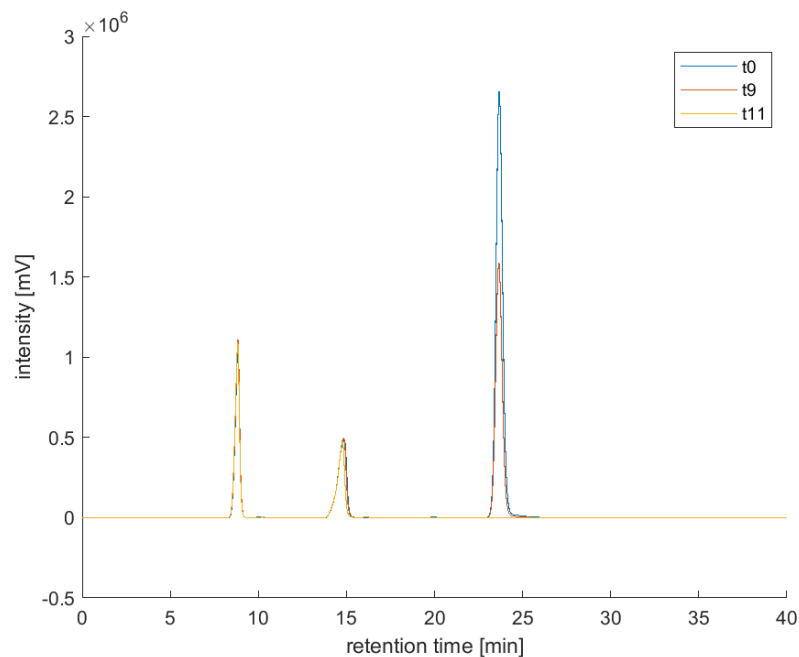


**Fig. 31:** Chromatograms of samples  $t_0$ ,  $t_9$  and  $t_{11}$  after begin of the fed batch during the first fermentation

In figure 31 three examples of a chromatogram of the supernatants of the first cultivation are shown. The peak at a retention time of around 24 min is dependent on the glycerol concentration in the medium. The area of this peak was used to calculate the concentrations using the calibration regression from figure 30.

The first peak from sample  $t_0$  is the biggest, as the glycerol concentration is highest here. The concentration of glycerol decreases, which is shown in the smaller

peak of sample  $t_9$  and reaches 0 with fed-batch, as the fed-batch is started with the depletion of the substrate. Sample  $t_{11}$  shows no peak at the retention time of 24 min.

The other two peaks which are shown are probably citrate and a water peak, as other chromatograms showed peaks of those substances at these retention times.

## 7.5 Fermentation 1

Two fermentations were carried out to help develop and test the app, as the data type and unit of the outputs had to be known.

**Table 17:** Set points for fermentation 1

Variable	Set point value	Unit
$\vartheta_L$	30	°C
$p_{O_2w}$	25	%
pH	5	
$c_{S1R}$	400	g/L
$F_{nG}$	4	L/min
$q_{X/Xw}$	0.15	1/h
$c_{XL0}$	1.25	g/L
$c_{S1L0}$	25	g/L

In figure 32 the cultivation course of the first fermentation is shown. The variables  $p_{O_2}$ ,  $N_{St}$ ,  $F_R$ , pH,  $Q_{T2in}$ ,  $Q_{S1in}$  and  $F_{nG}$  are shown over the time in hours.

In the batchphase, all parameters are stable for the most part. The pH is controlled well by the flow rate of the base during the whole fermentation. The addition of base is a necessary countermeasure against the pH lowering acid the cells produce and excrete. The dip at the beginning of the fermentation stems from the lower pH in the shaker flask culture broth, as the pH is uncontrolled during pre culture. The base simultaneously functions as a nitrogen source for the cells.

The stirrer speed and aeration rate are constant in the first phase, as the stirrer is not yet needed to control the  $p_{O_2}$ . The  $p_{O_2}$  shows the expected behavior, falling from 88 % to the set point of 25 %.

After the  $p_{O_2}$  reaches its set point of 25 %, the  $p_{O_2}$  controlled phase of the batch



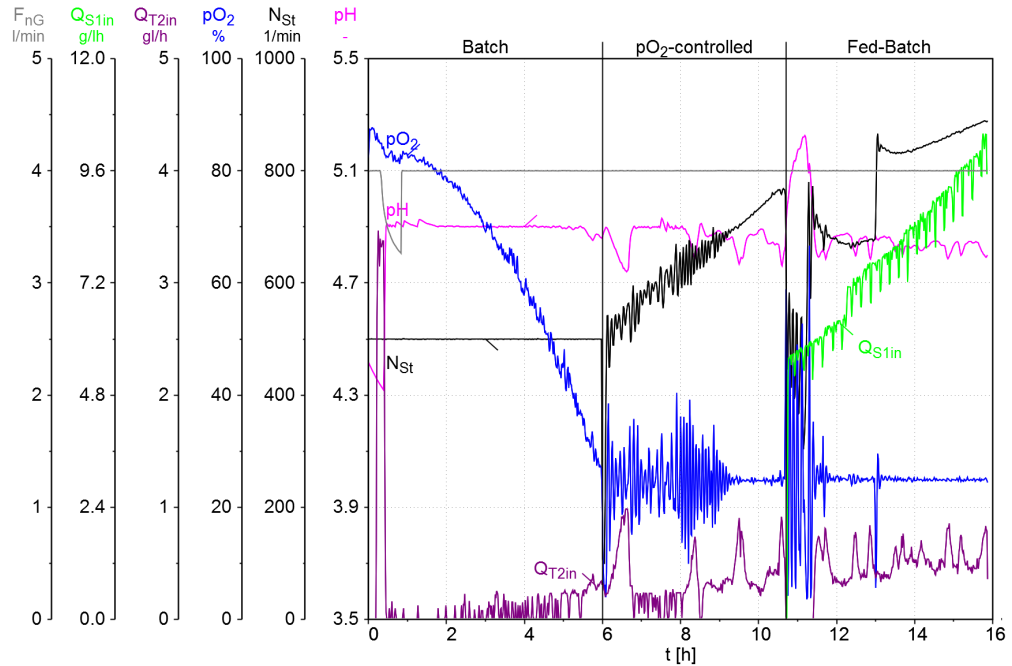


**Fig. 32:** Overview of the courses of  $F_{nG}$ ,  $Q_{S1in}$ ,  $Q_{T2in}$ ,  $pO_2$ ,  $N_{St}$  and pH for the first cultivation

begins. The stirrer speed slowly increases from the constant 300 rpm to around 750 rpm at the end of the batch, to meet the increasing oxygen demands caused by the growing cell concentration. The  $pO_2$  oscillates around 25 and becomes more stable at the end of the batch phase, as the  $pO_2$  control functions better at higher cell concentrations.

The end of the batch phase is indicated by a sharp increase in  $pO_2$  as well as a drop in  $N_{St}$ , which indicates that the substrate is used up and the cells do not need as much oxygen anymore as they can no longer grow with the maximal growth rate. Furthermore, the pH rises slightly as the cells now metabolize the acid in the medium.

The pump for the feed is started based on the variables for the open loop feed control. In the beginning of the fedbatch, the  $pO_2$  is very unstable, but becomes more constant over time. This might be due to a non-constant feed rate of the substrate, which leads to the cells growing in small 'bursts', as feeding solution is added in droplets.

The stirrer speed increases again in order to stabilize the  $pO_2$ , till it reaches its maximum of 950 rpm, when the fermentation is stopped after 15.5 h.

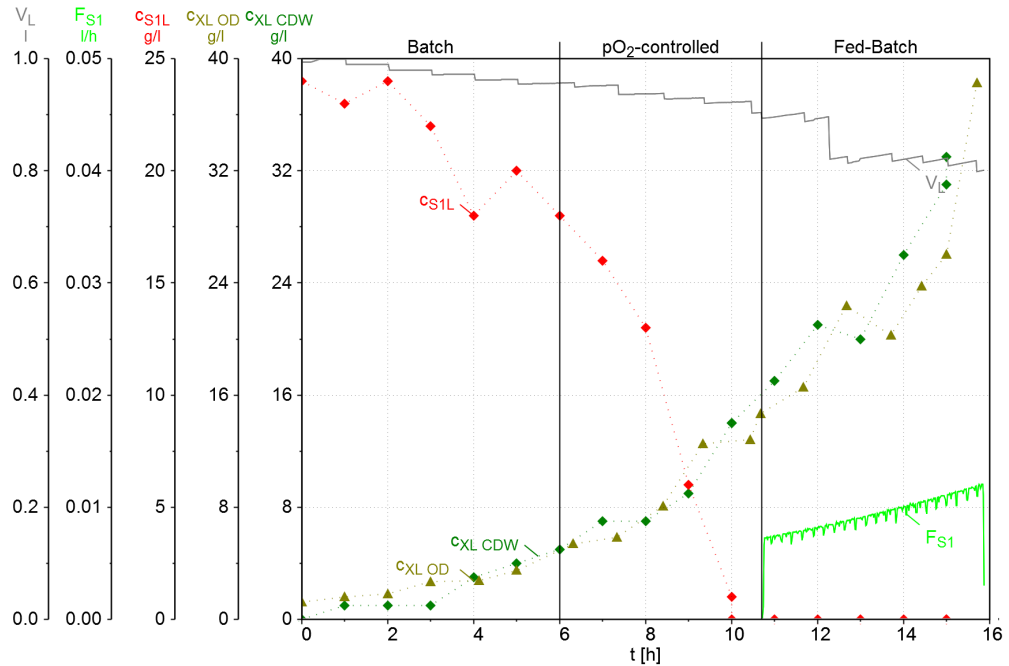


**Fig. 33:** Overview of the substrate uptake during the first fermentation, showing  $c_{XL}$ ,  $c_{S1L}$ ,  $F_{S1}$  and  $V_L$  over the time in hours

In fig. 33 the substrate uptake of the cells is shown by the concentration of glycerol  $c_{S1L}$  and the feed rate  $F_{S1}$ , as well as the cell concentration from the  $OD_{600}$ -measurement and the CDW measurement.

The cell concentration increases exponentially during the whole fermentation, with no stagnant phases visible.

The substrate concentration decreases during the batch until all the glycerol is consumed and it reaches 0 g/L at the end of the batchphase at 10.7 h. The feeding of substrate is started, which is indicated by the feed rate of substrate  $F_{S1}$ , but all available substrate is immediately taken up by the cells and the substrate concentration stays at 0 g/L. There is a substrate limited growth, as the cells can only grow as fast as the amount of substrate provided to them allows.

The sampling frequency and can be seen in the course of  $V_L$ , which is needed for the calculation of the concentration balance.

The feed rate follows an exponential profile after equation 4, increasing the flow rate as the cell concentration increases, which can be seen in the graph of  $F_{S1}$ .

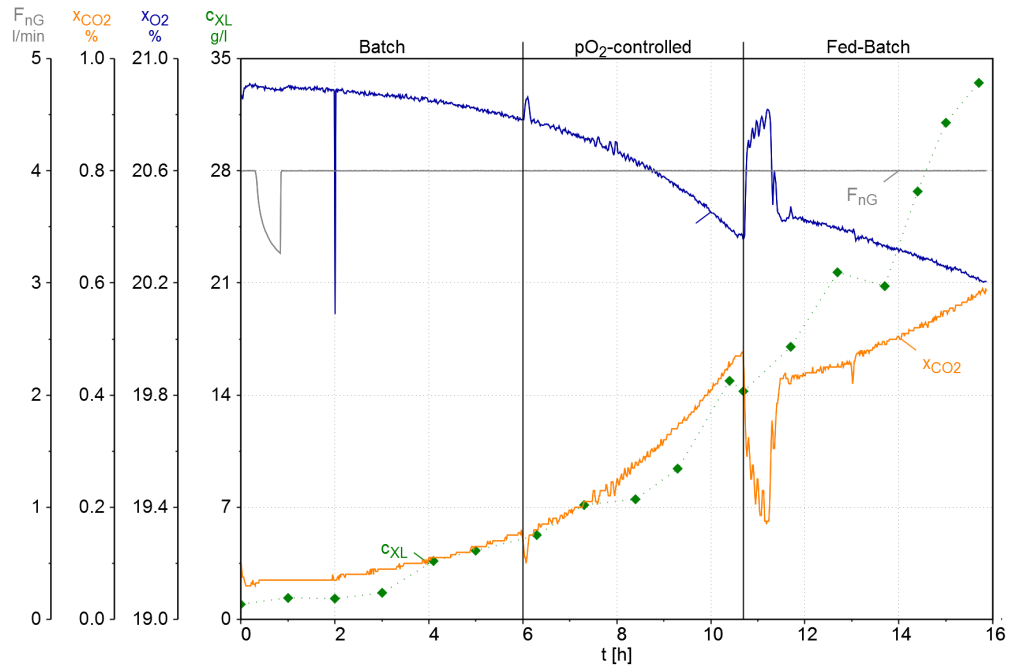


**Fig. 34:** Overview of the oxygen uptake during the first fermentation, showing  $c_{XL}$ ,  $x_{OG}$ ,  $x_{CG}$  and  $F_{nG}$  over the time in hours

In figure 34, the oxygen uptake and subsequent carbon dioxide production can be seen. The aeration is stable at 4 L/min during the fermentation. The oxygen mole fraction in the offgas decreases while the carbon dioxide mole fraction increases. At the switch to the fed-batch, the oxygen mole fraction sharply increases and the carbon dioxide mole fraction sharply decreases. They return to their previous behavior after around 1 h, albeit with a lower slope than before, due to the lower growth rate in the fed batch phase. The sharp peaks might indicate an inactive phase of the cell growth.

### 7.5.1 Discussion of the first fermentation

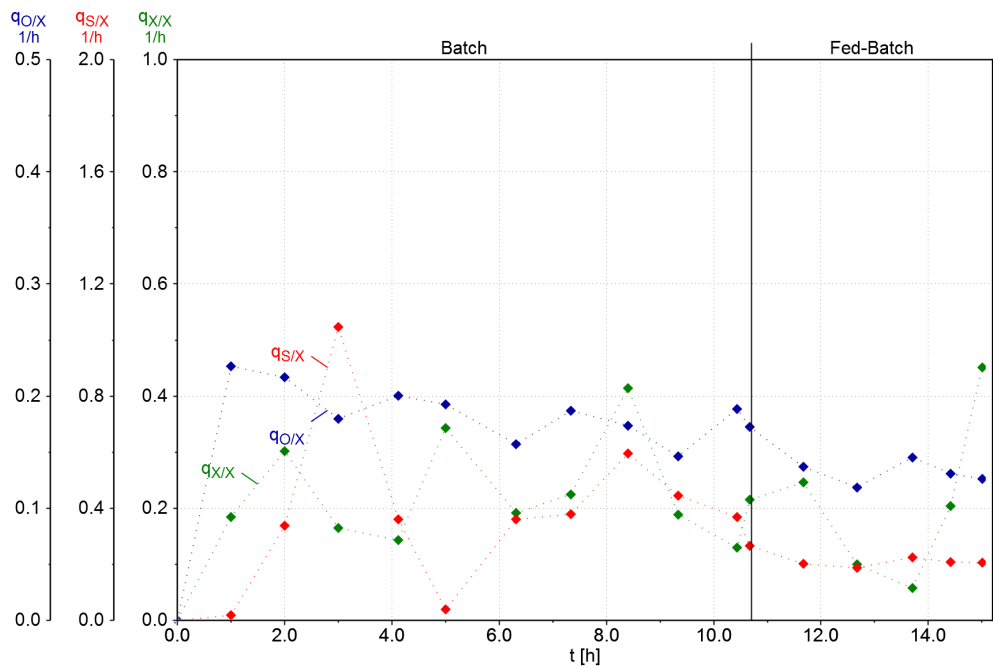


**Fig. 35:** Plots of the reaction rates  $q_{X/X}$ ,  $q_{S1/X}$  and  $q_{O/X}$  during the first fermentation calculated with the app using the  $OD_{600}$  measurements

In figure 35, the reaction rates during the cultivation, which were calculated by the app using the results from the  $OD_{600}$  measurement and the glycerol concentration in the supernatant, as well as the online data given by the reactor, are shown.

While the  $q_{O/X}$  is very stable during the whole fermentation, both  $q_{S1/X}$  and  $q_{X/X}$  fluctuate. Therefore it is hard to identify constant phases for the calculation of the global reaction parameters. Furthermore, the difference between the reaction rates during the batch and fed batch is not significant, which would be needed for the calculation of the global reaction parameters.

The ranges chosen for the calculation were 5 to 11 h for the batch and 11 to 15 hour for the fed batch. The resulting parameters are shown in table 20

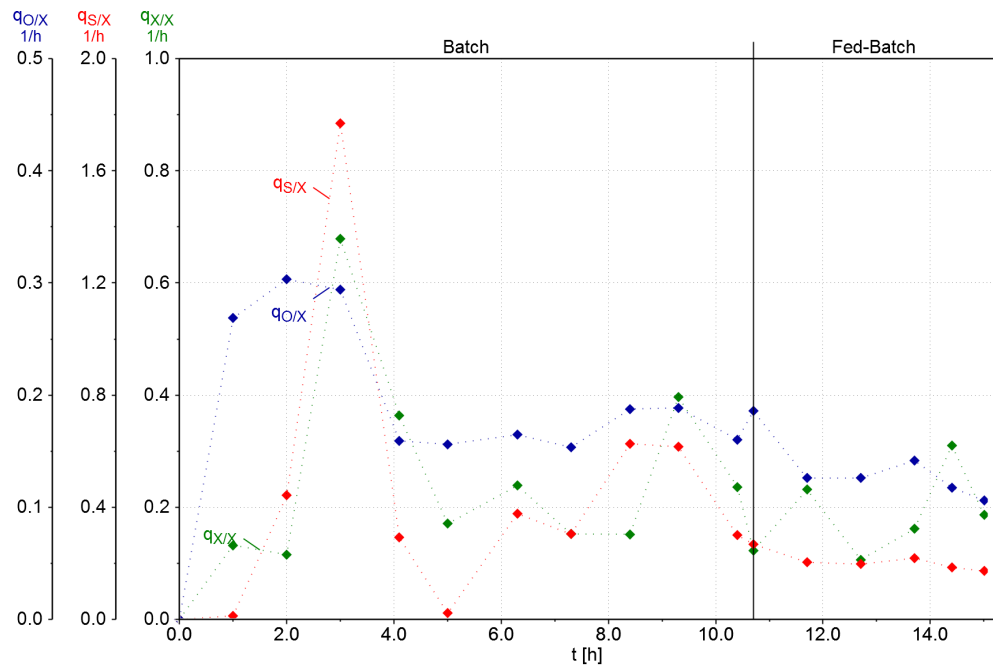


**Fig. 36:** Plots of the reaction rates  $q_{X/X}$ ,  $q_{S1/X}$  and  $q_{O/X}$  during the first fermentation calculated with the app using the CDW measurements

The reaction rates calculated with the results of the CDW-measurement show the same problem as the  $OD_{600}$ -measurements. Many fluctuations can be seen both in the batch and fed batch phase, making the identification of constant phases for the calculation of the global reaction parameters impossible.

The data for  $q_{X/X}$  during the fed-batch is even higher than in the previous analysis, making a differentiation between the two phases even harder.

$q_{S1/X}$  and  $q_{X/X}$  show a peak at 3 h. This peak can also be seen in the data from the  $OD_{600}$ -measurement, but is less pronounced there. The parameter  $q_{O/X}$  again shows the least fluctuations out of the three, but no significant difference between the batch and the fed batch phase can be observed.

The higher stability of the data for  $q_{O/X}$  is easily explained by the fact, that it is not dependent on the offline data and the taken samples. The sample taking procedure is the error prone step due to bad pre-flushing of the tubes or dilution of the samples, which leads to an inaccurate composition of the sample.

The reaction rates were used to calculate the global reaction parameters. The same ranges were chosen for both evaluations to make a comparison between the two data sets possible.

**Table 18:** Ranges for the calculations of the reaction parameters

Batch start	Batch end	Fed batch start	Fed batch end
4.2 h	9.3 h	11.7 h	13.7 h

**Table 19:** Reaction rates calculated from the OD<sub>600</sub>- and CDW-data from the first fermentation

	<b>k</b>	<b>q<sub>X/Xk</sub></b>	<b>q<sub>S1/Xk</sub></b>	<b>y<sub>X/S1k</sub></b>	<b>q<sub>O/Xk</sub></b>	<b>y<sub>X/Ok</sub></b>
OD <sub>600</sub>	max	0.2460 1/h	0.4440 1/h	0.5550	0.1610 1/h	1.5310
CDW	max	0.2590 1/h	0.4740 1/h	0.5550	0.1750 1/h	1.4780
OD <sub>600</sub>	w	0.1190 1/h	0.2040 1/h	0.5850	0.1320 1/h	0.9010
CDW	w	0.1570 1/h	0.2060 1/h	0.7590	0.1320 1/h	1.1900

The data for the batch phase, in which maximal growth occurs, still shows high similarities between the two different analysis methods, as the offline data is pretty similar.  $\mu_{\max}$  is in the range of expected values for *P. pastoris*.

In the fed batch phase, the deviations between the different methods of analysis are more apparent. The calculated  $\mu_w$  from the CDW-data is higher than the one using the OD<sub>600</sub> data. The set point for  $\mu_w$  was 0.15 1/h, which is close to the result using the CDW-data, while the result from the OD<sub>600</sub>-data is too low.

The cell specific substrate uptake rate is very similar between the two different data sets, but since the yield coefficients are calculated using the growth rate, the error is continued in these values, leading to higher values for the CDW-data, since the numerator of the fraction (equation 52) is bigger.

The same problem can be observed in the specific oxygen uptake rate and the oxygen yield coefficients. The value for  $q_{O/Xw}$  are equal, but the higher  $q_{X/Xw}$  leads to a higher yield coefficient for the CDW-data.

**Table 20:** Global reaction parameters calculated using data from the first fermentation

	<b>q<sub>S1/Xm</sub></b>	<b>y<sub>X/S1gr</sub></b>	<b>q<sub>O/Xm</sub></b>	<b>y<sub>X/Ogr</sub></b>
OD <sub>600</sub>	-0.0210 1/h	0.5310	0.1080 1/h	4.4170
CDW	-0.1990 1/h	0.3860	0.0980 1/h	2.3580

The global reaction parameters that were calculated using both data sets are shown in table 20. Notable at first glance is the negative values for  $q_{S1/Xm}$ . These are due to the substrate yield coefficients, as the  $y_{X/S1w}$  is bigger than the  $y_{X/S1max}$ ,

which is impossible. Possible errors for these results are, for example, (1) a problem in the concentration balances, as the volume of the reactor is not weighed but calculated from  $F_{in}$  and  $F_{out}$  and the sample volume is measured with the volume marks of the sample tube, (2) a deviation in the flow rate of substrate  $F_{S1}$  or (3) the fluctuations in the offline data. These all have significant influence on the result for the  $q_{S1/X}$ .

The  $q_{S1/Xm}$  is used in the equations for all other global reaction parameters, therefore these results will also be faulty.

The results for the global reaction parameters show, that the data sets are not suitable to calculate the global reaction parameters. The difference between the batch and fed batch phase is not significant enough, and the fluctuations in the offline data are too high.

## 7.6 Fermentation 2

**Table 21:** Set points for fermentation 2

Variable	Set point value	Unit
$\vartheta_L$	30	°C
$p_{O_2w}$	25	%
pH	5	
$c_{S1R}$	200	g/L
$F_{nG}$	1	L/min
$q_{X/Xw}$	0.1	1/h
$c_{XL0}$	1.25	g/L
$c_{S1L0}$	25	g/L

After the first fermentation, a couple of changes were made to the process.

The aeration rate was lowered from 4 L/min to 1 L/min, to increase the changes in the offgas data during the process. The concentration of glycerol in the feed reservoir was decreased from 400 g/L to 200 g/L, so the feed rate at the start of the fed-batch would be higher, to avoid the unstable  $p_{O_2}$  due to the growth pattern of the cells. Furthermore, the volume pumped by higher flow rates is more accurately calculated by the eve-system.

The set point for  $\mu_w$  was lowered from 0.15 to 0.1 to increase the difference to  $\mu_{max}$ , which in turn will increase the difference from  $q_{S1/Xw}$  and  $q_{O/Xw}$  to their counterparts from the maximal growth phase and the separation of the phases in the plots of the specific reaction rates and lead to more accurate results for the global reaction parameter.

Furthermore, more data points were collected for the fed batch phase, leaving it running for 2 h more than during fermentation 1.

The last change was the increase of the sample frequency. Between the normal, hourly samples for all three offline measurements, another sample is taken and only the OD and the glycerol concentration is measured. This enables the possibility to remove outliers from the results and still retain enough data points for the calculation, which should lead to smoother plot for the reaction parameters.



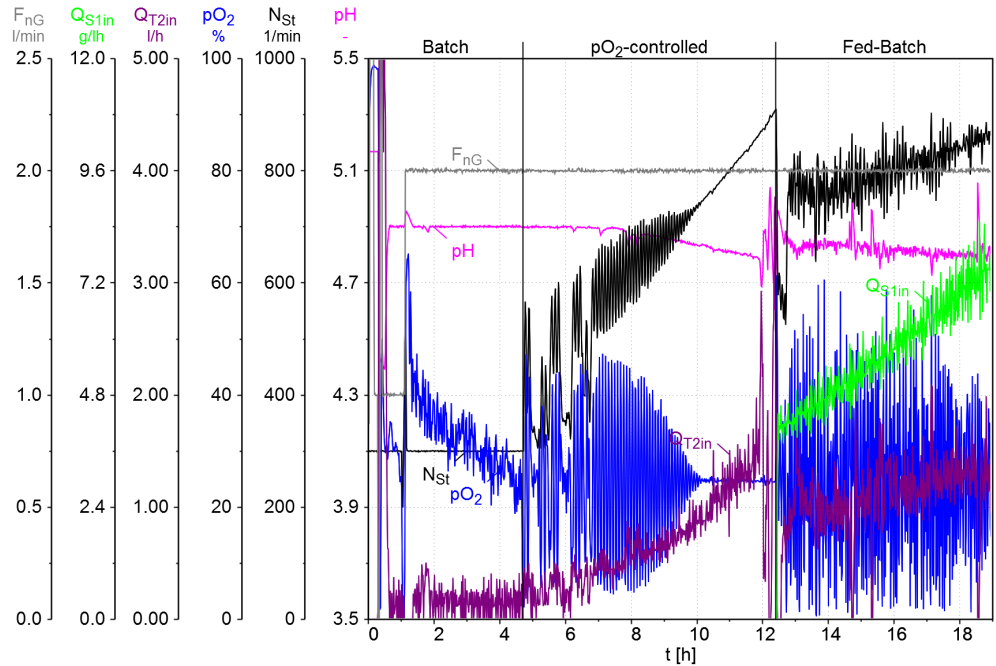


**Fig. 37:** Overview of the courses of  $F_{nG}$ ,  $Q_{S1in}$ ,  $Q_{T2in}$ ,  $pO_2$ ,  $N_{St}$  and pH for the second cultivation

In figure 37 an overview of fermentation number 2 is shown. As in the first fermentation, the pH is well controlled at its setpoint of 5 by the addition of base. The  $pO_2$  dropped very quickly at the beginning of the fermentation. The agitation control was not able to keep the  $pO_2$  at 25%, as the parameters of the agitation control did not lead to a change in the stirrer speed, even after the  $pO_2$  dropped to 4%. The aeration rate was subsequently increased to 2 L/min, which increased the  $pO_2$ . After that change, the agitation control increased the stirrer speed after the set point of 25% was reached, increasing the stirrer speed to meet the increasing oxygen demands of the cells.

The batch end can again be seen by a sharp increase in  $pO_2$ , while the  $N_{St}$  falls, as well as a spike in the pH.

At batch end, the feeding of glycerol is started with an exponential feed profile. During the fed batch phase, the  $pO_2$  is not controlled well, oscillating around its set point with the  $N_{St}$  also fluctuating. The parameters of the agitation control are not ideal for an aeration with 2 L/min, as the  $pO_2$  is not kept stable.

The  $Q_{S1in}$  is also fluctuating, which probably exacerbates the oscillation of the  $pO_2$ , as the growth rate of the cells is not kept constant with a non constant feeding of substrate, leading to varying oxygen demands.

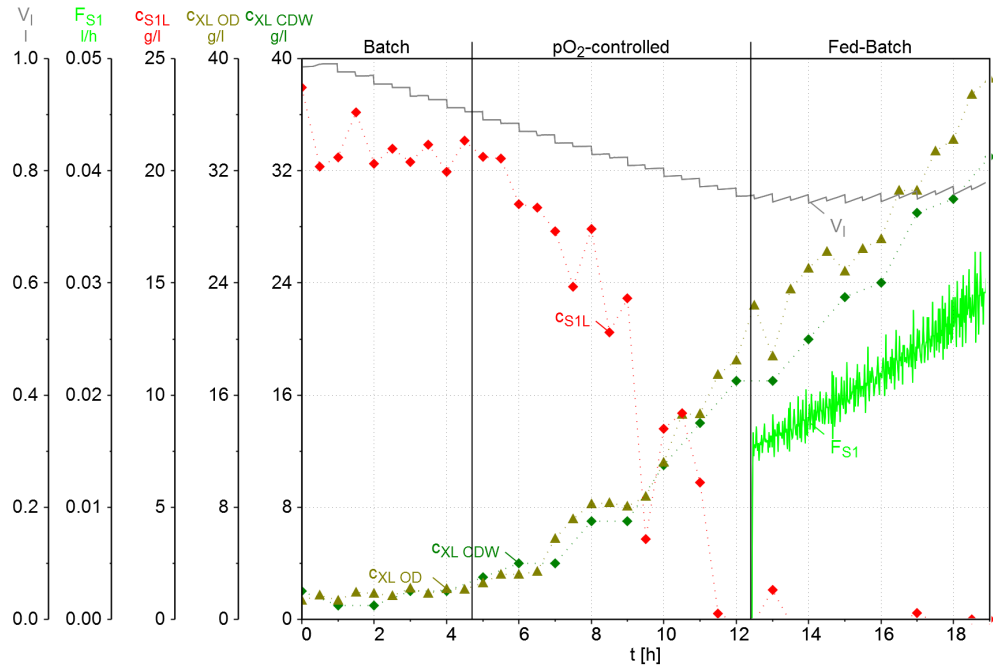


**Fig. 38:** Overview of the substrate uptake during the second fermentation, showing  $c_{XL}$ ,  $c_{S1L}$ ,  $F_{S1}$  and  $V_L$  over the time in hours

In figure 38 the glycerol concentration is shown together with the cell concentration and the substrate quantity. The glycerol concentration decreases until it reaches 0 at 11.5 h, which is before the batch end detection of the online data. Since all three parameters of the batch end detection are met in the online data, the spike in  $pO_2$ , the drop in  $N_{St}$  and the spike in the pH, that time is chosen for the batch end at 12.7 hour.

The substrate concentration shows an increase to 1.3 g/L after the fed batch already started, indicated by the feed rate of substrate  $F_{S1}$ . The substrate concentration should be 0 g/L during the fed batch, as the substrate is consumed by the cells immediately, since they are in substrate limited growth. Therefore, the cells were not consuming all available substrate at the beginning of the fed batch and were probably not growing with the set growth rate  $q_{X/Xw}$ .

The cell concentration is increasing exponentially during the whole fermentation. During the batch phase, the data from the  $OD_{600}$ -measurement and the data from the CDW-measurement match up well, but in the fed batch, the CDW-data is lower than the  $OD_{600}$ -data.

The sampling frequency can be observed in the course of the volume of the reactor  $V_L$ , which is needed in the calculation of the concentration balances.

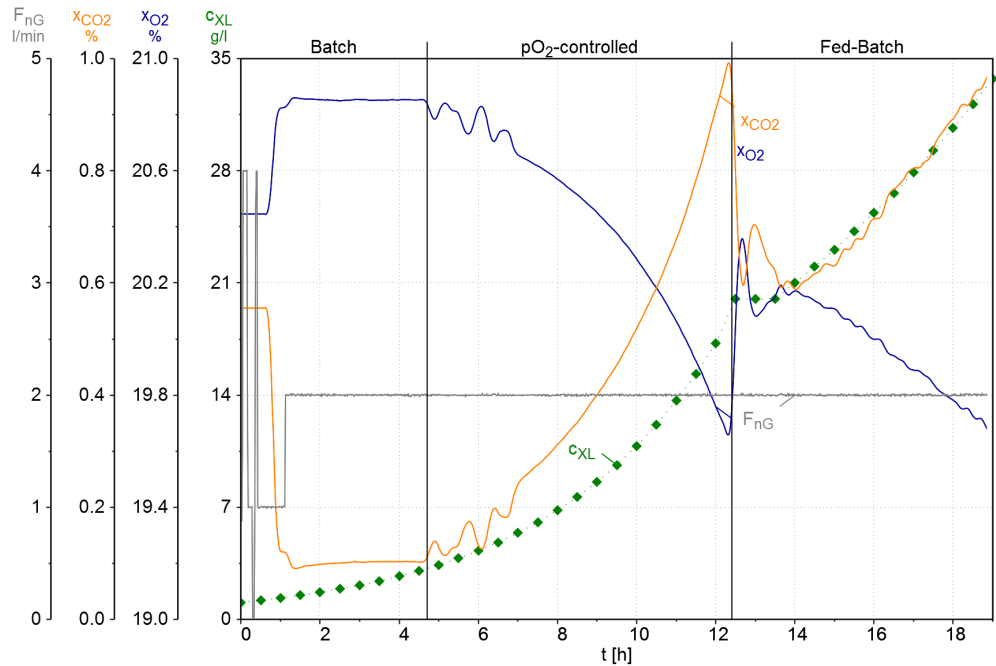


**Fig. 39:** Overview of the oxygen uptake during the second fermentation, showing  $c_{XL}$ ,  $x_{OG}$ ,  $x_{CG}$  and  $F_{nG}$  over the time in hours

In figure 39 the oxygen uptake and subsequent carbon dioxide production can be seen. The change in aeration rate after 1 h leads to a jump in both and both stay mostly stable until the beginning of the  $pO_2$  controlled phase. After that, the oxygen fraction is decreasing while the carbon dioxide fraction is increasing. The jump at the beginning of the fed batch can again be observed, after which the in-, respectively decrease continues slower.

The inactive phase, where no change in the offgas mole fractions can be observed, lasts much longer than during the first fermentation, to around 14 h. This together with the fact that the substrate concentration increased again after the fed batch was started, shows that the cells were not growing significantly during this time.

### 7.6.1 Disussion of the second fermentation

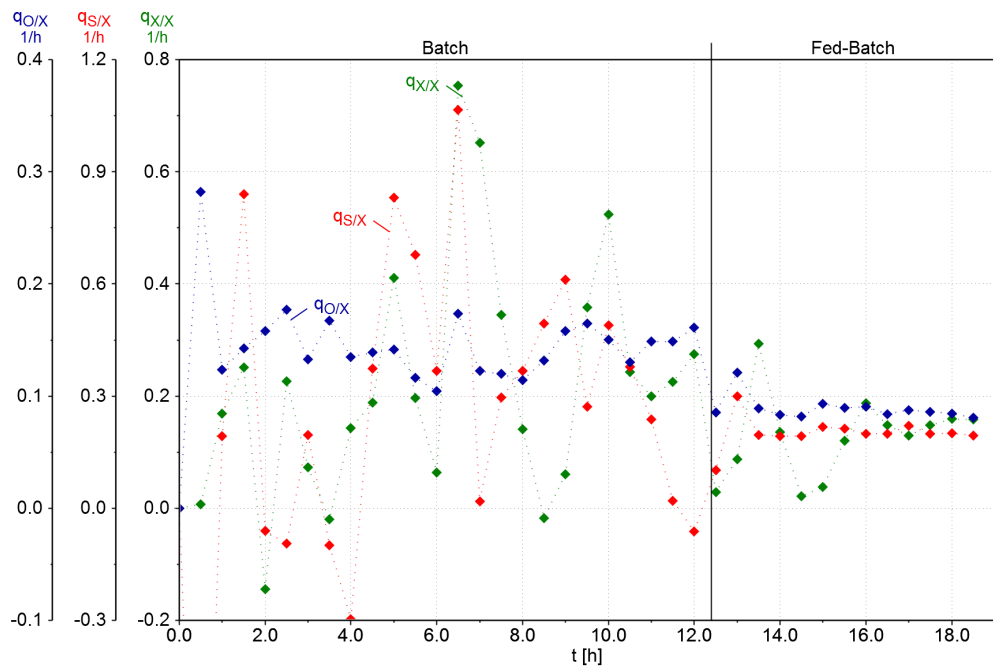


**Fig. 40:** Plots of the reaction rates  $q_{X/X}$ ,  $q_{S1/X}$  and  $q_{O/X}$  during the second fermentation calculated with the app from the offline measurements  $OD_{600}$  and glycerol concentration in the supernatant

In figure 40 the reaction rates calculated using the  $OD_{600}$ -data is shown. The  $q_{X/X}$  and  $q_{S1/X}$  again show many fluctuations during the fermentation, even reaching negative values for the growth and substrate uptake. Only the oxygen uptake rate is smooth, indicating a problem with the samples and offline measurements.

A significant difference between the batch and fed batch can be seen in the values for  $q_{O/X}$ , but the fluctuations in the other two variables make an identification of constant ranges impossible. Therefore, no global reaction parameters were calculated with this data.

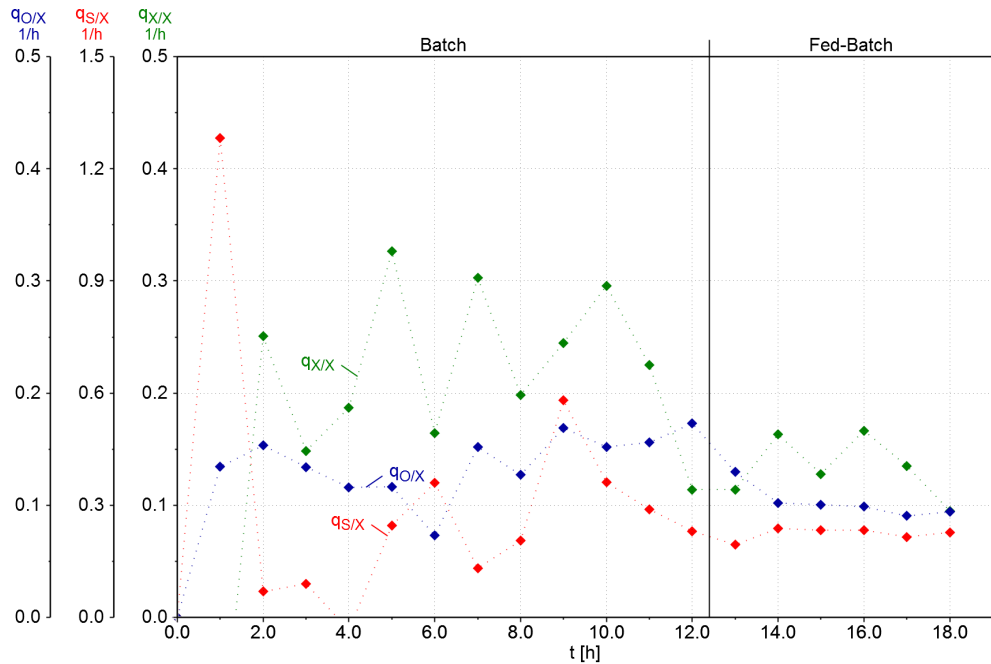


**Fig. 41:** Plots of the reaction rates  $q_{X/X}$ ,  $q_{S1/X}$  and  $q_{O/X}$  during the second fermentation calculated with the app from the offline measurements CDW and glycerol concentration in the supernatant

The data obtained from the CDW-measurements shown in figure 41 again shows high fluctuations as well, but there are no negative results in contrast to the data from the  $OD_{600}$ .

A difference between the batch and fed batch phase can also be observed for the first time in the data for  $q_{X/X}$  and  $q_{O/X}$ , with a decrease of the reaction rates during the fed batch.

The cell specific substrate uptake rate does not show two different phases with very low values at the beginning of the batch phase. A calculation of the global reaction parameters was attempted with this data, with the ranges for calculation shown in table 22. The low values of  $q_{S1/X}$  at the beginning of the batch phase were avoided while choosing the ranges.

**Table 22:** Ranges for the calculations of the reaction parameters

Batch start	Batch end	Fed batch start	Fed batch end
4 h	10 h	14 h	18 h

**Table 23:** Reaction rates calculated from the CDW-data from the second fermentation

	<b>k</b>	<b>q<sub>X/Xk</sub></b>	<b>q<sub>S1/Xk</sub></b>	<b>y<sub>X/S1k</sub></b>	<b>q<sub>O/Xk</sub></b>	<b>y<sub>X/Ok</sub></b>
CDW	max	0.2570 1/h	0.3450 1/h	0.7460	0.1430 1/h	1.8000
CDW	w	0.1320 1/h	0.2280 1/h	0.5800	0.0960 1/h	1.3760

Table 23 shows the results of the reaction parameters for the maximal and controlled growth phase for the second fermentation. Only the data from the CDW measurement was used for a calculation.

All values from the controlled growth phase are lower than the values from the maximal growth, which is the expected result.

The  $q_{X/X_{max}}$  and  $q_{S1/X_{max}}$  are close to the expected result during a *Pichia pastoris* cultivation.

$q_{X/X_w}$  is higher than the set point of the growth rate of 0.1 1/h at 1.1320 1/h, which indicates a higher supply of substrate than needed for the set point of the growth rate.

In table 24 the global reaction parameters calculated using data from the second fermentation are shown

**Table 24:** Global reaction parameters calculated using data from the second fermentation of *P. pastoris*

	<b>q<sub>S1/Xm</sub></b>	<b>y<sub>X/S1gr</sub></b>	<b>q<sub>O/Xm</sub></b>	<b>y<sub>X/Ogr</sub></b>
CDW	0.1040 1/h	1.0670	0.0050 1/h	2.6690

## 8 Exemplary calculated data

### 8.1 Data fit

To provide an exemplary model plot, data was optimized by the Matlab® smooth-data function and offline data was fitted to plots with the Matlab Curve Fitting Tool. In figure 42, the smoothed data of the second fermentation is shown.

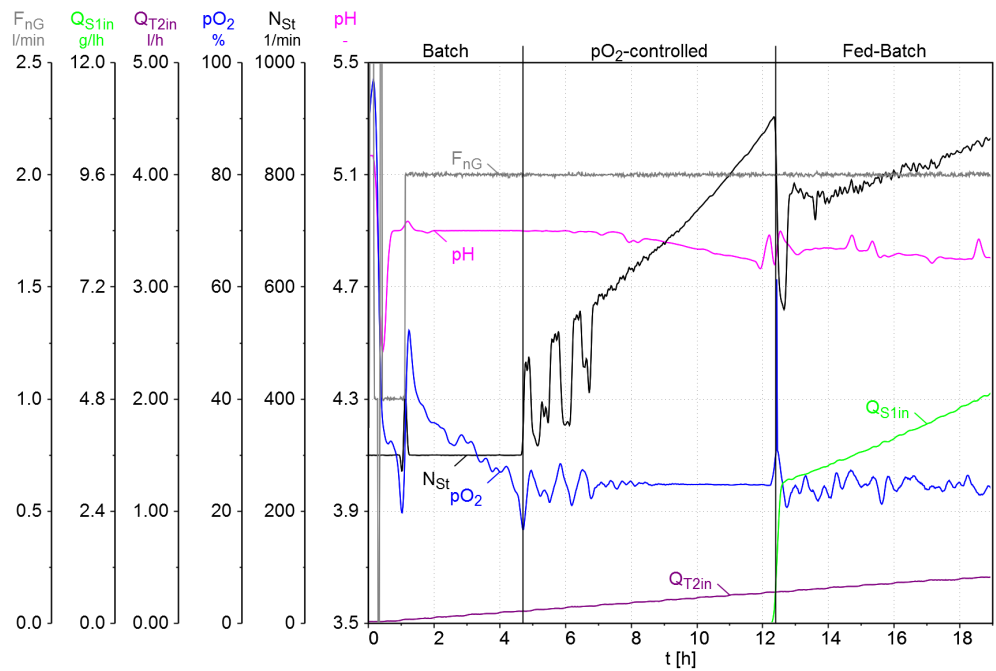


**Fig. 42:** Overview of the smoothed data of  $pO_2$ ,  $N_{St}$ ,  $Q_{S1in}$ ,  $pH$ ,  $Q_{T2}$  and  $F_{NG}$  from data from the second fermentation

To create optimized data, functions were fitted to the CDW-data of the second cultivation. The functions were then used to calculate the theoretical, perfected offline data. Firstly, the cell concentration was fitted by using the equation

$$c_{XL}(t) = c_{XL0} * e^{q_{X/X} * t} \quad (77)$$

were  $c_{XL0}$  and  $q_{X/X}$  were the unknowns fitted by Matlab. The data for  $c_{S1L}$  was fitted using the general equation

$$c_{S1L}(t) = c_{S1L0} - c_{XL}(t) * q_{S1/X} \quad (78)$$

containing the equation for  $c_{XL}(t)$  with  $q_{S1/X}$  as the unknown.  $c_{S1L0}$  was set as 25 g/L, as this was the set point of the fermentation, in contrast to  $c_{XL0}$  which was determined by measurements, and was therefore used as an unknown.

The data for  $c_{XL}$  was fitted in two phases, the batch and the fed batch. The batch phase data was fitted from 0 to 12 h, while the fed batch phase beginning was set to 14 h, as an inactive phase in the cell growth is apparent in the data from the fermentation.

The substrate concentration was only fitted for the batch phase, as the concentration during the fed batch is 0.

The resulting formulas for the curve fittings are for the batch phase

$$c_{XL}(t) = 1.064 * e^{0.232*t} \quad (79)$$

for the cell concentration and

$$c_{S1L}(t) = 25 - c_{XL}(t) * 1.668 \quad (80)$$

for the substrate concentration and for the fed batch phase

$$c_{XL}(t) = 21 * e^{0.09477*t} \quad (81)$$

for the cell concentration.

The evaluation of the fit is shown in table 25.

**Table 25:** Evaluation of fit

	SSE	R <sup>2</sup>	adjusted R <sup>2</sup>	RMSE
C <sub>XL</sub> Batch	4.452	0.9856	0.9843	0.6362
C <sub>XL</sub> Fedbatch	4.112	0.9656	0.957	1.014
C <sub>S1L</sub> Batch	38.26	0.9525	0.9525	1.786

The R<sup>2</sup> and the adjusted R<sup>2</sup> are all over 0.95, indicating a good correlation of the fit to the data in all functions.

The residual errors SSE are very high for the fit of the  $c_{S1L}$  during the batch phase, but the data has many variations and it is a nested fit, as the functions contains the fit for the cell concentration.

The root mean squared error is below or close to 1 for all fits, meaning the stan-



standard error of the regression is not very high.

All in all, the fits are useful for a calculation of the offline data.

In figure 43 the data points and the fitted function can be seen. A data point was calculated every 0.5 h.

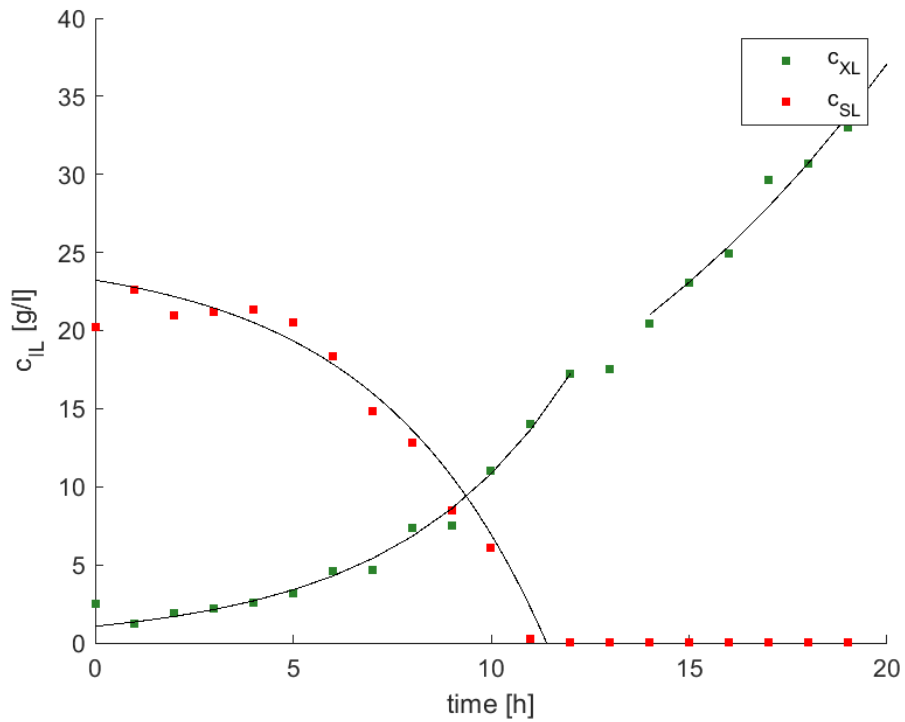


**Fig. 43:** Fitted and actual data using the Matlab® curve fitting tool

## 8.2 Fermentation overview using the calculated data

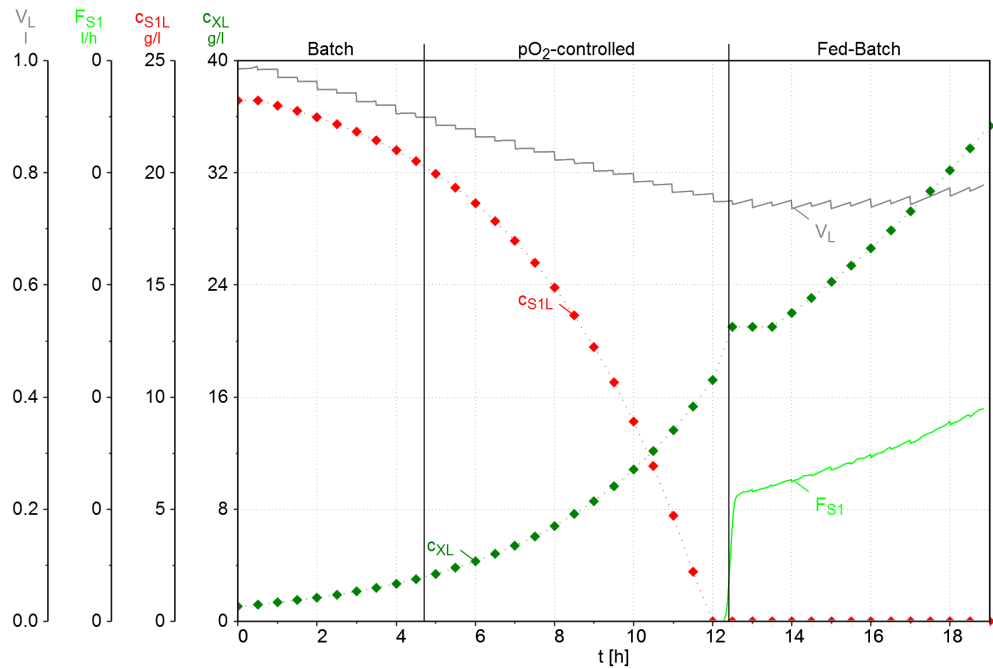


**Fig. 44:** Overview of the substrate uptake of the optimized data, showing  $c_{XL}$ ,  $c_{S1L}$ ,  $F_{S1}$  and  $V_L$  over the time in hours

In figure 44, the calculated data points of the cell and substrate concentration, as well as the flow rate of substrate and the volume of the reactor are plotted. The inactive phase from 12 to 14 h is clearly visible at the beginning of the fed batch. The substrate reaches 0 g/L before the actual batch end at 12 h, which is resulting from the real data arriving at a substrate concentration of 0 g/L before the batch end detection. Of course, this is improbable, as the batch end detection indicates the batch end at 12.7 h, but the fit can not be forced through this point. The fitted function reaches a substrate concentration of 0 g/L at 11.4 h.

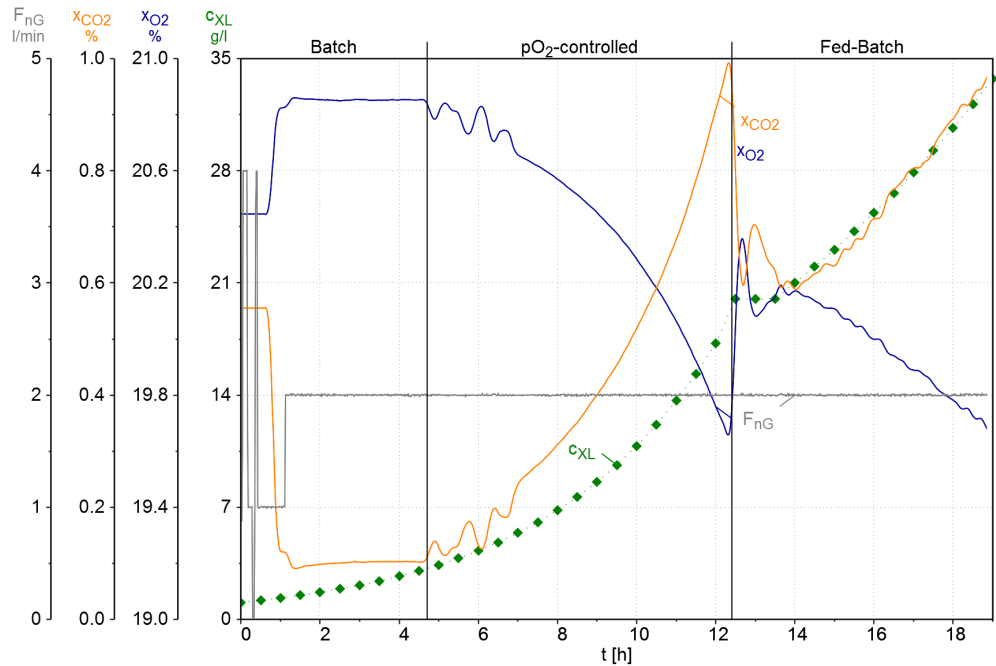


**Fig. 45:** Overview of the oxygen uptake using the calculated data, showing  $c_{XL}$ ,  $x_{OG}$ ,  $x_{CG}$  and  $F_{nG}$  over the time in hours

In figure 45 the smoothed offgas data is displayed. It shows the expected course, with the  $x_{O_2}$  decreasing during the batch phase, a jump at the batch end and then a further decline, while the  $x_{CO_2}$  does the opposite. The inactive phase after the beginning of the fed batch is still visible, where the two courses show the opposite of their expected behavior, indicating that no major cell growth was happening during this time. The cell concentration increases again with the end of the stagnant phase in the offgas data.

### 8.2.1 Discussion of the results using the calculated data

The smoothed data as well as the new offline data was loaded into the app to calculate the reaction parameters of the theoretical fermentation. The results can be seen in figure 46. A significant difference in the values for the batch and the fed batch phase is clearly visible, as all values in the batch phase are higher than the fed batch phase values.

Furthermore, the values for  $q_{X/X}$  and  $q_{S1/X}$  now show a very constant course over the respective phases which was expected with the calculated data.

The inactive phase at the beginning of the fed batch phase is visible through a drop in the values, which stabilizes at 14 h with the end of the inactive phase.

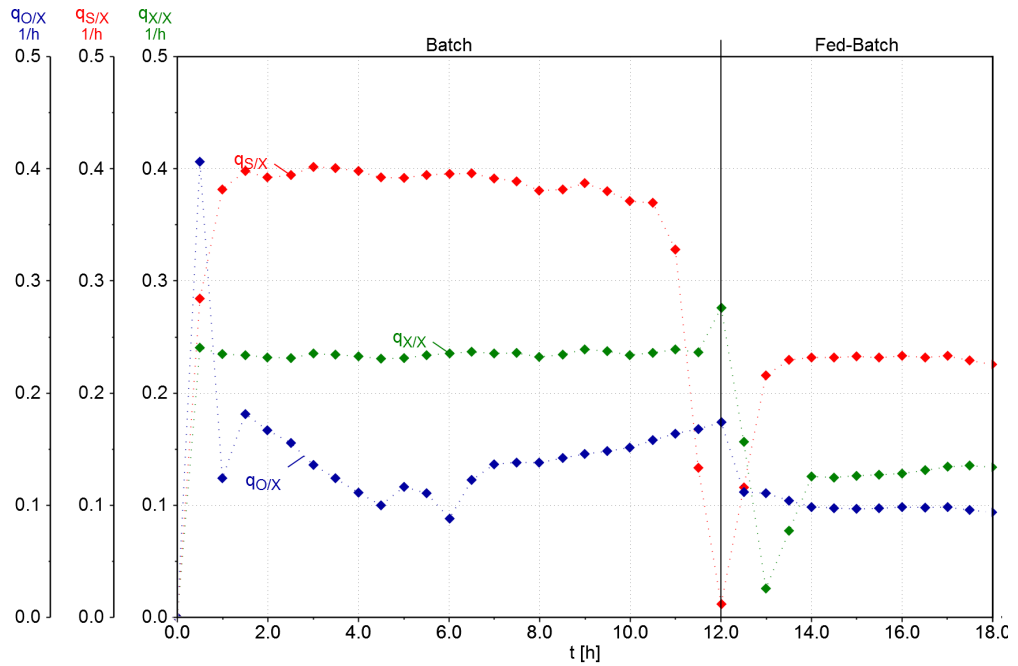


**Fig. 46:** Plots of the reaction rates  $q_{X/X}$ ,  $q_{S1/X}$  and  $q_{O/X}$  using the smoothed and calculated data using CDW- and online data from the second fermentation

The ranges chosen for the calculation of the reaction parameters is shown in table 26. The drop at the beginning of the fed batch, as well as the non-constant range in the course of  $q_{O/X}$  were avoided in the choosing of the ranges.

**Table 26:** Ranges for the calculations of the reaction parameters using the calculated data

Batch start	Batch end	Fed batch start	Fed batch end
6.5 h	11 h	15 h	17 h

The resulting parameters are shown in tables 27 and 28.

**Table 27:** Reaction rates calculated using the fitted data

<b>k</b>	$q_{X/Xk}$	$q_{S1/Xk}$	$y_{X/S1k}$	$q_{O/Xk}$	$y_{X/Ok}$
max	0.2360 1/h	0.3670 1/h	0.6440	0.1520 1/h	1.5650
w	0.1300 1/h	0.2320 1/h	0.5580	0.0990 1/h	1.3130

**Table 28:** Global reaction parameters calculated using the fitted data

	$q_{S1/Xm}$	$y_{X/S1gr}$	$q_{O/Xm}$	$y_{X/Ogr}$
Fit	0.0690 1/h	0.7930	0.0090 1/h	2.0430

### 8.3 Comparison of the results

**Table 29:** Comparison of the results from the actual and fitted data from the second fermentation

	<b>k</b>	<b>q<sub>X/Xk</sub></b>	<b>q<sub>S1/Xk</sub></b>	<b>y<sub>X/S1k</sub></b>	<b>q<sub>O/Xk</sub></b>	<b>y<sub>X/Ok</sub></b>
Data	max	0.2570 1/h	0.3450 1/h	0.7460	0.1430 1/h	1.8000
Fit	max	0.2360 1/h	0.3670 1/h	0.6440	0.1520 1/h	1.5650
Data	w	0.1320 1/h	0.2280 1/h	0.5800	0.0960 1/h	1.3760
Fit	w	0.1300 1/h	0.2320 1/h	0.5580	0.0990 1/h	1.3130

**Table 30:** Comparison of the global reaction parameters using the actual and fitted data from the second fermentation

	<b>q<sub>S1/Xm</sub></b>	<b>y<sub>X/S1gr</sub></b>	<b>q<sub>O/Xm</sub></b>	<b>y<sub>X/Ogr</sub></b>
Data	0.1040 1/h	1.0670	0.0050 1/h	2.6690
Fit	0.0690 1/h	0.7930	0.0090 1/h	2.0430

Table 29 and 30 show a comparison of the data calculated using the actual fermentation data, and the data fitted and smoothed using Matlab.

The parameters are very close together, which is expected, as one data set was calculated using the other one. The functions for the fit already contain a version of  $q_{X/X_{max}}$ ,  $q_{X/X_w}$  and  $q_{S1/X_w}$  without the influence of the changing reactor volume. The results of  $q_{X/X_k}$ ,  $y_{X/S1k}$  and  $y_{X/Ok}$  is lower for the fitted than the actual data, while  $q_{S1/Xk}$  and  $q_{O/Xk}$  are higher.

In the global parameters, the values are much further apart from each other, showing that good data is very important for accurate calculations, as every value has a big influence on the end result

All values for the fitted data are lower than the values calculated from the non-edited data, except the  $q_{O/Xm}$ .

## 9 Summary and Conclusion

In this thesis an app was developed using the Matlab App Designer that calculates the global reaction parameters of a strain with fermentation data produced with the Infors reactor and the eve-software or the MFCS-software. A two phase fermentation with a batch and a fed batch phase is needed for the calculations.

The data is uploaded into the app from the files produced by the software and offline data is added. The data can be visually checked in a plot. After calculating the specific reaction parameters, constant ranges can be chosen in plots for the calculation of the global reaction parameters. The results of the app can be saved in a PDF or mat-file for further use.

For the validation of the app, two fermentations were carried out and the data was used for a calculation. The cell concentration was analyzed with two different methods,  $OD_{600}$  and CDW, while a HPLC was employed for the glycerol measurement.

The first fermentation showed, that a significant difference in the growth rates of the two phases is necessary for good results, otherwise the calculations will not lead to reasonable results. After changing the parameters, the second fermentation had better results with the CDW method, while the  $OD_{600}$ -method showed too many fluctuations in the data of the specific reaction rates, which made it impossible to choose constant ranges for the calculation. The CDW-data could be used to calculate global reaction parameters and reasonable results were achieved.

For an example of how the plots should look, the data of the second fermentation was smoothed and the offline data was fitted to functions, which were used to calculate new offline data. This edited data was used again in the app. The reaction rates showed a very smooth behavior, and the results were close to the results with the non-edited data from the second fermentation. The optimized data was beneficial in showing the function of the application.

In conclusion, the app is useful for the automation of the calculation of global reaction parameters. Data can easily be uploaded and checked. The batch and fed batch ranges can be chosen in the plot and saved by the click of a button. The data transformations and the calculations are all done automatically and the results can be saved for further use. However, it is vital to make sure the data set provided to the app is suitable for the analysis to acquire reliable results.

## 9.1 Outlook

In the future, the app could be extended to also calculate the production rate and yield coefficient of a product. An option to calculate the reaction rates for an organism growing on 2 substrates could also be added.

The selection of the ranges could be automated, although a confirmation of the ranges through the user would probably be necessary, as high fluctuations in the reaction rates are likely to occur, which will make the automation unreliable.

Right now the app only works reliably with data from the Infors reactor, as this was the data it was tested with. The data from the MFCS-system needs to be tested more, to make sure it also operates correctly.

Furthermore, a more general way to upload the data could be developed, to work with many different data types. At the moment, data not produced with the Infors reactor and the eve-system can be added to a template resembling the eve-data using Excel, but that requires a lot of work previous to the calculation to make the data usable.

## References

- Cornelissen, Gesine (2004). *Integrierte Bioprozessentwicklung zur Herstellung pharmakologisch wirksamer Proteine mit Pichia Pastoris*. Universität Hannover.
- Cregg, J M et al. (1989). "Functional characterization of the two alcohol oxidase genes from the yeast *Pichia pastoris*." In: *Molecular and Cellular Biology* 9.3, pp. 1316–1323. DOI: 10.1128/mcb.9.3.1316.
- Dietzsch, Christian, Oliver Spadiut, and Christoph Herwig (2011). "A fast approach to determine a fed batch feeding profile for recombinant *Pichia pastoris* strains". In: *Microbial Cell Factories* 10.1, p. 85. DOI: 10.1186/1475-2859-10-85.
- Garcia-Ochoa, Felix et al. (2010). "Oxygen uptake rate in microbial processes: An overview". In: *Biochemical Engineering Journal* 49.3, pp. 289–307. DOI: 10.1016/j.bej.2010.01.011.
- Hamilton Company (last accessed: 14.04.2021 12:00). *Optical Dissolved Oxygen Sensors*. URL: <https://www.hamiltoncompany.com/process-analytics/sensors/dissolved-oxygen/optical#support>.
- Heyland, Jan et al. (2011). "Carbon metabolism limits recombinant protein production in *Pichia pastoris*". In: *Biotechnology and Bioengineering* 108.8, pp. 1942–1953. DOI: 10.1002/bit.23114.
- Higgins, David R. and James M. Cregg (2000). "Introduction to *Pichia pastoris*". In: *Pichia Protocols*. Humana Press, pp. 1–16. DOI: 10.1385/0-89603-421-6:1.
- Johnson, I. (1983). "Human insulin from recombinant DNA technology". In: *Science* 219.4585, pp. 632–637. DOI: 10.1126/science.6337396.
- Krainer, Florian W et al. (2012). "Recombinant protein expression in *Pichia pastoris* strains with an engineered methanol utilization pathway". In: *Microbial Cell Factories* 11.1, p. 22. DOI: 10.1186/1475-2859-11-22.
- Kurtzman, Cletus Paul (2009). "Biotechnological strains of *Komagataella (Pichia) pastoris* are *Komagataella phaffii* as determined from multigene sequence analysis". In: *Journal of Industrial Microbiology & Biotechnology* 36.11, pp. 1435–1438. DOI: 10.1007/s10295-009-0638-4.
- Li, Pingzuo et al. (2007). "Expression of Recombinant Proteins in *Pichia Pastoris*". In: *Applied Biochemistry and Biotechnology* 142.2, pp. 105–124. DOI: 10.1007/s12010-007-0003-x.
- Looser, V. et al. (2015). "Cultivation strategies to enhance productivity of *Pichia pastoris*: A review". In: *Biotechnology Advances* 33.6, pp. 1177–1193. DOI: 10.1016/j.biotechadv.2015.05.008.



- Lopes, Marlene, Isabel Belo, and Manuel Mota (2012). "Batch and fed-batch growth of *Pichia pastoris* under increased air pressure". In: *Bioprocess and Biosystems Engineering* 36.9, pp. 1267–1275. DOI: 10.1007/s00449-012-0871-5.
- Luttmann, Reiner, Gerhard Bitzer, and Jens Hartkopf (1994). "Development of control strategies for high cell density cultivations". In: *Mathematics and Computers in Simulation* 37.2-3, pp. 153–164. DOI: 10.1016/0378-4754(94)00004-2.
- Luttmann, Reiner, Elisabeth Hukelmann, et al. (2010). "A Cybernetic Approach for Modelling of Complex Dynamic Expression in Recombinant Protein Production with *Pichia pastoris*". In: *IFAC Proceedings Volumes* 43.6, pp. 383–388. DOI: 10.3182/20100707-3-be-2012.0020.
- MathWorks Inc (last accessed: 17.06.2021 08:34). *Develop Apps Using App Designer*. URL: <https://de.mathworks.com>.
- (last accessed: 17.06.2021 09:01). *Curve Fitting Toolbox*. URL: <https://de.mathworks.com/products/curvefitting.html>.
- (last accessed: 17.06.2021 15:12). *Documentation*. URL: <https://de.mathworks.com/help/>.
- Ogata, Koichi, Hideo Nishikawa, and Masahiro Ohsugi (1969). "A Yeast Capable of Utilizing Methanol". In: *Agricultural and Biological Chemistry* 33.10, pp. 1519–1520. DOI: 10.1080/00021369.1969.10859497.
- Porro, Danilo et al. (2005). "Recombinant Protein Production in Yeasts". In: *Molecular Biotechnology* 31.3, pp. 245–260. DOI: 10.1385/mb:31:3:245.
- Scheunemann, Maria (2020). *Analysis of *P. pastoris* growth on yeast extracts and classification and prediction via different cluster functions*. Masterthesis.
- Schügerl, Karl and Karl-Heinz Bellgardt (2011). *Bioreaction Engineering*. Springer Berlin Heidelberg. 648 pp. ISBN: 3642641032.
- Tribe, L. A., C. L. Briens, and A. Margaritis (1995). "Determination of the volumetric mass transfer coefficient (kLa) using the dynamic ?gas out-gas in? method: Analysis of errors caused by dissolved oxygen probes". In: *Biotechnology and Bioengineering* 46.4, pp. 388–392. DOI: 10.1002/bit.260460412.
- Trinh, L. B., J. N. Phue, and Joseph Shiloach (2003). "Effect of methanol feeding strategies on production and yield of recombinant mouse endostatin from *Pichia pastoris*". In: *Biotechnology and Bioengineering* 82.4, pp. 438–444. DOI: 10.1002/bit.10587.

## Appendix

Table A: Data of fermentation 1

time	time[h]	OD	Median	Dilution	OD*Dilution	Supernatant	OD - supernatant	Cellconc [g/l] OD	CDW[g]	MEAN CDW	Cellconc [g/l] CDW	CSL[g/l]
03.03.2021 10:20	0,0	0,547	0,577	4,000	2,248	0,019	2,248	1,238	0,001	0,000	0,001	0,95
03.03.2021 11:20	1,0	0,294	0,287	10,000	2,905	0,127	2,905	1,599	0,001	0,001	0,001	1,35
03.03.2021 12:20	2,0	0,327	0,334	10,000	3,305	0,095	3,305	1,820	0,002	0,001	0,001	1,3
03.03.2021 13:20	3,0	0,442	0,538	10,000	4,900	0,009	4,900	2,698	0,002	0,002	0,002	1,655
03.03.2021 14:27	4,1	0,244	0,257	20,000	5,010	0,008	5,010	2,759	0,003	0,004	0,004	3,65
03.03.2021 15:20	5,0	0,323	0,310	20,000	6,330	0,004	6,330	3,485	0,005	0,004	0,004	4,3
03.03.2021 16:39	6,3	0,478	0,499	20,000	9,770	0,007	9,770	5,379	0,005	0,005	0,005	5,25
03.03.2021 17:40	7,3	0,272	0,260	40,000	10,640	0,005	10,640	5,858	0,007	0,007	0,007	7,15
03.03.2021 18:44	8,4	0,148	0,146	100,000	14,700	0,005	14,700	8,094	0,007	0,008	0,008	7,5
03.03.2021 19:40	9,3	0,238	0,217	100,000	22,750	0,005	22,750	12,526	0,009	0,009	0,009	9,4
03.03.2021 20:46	10,4	0,242	0,224	100,000	23,300	0,005	23,300	12,829	0,015	0,015	0,015	14,9
03.03.2021 21:00	10,7	0,270	0,263	100,000	26,650	0,006	26,650	14,673	0,014	0,015	0,014	14,25
03.03.2021 22:00	11,7	0,290	0,311	100,000	30,050	0,005	30,050	16,546	0,016	0,018	0,017	17
03.03.2021 23:00	12,7	0,375	0,416	100,000	40,650	0,016	40,650	22,382	0,022	0,021	0,022	21,55
04.03.2021 00:02	13,7	0,375	0,361	100,000	36,800	0,007	36,800	20,262	0,021	0,021	0,021	20,8
04.03.2021 00:45	14,4	0,416	0,447	100,000	43,150	0,011	43,150	23,758	0,027	0,027	0,027	26,7
04.03.2021 01:20	15,0	0,226	0,247	200,000	47,300	0,007	47,300	26,043	0,031	0,031	0,031	31
04.03.2021 02:02	15,7	0,333	0,362	200,000	69,500	0,099	69,500	38,267	0,034	0,033	0,034	33,5
												0,00

Table B: Data of fermentation 2

time	time[h]	OD		Median	Dilution	OD*Dilution	Cellconc [g/l]	OD	CDW[g]	MEAN CDW	Cellconc [g/l]	CDW	csL [g/l]
03.03.2021 10:43	0.0	0,507	0,507	0,507	4	2,028	1,22	0,0020	0,0025	0,0022	2,25	20,193	
03.03.2021 11:13	0,5	0,31	0,33	0,320	8	2,560	1,54					20,607	
03.03.2021 11:43	1,0	0,261	0,145	0,203	10	2,030	1,22	0,0013	0,0012	0,0012	1,25	22,610	
03.03.2021 12:13	1,5	0,297	0,283	0,290	10	2,900	1,74					20,327	
03.03.2021 12:43	2,0	0,27	0,281	0,276	10	2,755	1,65	0,0022	0,0016	0,0019	1,9	20,993	
03.03.2021 13:13	2,5	0,248	0,252	0,250	10	2,500	1,50					20,395	
03.03.2021 13:43	3,0	0,297	0,367	0,332	10	3,320	1,99	0,0021	0,0023	0,0022	2,2	21,171	
03.03.2021 14:13	3,5	0,267	0,281	0,274	10	2,740	1,64					19,954	
03.03.2021 14:43	4,0	0,324	0,329	0,327	10	3,265	1,96	0,0023	0,0028	0,0025	2,55	21,338	
03.03.2021 15:13	4,5	0,32	0,321	0,321	10	3,205	1,92					20,623	
03.03.2021 15:43	5,0	0,393	0,38	0,387	10	3,865	2,32	0,0030	0,0033	0,0032	3,15	20,545	
03.03.2021 16:13	5,5	0,234	0,245	0,240	20	4,790	2,87					18,521	
03.03.2021 16:43	6,0	0,235	0,245	0,240	20	4,800	2,88	0,0041	0,0051	0,0046	4,6	18,367	
03.03.2021 17:13	6,5	0,247	0,262	0,255	20	5,090	3,05					17,315	
03.03.2021 17:43	7,0	0,478	0,385	0,432	20	8,630	5,18	0,0045	0,0048	0,0047	4,65	14,843	
03.03.2021 18:13	7,5	0,107	0,107	0,107	100	10,700	6,42					17,415	
03.03.2021 18:43	8,0	0,124	0,122	0,123	100	12,300	7,38	0,0072	0,0076	0,0074	7,4	12,800	
03.03.2021 19:13	8,5	0,124	0,124	0,124	100	12,400	7,44					14,311	
03.03.2021 19:43	9,0	0,121	0,12	0,121	100	12,050	7,23	0,0077	0,0074	0,0076	7,55	8,498	
03.03.2021 20:13	9,5	0,133	0,129	0,131	100	13,100	7,86					9,191	
03.03.2021 20:43	10,0	0,158	0,176	0,167	100	16,700	10,02	0,0111	0,0110	0,0111	11,05	6,116	
03.03.2021 21:13	10,5	0,205	0,231	0,218	100	21,800	13,08					3,583	
03.03.2021 21:43	11,0	0,224	0,214	0,219	100	21,900	13,14	0,0147	0,0133	0,0140	14	0,267	
03.03.2021 22:13	11,5	0,256	0,265	0,261	100	26,050	15,63					-0,131	
03.03.2021 22:43	12,0	0,277	0,275	0,276	100	27,600	16,56	0,0168	0,0176	0,0172	17,2	-0,113	
03.03.2021 23:13	12,5	0,359	0,31	0,335	100	33,450	20,07					1,310	
03.03.2021 23:43	13,0	0,282	0,279	0,281	100	28,050	16,83	0,0173	0,0178	0,0176	17,55	-0,119	
04.03.2021 00:13	13,5	0,352	0,352	0,352	100	35,200	21,12					-0,135	
04.03.2021 00:43	14,0	0,349	0,399	0,374	100	37,400	22,44	0,0207	0,0202	0,0205	20,45	-0,147	
04.03.2021 01:13	14,5	0,385	0,399	0,392	100	39,200	23,52					-0,106	
04.03.2021 01:43	15,0	0,354	0,388	0,371	100	37,100	22,26	0,0231	0,0230	0,0231	23,05	-0,130	
04.03.2021 02:13	15,5	0,393	0,396	0,395	100	39,450	23,67					-0,135	
04.03.2021 02:43	16,0	0,4	0,411	0,406	100	40,550	24,33	0,0252	0,0246	0,0249	24,9	-0,132	
04.03.2021 03:13	16,5	0,451	0,462	0,457	100	45,650	27,39					0,288	
04.03.2021 03:43	17,0	0,447	0,467	0,457	100	45,700	27,42	0,0280	0,0313	0,0297	29,65	-0,132	
04.03.2021 04:13	17,5	0,499	0,498	0,499	100	49,850	29,91					-0,128	
04.03.2021 04:43	18,0	0,26	0,251	0,256	200	51,100	30,66	0,0300	0,0314	0,0307	30,7	0,000	
04.03.2021 05:13	18,5	0,28	0,279	0,280	200	55,900	33,54					0,000	
04.03.2021 05:43	19,0	0,28	0,296	0,288	200	57,600	34,56	0,0334	0,0326	0,0330	33	0,000	

## Herkunft

## Empfänger

<b>HAW Hamburg</b> Fakultät LS – Department Biotechnologie Ulmenliet 20 21033 Hamburg  <b>AG: Prof. Dr. Stephan Noll</b>	<b>HAW Hamburg</b> Fakultät LS – Department Biotechnologie Ulmenliet 20 21033 Hamburg  <b>AG: Prof. Dr. Gesine Cornelissen</b>
---	---

Datum der Abgabe: 06.05.2020

Stammsname: ***Pichia pastoris* LM1**

Risikogruppe: 1

Herkunft des parentalen Stamms: **bisy e.U.**  
 Wetzawinkel 20/2, 8200 Hofstätten/ Raab  
 Austria

Material:
 

- Ausstrich auf Agarplatte
- Flüssigkultur
- Glycerin-Dauerkultur

### Weiter Informationen für GVOs:

Plasmid:
 

- kein Plasmid enthalten
- Klicken oder tippen Sie hier, um Text einzugeben.

*Nähere Informationen zum Plasmid sind der Infokarte zu entnehmen.*

Genomische Modifikation:
 

- keine
- Genom wurde modifiziert

**Zusätzliche Informationen:** verfügt über Zeocin-Resistenz (100 µg/mL)

### Beschreibung der Modifikation:

*P. pastoris* LM1 basiert auf BSYBG11 (bisy) und wurde so modifiziert, dass durch Zugabe von Methanol eine Expression eines Fusionsproteins (8His\_eGFP\_TEV(G)\_NK2-ALK) induziert wird, welches extrazellulär sekretiert wird (s. Abb. 1).

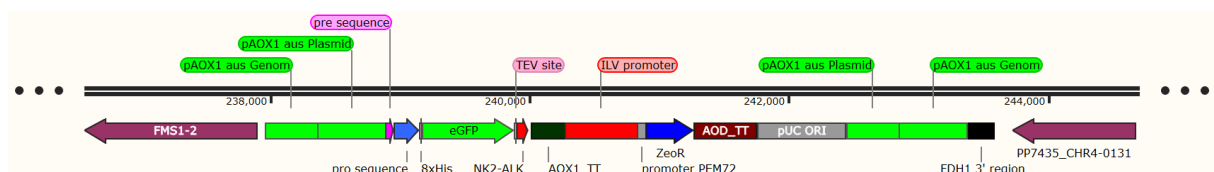


Abbildung 1: Schematische Darstellung der homologen Rekombination von Plasmid 43 in das Genom von *P. pastoris* BSYBG11 (erstellt mit SnapGene).

In pAXO1 auf Chromosom 4 des Genoms von *P. pastoris* BSYBG11 wurde Plasmid 43 über homologe Rekombination integriert.

Die Übergänge zwischen Genom und Plasmid befinden sich an den Positionen 238.373 und 242.858.

## Qualitätskontrolle:

Die Übergänge zwischen Genom und Plasmid (rechte und linke Flanke der Rekombination, jeweils über pAOX1 hinaus), sowie der Expressionsbereich (pre\_pro\_8His\_eGFP\_TEV(G)\_NK2-ALK) wurden vollständig mittels Sangersequenzierung überprüft (vgl. Abb. 2). Die Sequenzdaten sind verfügbar unter dem Laufwerk der Mikrobiologie, AG Noll, Projekt 14.

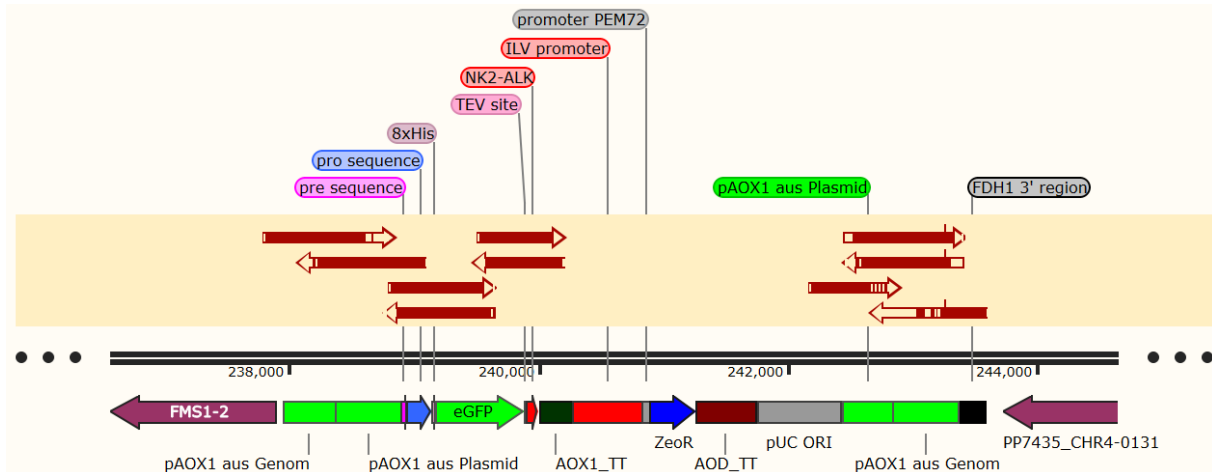


Abbildung 2: Schematische Darstellung der sequenzierten Genomabschnitte des konstruierten Stammes *P. pastoris* LM1 (erstellt mit SnapGene). Die Pfeile stellen die sequenzierten Bereiche dar. Ausgefüllte Bereiche in den Pfeilen zeigen eine Übereinstimmung mit dem Sequenztemplate.

In den sequenzierten Bereichen sind keine Abweichungen zum Sequenztemplate aufgetreten.

Zur Überprüfung der Sekretion wurde eine *Small-Scale-Expression* entsprechend ROP\_LP19\_01 durchgeführt.

Mittels SDS-PAGE konnte eine Bande von etwa 30 kDa nachgewiesen werden. Dies entspricht der theoretischen Größe des rekombinanten Proteins (28,2 kDa) (s. Abb. 3).

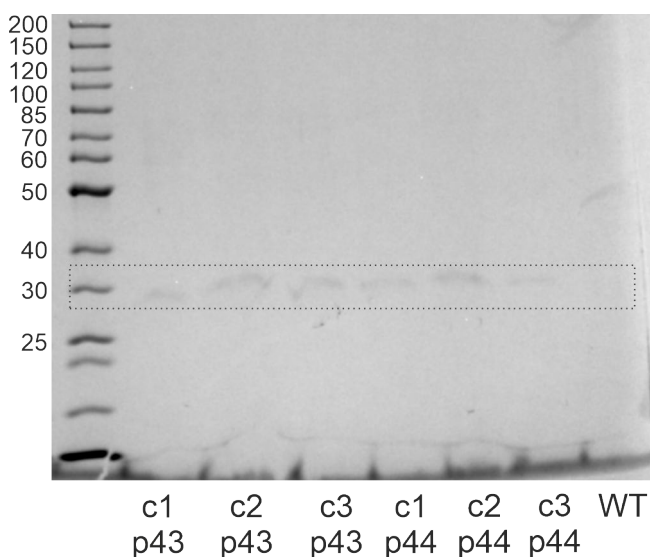


Abbildung 3: Gezeigt ist eine SDS-PAGE der Kulturüberstände der durchgeführten Small-Scale-Expression. Von links nach rechts wurden aufgetragen: Marker, die Klone 1 bis 3 des Stammes *P. pastoris* LM1 (*P. pastoris* BSYBG11 + Plasmid 43 (p43)), die Klone 1 bis 3 des Stammes *P. pastoris* LM2 (*P. pastoris* BSYBG11 + Plasmid 44 (p44)) sowie der parentale Stamm *P. pastoris* BSYBG11 (Wildtyp (WT)).

Unter dem Fluoreszenzmikroskop konnte bei dem Stamm *P. pastoris* LM1 nach Methanol-Induktion eine grüne Fluoreszenz beobachtet werden ( $\lambda_{A \max} = 488 \text{ nm}$ ,  $\lambda_{E \max} = 509 \text{ nm}$ ) (vgl. Abb. 4), die vermutlich auf das eGFP zurückzuführen ist, da sie beim parentalen Stamm (*P. pastoris* BSYBG11) nicht beobachtet wurde (Daten nicht gezeigt).

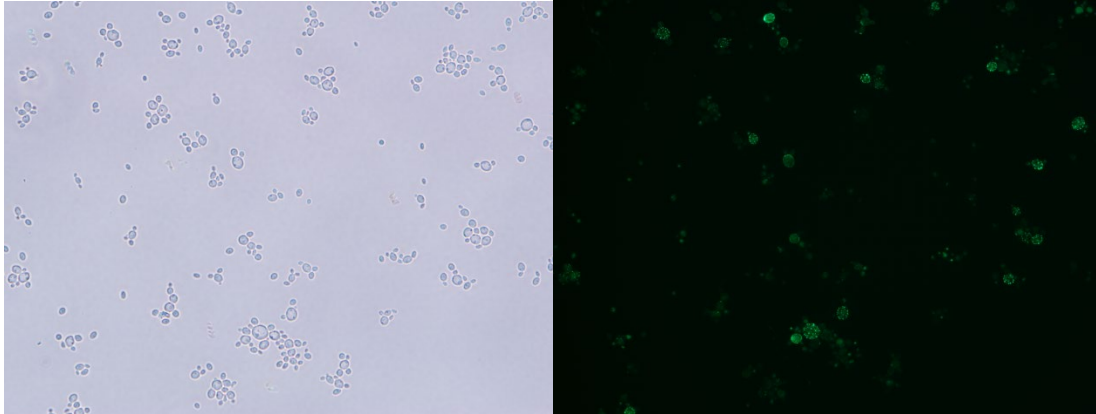


Abbildung 4: Vergleich des gleichen Bildausschnitts bei Hellfeld- (links) und Fluoreszenzmikroskopie (rechts).

## Kultivierung:

Der Stamm wurde in folgenden Medien kultiviert.

### YPD-Medium mit Zeocin

- 10 g/L Hefeextrakt
- 20 g/L Pepton
- 20 g/L Glucose
- 100 mg/L Zeocin

### BMG1 mit Zeocin

- 4,6 g/L  $K_2HPO_4$
- 23,6 g/L  $KH_2PO_4$
- 6,7 g/L Hefe-Stickstoff-Basis (YNB), ohne Aminosäuren (Carl Roth, #HP26)
- 10,0 g/L Glucose
- 100,0 mg/L Zeocin